NASr-21(02)

MEMORANDUM
RM-4048-NASA
APRIL 1964

DYNAMIC ANALYSIS OF A PASSIVE SATELLITE STABILIZATION TECHNIQUE

T. B. Garber

This research is sponsored by the National Aeronautics and Space Administration under Contract No. NASr-21. This report does not necessarily represent the views of the National Aeronautics and Space Administration.

The RAND Corporation
1700 MAIN ST. • SANTA MONICA • CALIFORNIA

PREFACE

This study analyzes a proposed passive attitude-stabilization concept for artificial satellites. The analysis was carried out at the request of Mr. A. M. Andrus, Office of Space Sciences and Applications, National Aeronautics and Space Administration, as part of RAND's work for NASA on communication satellite technology.

SUMMARY

For some applications, artifical earth satellites must be stabilized in attitude with respect to the earth or some other reference. The attitude requirements for certain missions are more severe than for others. For example, a communication satellite, which is simply required to floodlight the earth, might function quite well without regard to whether it were oriented frontward or backward, while an observation satellite with very directional sensors may require exceptional attitude accuracy.

It is possible to design a satellite so that gravity alone will keep it approximately stabilized. The resulting stabilization is not as precise as may be possible with an active system, and so may be valuable for applications in which the satellite must be stabilized, but not necessarily with great precision. Such a passive system should function as long as the satellite stays in orbit.

The present study analyzes a gravity-stabilized satellite, proposed by workers at the Ames Research Center. This concept has been previously analyzed on an approximate, or linear, basis. The present analysis is nonlinear, and hence more complicated, but should also yield more general results.

The analysis takes into account deviations from the desired attitude due to initial errors, due to deviations of the satellite from a circular orbit, and due to external forces such as radiation pressure. The particular stabilization concept under consideration gives excellent performance in making corrections for initial attitude errors. However, some subsequently applied forces, such as those resulting

if the orbit had to be corrected by a thrust impulse, might unduly perturb the satellite's attitude, so that stabilization could not be maintained. This could be alleviated at the expense of some degradation in transient response by an appropriate small design change.

ACKNOWLEDGMENT

The author wishes to thank Susan Belcher who prepared the machine computation program and Bruce Tinling and Vernon Merrick, of Ames Research Center, NASA, who supplied the values of the parameters for the stabilization scheme analysed in this Memorandum.

CONTENTS

LIST OF FIGURES

LIST OF SYMBOLS

Coordinate Systems (See Figs. 1-3)

X_I, Y_I, Z_I	Earth-centered inertial axes.
X, Y, Z	Earth-centered axes.
i, j, k	Local horizontal axes.
x, y, z	Principal axes of primary body.
x_1, y_1, z_1	Principal axes of damper-rod.
x_p, y_p, z_p	Principal axes of damper-rod, body combination.

Orbital Parameters (See Fig. 1 and Appendix B)

r, θ, γ	Spherical coordinates used to specify the position of the center of mass of the satellite with respect to the nominal orbit plane.
Ψ	Angle between X and X_I.
i_o	Inclination of the nominal orbit plane.
e	Orbit eccentricity.

Orientation Angles (See Figs. 2-3)

α, β, φ	Orientation angles relating the body x, y, z axes to the i, j, k axes. For small angles α is the pitch angle, β is the roll angle and $\Delta\varphi$ is the yaw angle.
α_1, β_1, φ_1	Angles relating the damper-rod axes, x_1, y_1, z_1 to the i, j, k axes.
α_p, β_p, φ_p	Angles relating the x_p, y_p, z_p axes to the i, j, k axes.
ρ_1, ρ_2	Angles relating the damper-rod to the body.

Angular Rates

$\omega_x, \omega_y, \omega_z$	The x, y, z components of the angular rate of the body with respect to inertial space.
$\omega_{xp}, \omega_{yp}, \omega_{zp}$	The x_p, y_p, z_p components of the angular rate of the damper-rod, body combination with respect to inertial space.

Moments of Inertia

I_x, I_y, I_z	The principal moments of inertia of the body alone (i.e., without damper-rod).
I_{xl}, I_{yl}, I_{zl}	The principal moments of inertia of the damper-rod. In this study $I_{xl} = 0$ and $I_{yl} = I_{zl} = I_{dr}$.
I_{xp}, I_{yp}, I_{zp}	The instantaneous principal moments of inertia of the damper-rod, body combination. For small disturbances they are approximately constant.

Miscellaneous Quantities

$\dot{\theta}_c$	Constant orbital angular rate for an ideal circular orbit.
r_c	Orbital radius of ideal circular orbit.
g_o	Acceleration of gravity at the surface of a spherical earth.
ρ_L	The limit value of ρ_2.
$(\dot{})$	Time derivative of a quantity.

I. INTRODUCTION

The passive attitude stabilization of satellites by means of gravitational gradient torques has been under study for at least the last 10 years.[1] Such an approach is attractive, since under idealized conditions, a satellite will maintain a particular orientation with respect to the local vertical without the expenditure of energy.* However, even in the absence of external disturbing torques, the satellite can tumble or oscillate continuously due to initial errors in body attitude angles and angular rates, orbital eccentricity, or perturbations due to the higher-order harmonics in the earth's potential function. Thus for any practical application some sort of damping mechanism must be employed so that the oscillations due to initial errors will decay with time.

A number of ingenious schemes have been proposed.[2-4] If precise attitude control is required, active systems employing reaction wheels or gyros in conjunction with a sensor such as an horizon scanner are utilized.[5] However, if extreme pointing accuracy is not a requirement, then passive damping techniques can be employed. The term "passive" implies that the damping system does not require a power supply.

The passive stabilization concept under consideration in this Memorandum is directly related to the Vertistat as proposed by Kamm.[6] Since a number of stabilization schemes employing the principles of the Vertistat have been proposed, a discussion of the basic features

*The local vertical is assumed to be the direction of the maximum of the gravitational gradient.

of this concept is of value.[7-10]

In order to achieve three-axis stabilization, the moments of inertia of a vehicle must have a certain order insofar as their magnitudes are concerned.[11] Thus the largest moment of inertia must correspond to the pitch axis, which is ideally normal to the orbital plane. The yaw axis, ideally aligned with the vertical, is the axis of minimum moment of inertia. The roll axis, of intermediate moment of inertia, is colinear with the vehicle's velocity vector.

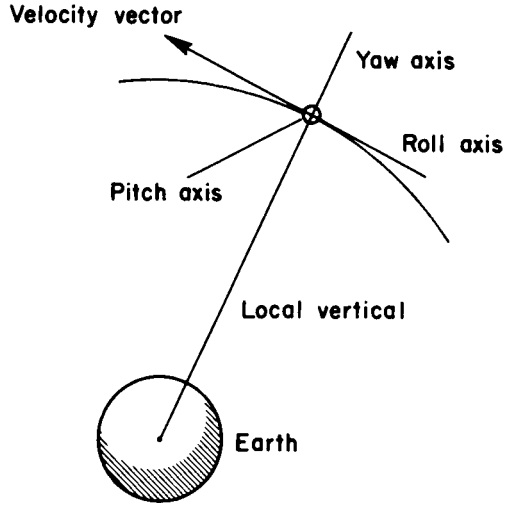

A satellite is not always constructed with the proper mass distribution for the required order of the moments of inertia. This difficulty is circumvented in the Vertistat by utilizing rods or booms that can be stored compactly and then extended once the vehicle is in orbit.[12] For a nominal weight penalty the moment of inertia about a given axis, and thus the gradient torque, can be greatly enhanced.

Two bodies with differing pitch moments of inertia will have different periods of oscillation about the pitch axis. Thus if two such bodies are coupled together by means of a dissipative mechanism,

their relative angular velocity will be damped until, in the absence of external disturbances, both bodies no longer oscillate with respect to each other or to the local vertical. For small displacements from a stable orientation the pitch motion is independent of the coupled roll-yaw motion. Thus Kamm suggested that one boom be viscously coupled to the main body so that its equilibrium position would be along the roll axis. Since this is an attitude of unstable equilibrium, due to the gradient torques, a spring must be used to maintain the desired body-boom angular relationship. Another boom is viscously coupled to the body so that it is nominally along the pitch axis. Again a spring is required to keep the boom in the horizontal plane under equilibrium conditions. (See the following sketch.)

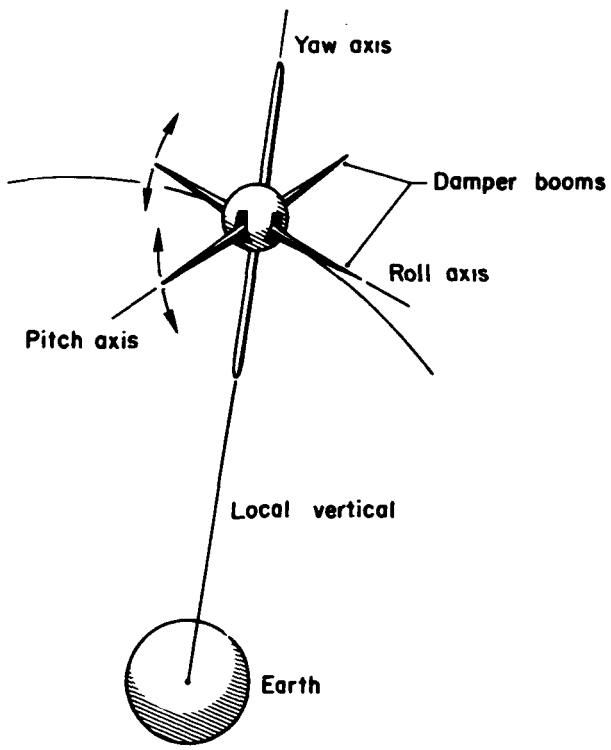

The lengths of the booms along the yaw, pitch and roll axes are chosen so that the magnitude of the moments of inertia have the required order. In addition, the booms along the roll and pitch axes are viscously spring coupled to the body so that disturbances will cause relative motion and will thus dissipate energy.

The specific concept considered in this Memorandum is due to Bruce E. Tinling and Vernon K. Merrick[8] of the Ames Research Center, Moffett Field, California.* It is a variation of the Vertistat, employing only one damping rod or boom which moves relative to the body.

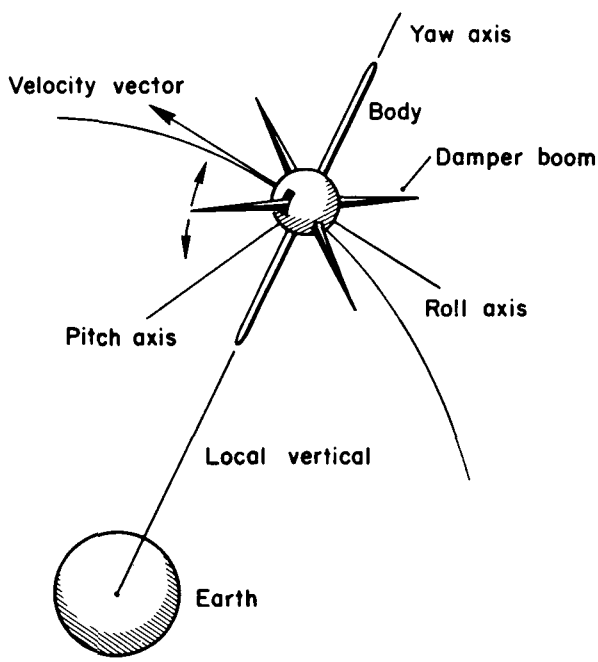

The mass distribution of the damper-rod, combined with the mass distribution of the fixed rods and the body, is such that the principal axes are along the pitch, yaw and roll axes as shown in the sketch.

*A similar approach has been analysed in unpublished work by the General Electric Company, Valley Forge, Pennsylvania.

Thus the damper-rod, under equilibrium conditions, lies in the horizontal plane at an angle with respect to the orbital plane. Due to the gyroscopic terms in the rotational equations of motion, the pitch, roll and yaw equations are coupled even for small oscillations. As a consequence, damping the relative angular rate between the damper-rod and the body also damps the pitch, roll and yaw modes. (See Appendix A.)

The system parameters which are utilized in this study have been selected on the basis of a linearized analysis of the rotational equations of motion.[8] The purpose of this study is to examine the rotational motion of a satellite which uses the Ames damping scheme when the complete nonlinear equations of motion are considered.

II. BASIC ASSUMPTIONS AND DEFINITIONS

The primary force acting on the center-of-mass of the satellite is derived from an inverse-square gravitational field. All other forces are either neglected, or else they are treated as small perturbations. Thus, for example, the influence of the earth's oblateness upon the center-of-mass motion can be included, approximately, if desired. Those force terms which arise as functions of body attitude about the center-of-mass are neglected.[13,14]

The primary external moments-of-force, or torques, which act about the body center-of-mass are those due to the gradient of the inverse-square gravitational field. Provision is also made for the inclusion of external disturbing torques of arbitrary magnitude and frequency. Gradient torques due to the higher-order harmonics of the earth's gravitational field and those due to gravitational fields external to the earth are neglected.

The coordinate systems which are used to describe the orbital motion of the vehicle are shown in Fig. 1.

A set of inertial axes, X_I, Y_I, Z_I, are located at the center of the earth. The nominal orbital plane is fixed with respect to the X Y Z coordinates and inclined at an angle i_o with respect to the X Y plane. If the earth's oblateness is included as an orbital disturbance, the X Y Z axes rotate about Z_I through ψ, the regression angle. The spherical coordinates r, θ, and γ serve to establish the location of the center-of-mass of the vehicle with respect to the nominal orbital plane.

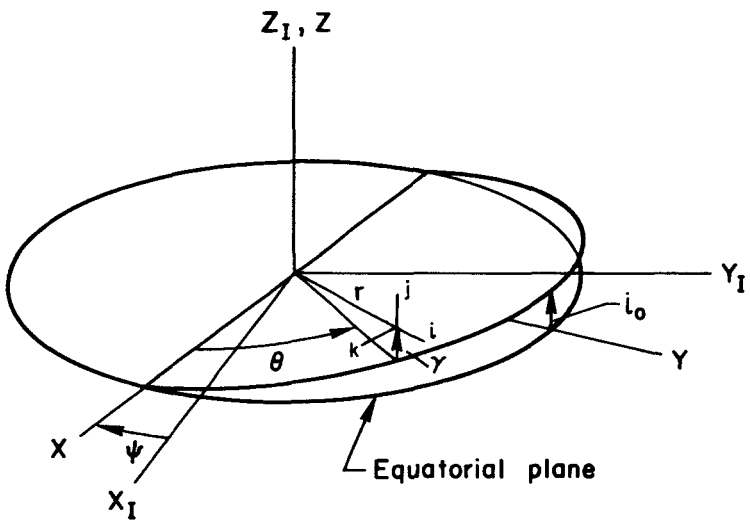

Fig. 1—Inertial and orbital coordinates

Another set of axes, i j k, located at the center-of-mass, are used in relating the attitude of the body to the gravitational field. The i axis is along r, the k axis is parallel to the nominal orbital plane and perpendicular to r, while j is perpendicular to i and k, forming a right-handed system. This set of axes will be called the local horizontal axis system, although this is strictly true only for a spherical earth. Figure 2 shows the relationship between the satellite and the local horizontal axes.

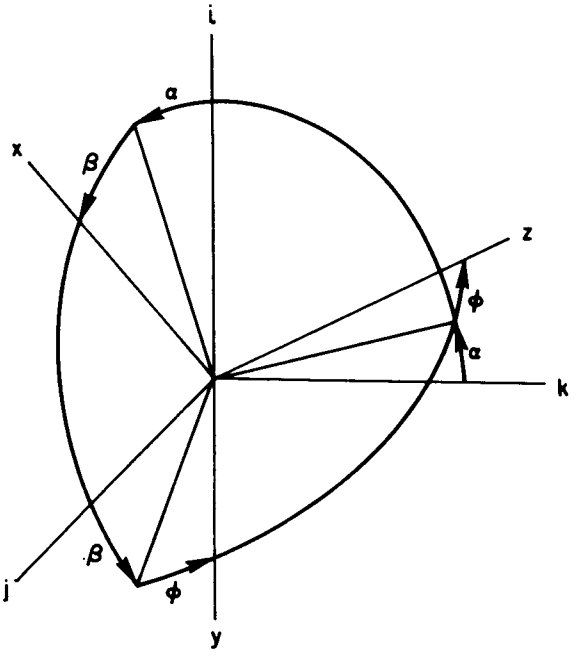

Fig. 2—Relationship between local horizontal axes and body principal axes

The x y z set of coordinates are the central principal axes of the body. In Fig. 2, α is a positive rotation about j (pitch), β is a positive rotation about the intermediate z axis (roll), and φ is a positive rotation about the x axis (yaw).

To introduce damping, another body called the damper-rod, is coupled with the primary body or satellite so that their relative motion dissipates energy. By making the centers-of-mass of the two bodies coincident, only one set of translational equations is required. Thus the coordinate systems and parameters defined in Fig. 1 pertain to both bodies.

Figure 3 shows the relationship of the damper-rod with respect to the vehicle's central principal axes.

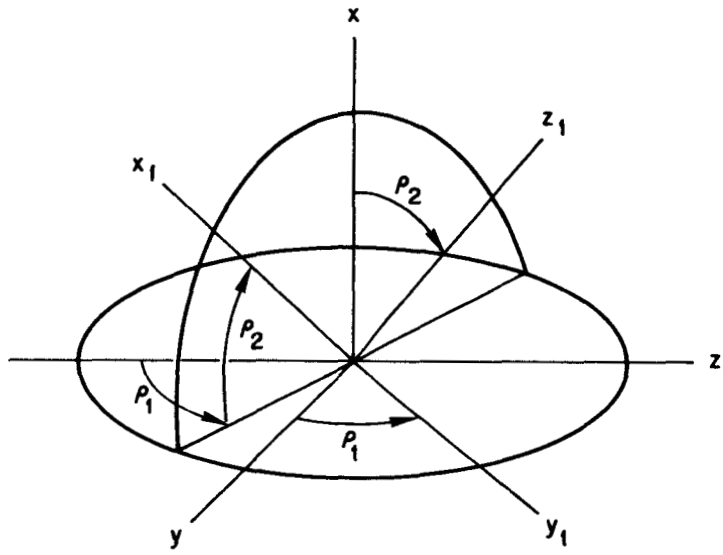

Fig. 3— Damper-rod, body axes geometry

In Fig. 3, the central principal axes of the damper-rod are designated by the subscript 1. The damper-rod has one rotational degree-of-freedom, ρ_2, with respect to the primary body, and the axis of rotation, y_1, is constrained to remain at an angle, ρ_1, in the y z plane.

In order to specify the attitude of the damper-rod with respect to the local horizontal coordinates, a set of angles, α_1, β_1, φ_1, analogous to α, β, φ shown in Fig. 2, are introduced.

It is convenient to define another set of principal axes, x_p, y_p and z_p. These are the instantaneous central principal axes of the body and damper-rod combined. Under ideal equilibrium conditions, x_p is along i, y_p is along j and z_p is along k.

III. COMPUTATIONAL RESULTS

Under ideal equilibrium conditions, the damper-rod would lie in the y z plane of the body, which in turn is coincident with the local-horizontal plane.* (See Figs. 2,3.) Due to the gyroscopic torques which act on the rod and, in turn, are applied to the body, the y axis is displaced from j by a steady-state angle, φ_{ss}. Since dynamically there is no distinction between x along i or minus i or between y along j or minus j, there are four orientations of the satellite which are nominally stable. The values of φ_{ss} and the other orientation angles for which stable motion is possible are dependent on the specific design. Table 1 lists the various damper-rod, body parameters which have been utilized in this study. (See Appendix A.)

Table 1

DESIGN PARAMETERS

Inertia Ratios	Damper-rod Parameters
$(I_y/I_z) = 1.12$	$(c_1/I_{dr}) = 1.545 \times 10^{-3}$ rad/sec
$(I_x/I_z) = 0.12$	$(c_2/I_{dr}) = 4.538 \times 10^{-6}$ (rad/sec)^2
$(I_{dr}/I_x) = 0.666$	$\rho_1 = 1.0929$ rad
$(I_{dr}/I_z) = 0.08$	

Also it is assumed that the magnitude of ρ_2 is physically limited to some maximum value, $|\rho_L|$. See Fig. 3 and Appendix A.

For the conditions of Table 1, the four stable orientations are:

*Ideal conditions imply a circular orbit and no external disturbing forces or torques.

1) $\alpha_{ss} = \beta_{ss} = \rho_2 = 0$; $\varphi_{ss} = -0.3622$ or 5.921 rad

2) $\alpha_{ss} = \beta_{ss} = \rho_2 = 0$; $\varphi_{ss} = -3.5038$ or 2.7794 rad

3) $\alpha_{ss} = \pm \pi$ rad ; $\beta_{ss} = \rho_2 = 0$; $\varphi_{ss} = 0.3622$ or -5.921 rad

4) $\alpha_{ss} = \pm \pi$ rad ; $\beta_{ss} = \rho_2 = 0$; $\varphi_{ss} = 3.5038$ or -2.7794 rad

In Case 1, the vehicle is right side up and by definition oriented properly. Case 2 represents a vehicle right side up but moving backwards. Cases 3 and 4 correspond to 1 and 2 respectively except that the vehicle is upside down.

As a matter of convenience Case 1 has been selected as the standard vehicle orientation, and thus represents perfect three-axis attitude control. For these ideal conditions, the body angular rates are

$$\omega_x = 0$$

$$\omega_y = \dot{\theta}_c \cos \varphi_{ss}$$

$$\omega_z = -\dot{\theta}_c \sin \varphi_{ss}$$

where $\dot{\theta}_c$ is the constant orbital angular rate.

The design parameters, c_1, c_2, etc., have been chosen such that the time required to damp small disturbances is the same about each axis. The purpose of this study is to examine the response of the design to large initial disturbances, and to determine the steady-state angular motion under external forcing. (See Figs. 4-32, Appendix E.)

INITIAL ANGLE ERRORS

An obvious type of initial condition error that might occur is

for $\alpha(0)$, $\beta(0)$ and $\varphi(0)$ to be, singly or in combination, different from the required steady-state values. For small initial attitude errors the linearized and nonlinear results are in good agreement.* (See Fig. 4.) When large angle errors are considered, the nonlinear response deviates from the linear results. Of course, if limiting occurs the difference between the two solutions can be very great. (See Figs. 5,6.)

The response due to initial angle errors damps to essentially zero in three to five orbits if limiting does not occur. This is true for errors as large as 45°. (See Fig. 7.) When limiting is involved the time to damp is dependent on the specific initial angle errors present. (See Figs. 8 and 9.) For $\rho_L \pm 30^{\circ}$ limiting occurs for initial error angles of 20° or greater.

Another point that should be noted from Figs. 8 and 9 is that it is very possible for the vehicle to stabilize in a backward position. Whether or not this is of importance depends upon the particular mission.

In any case if the limiting value of ρ_2 is $\pm 30^{\circ}$ or greater, the time to damp the response due to initial angle errors is from three to six orbitals periods.

INITIAL ANGULAR RATE ERRORS

There will almost certainly be angular rate errors at the initiation of the stabilization process. The manner in which the angular rate error is distributed between x_p y_p and z_p depends to a great extent

*The linear solutions were supplied by B. E. Tinling, Ames Research Center, private communication.

on the details of the orbital injection procedure.

If the final-stage vehicle is spin-stabilized, then a residual value of $\omega_{xp}(o)$ can be expected. At the same time the x_p axis is inertially stable so that, ideally, $\omega_{yp}(o)$ and $\omega_{zp}(o)$ are zero. Figure 10 shows the attitude response of the vehicle as a function of time when the only initial error is $\omega_{xp}(o)$. Again with the exception of the yaw motion, the disturbances are well damped within three to five orbits. Initial errors in pitch attitude in conjunction with $\omega_{xp}(o)$ do not substantially alter the time to damp. (See Figs. 11-12.)

Another case of interest is if the vehicle has a residual angular rate error about an axis perpendicular to the orbital plane.* Due to the gradient restoring torques the body will rotate with respect to the local vertical only if the initial pitch angular rate exceeds a certain value. (See Appendix C.) For positive pitch rates this value is approximately $2.75\ \dot{\theta}_c$, where $\dot{\theta}_c$ is the orbital angular rate. For negative pitch rates the minimum value is approximately $-0.75\ \dot{\theta}_c$. Thus for the range of pitch rates less than $2.75\ \dot{\theta}_c$ and greater than $-0.75\ \dot{\theta}_c$ the vehicle will oscillate and not rotate with respect to the local vertical. Under these conditions the oscillations of the vehicle damp in about five orbits. (See Figs. 13-14.) When the pitch rate is increased (or decreased) until tumbling occurs, the time required to damp the motion changes markedly. For example, if the pitch angular rate is increased from $2.5\ \dot{\theta}_c$ to $3\ \dot{\theta}_c$ the time to damp increases from about five orbital periods to approximately 15 orbital periods. (See Fig. 15.)

*This axis is the nominal pitch axis, y_p, of the damper-rod, body combination.

For the first ten orbits the body rotates with respect to the local vertical and then begins to oscillate. This behavior can be explained as follows: With the vehicle rotating about the pitch axis the gradient torque acting on the damper-rod tends to be averaged to zero. Thus, after the transient phase, ρ_2 is small in amplitude and the removal of energy is slow. Limiting has very little influence on the damping time, as can be seen from Fig. 16, which is a repeat of the previous case, but without limits. The same sort of behavior occurs for negative pitch rates. (See Fig. 17.) In this case even the transient motion of the damper-rod is small, so that the damping rate is very slow. The vehicle does not stop tumbling until approximately 30 orbital periods have elapsed!

If the initial value of the pitch angular rate is increased to $4\dot{\theta}_c$, the number of orbits that are completed before tumbling stops is 24, when there are no limits on ρ_2. If ρ_2 is limited to $\pm 30^\circ$ the tumbling stops in approximately 34 orbits! The reason for this behavior is that as the initial pitch rate increases, another mode of motion is possible if there is a limit imposed upon the magnitude of ρ_2. The damper-rod, during the initial transient response, moves to the limit and subsequently does not depart very far from that limit. As a consequence there is very little relative motion and the damper-rod and body tend to rotate as a single unit. (See Appendix C.) As is indicated in Appendix C, the rod is held on the limit by the gyroscopic torque term in the equations of motion of the damper-rod. The same type of behavior as described above occurs if the initial pitch rate is $-4\dot{\theta}_c$.

The initial pitch rate required for continuous limiting is a function of the remaining initial conditions. If the damper-rod starts on a limit of $\pm 30^{\circ}$, the analysis of Appendix C indicates that an initial pitch rate of approximately $+4.1\ \dot{\theta}_c$ rad/sec or $-6.0\ \dot{\theta}_c$ rad/sec is sufficient to maintain continuous limiting. (See Figs. 18-19.) Of course ρ_2 would usually be zero, initially, rather than $\pm 30^{\circ}$. A number of runs have been made in the investigation of the conditions for continuous limiting. A typical result is a case in which the pitch rate is initially $5\dot{\theta}_c$ rad/sec, all other conditions being standard. After 55 orbits the vehicle still tumbles and the damper-rod practically never leaves the limit.

The analysis of Appendix C indicates that, when the damper-rod is initially on the limit, there is a value of $|\rho_L|$, between 0° and 90°, for which the required initial pitch rate for continuous limiting is a minimum. As $|\rho_L|$ approaches either 0° or 90° the required initial pitch rate for continuous limiting approaches infinity.

FORCING DUE TO ORBITAL MOTION

Under idealized conditions the vehicle's center-of-mass is on a circular orbit about an earth which has an inverse-square gravitational field. In practice, the orbit is apt to be somewhat eccentric, and the earth's field is only approximately inverse-square in nature.

The magnitude of the orbital eccentricity is dependent upon the guidance accuracy associated with orbit injection. Since guidance accuracy is a function of the particular system involved, eccentricities of from 0.01 to 0.1 have been arbitrarily chosen for this study. Figures 20-21 show typical examples of the forced responses due to eccentricity.

One of the interesting features of Figs. 20-21 is the amplitude of the yaw response. It is obvious that the yaw mode is particularly susceptible to disturbances at orbital frequency.

Over the range of values, 0.01 to 0.07, the amplitudes of the various steady-state responses vary linearly with eccentricity.

The oblateness of the earth causes by far the most important deviation from an inverse-square gravitational field. Insofar as body attitude is concerned, the major influence of oblateness is the forcing due to the regression of the orbital plane. (See Appendix B.) Figures 22-23 show the influence of oblateness with and without eccentricity. A comparison of Figs. 20 and 23 gives an indication of the small effect of oblateness. Furthermore, the runs that are presented in Figs. 20 and 23 are for an orbit altitude of 625 miles. Since, relative to the inverse-square force, the magnitude of the oblateness term diminishes by the additional factor, $(r_E/r_c)^2$, its effect is quite negligible for higher orbits.

FORCING DUE TO EXTERNAL DISTURBING TORQUES

Up to this point the vehicle attitude response to the various disturbances considered has been independent of the orbital altitude.* Thus Figs. 4-21 are valid for a given vehicle for near-earth to synchronous orbits with only the time per orbit varying. However, when disturbances external to the satellite and its motion are considered, the relative magnitudes of the gradient-restoring torques and other sources of torque must be compared on an absolute basis.

*The one exception is the earth's oblateness which has decreasing influence with increasing altitude.

As an indication of the variation in the magnitude of the gradient torques let us examine the influence of the following constant disturbing torque:

$$M_D = I_{yp} \times 10^{-7}$$

where I_{yp} is the principal moment-of-inertia about the pitch axis of the damper-rod, body combination. Such a disturbance torque produces a steady-state error in pitch of approximately 2.6^o, if the orbit altitude is 625 miles. (See Fig. 24.) The same vehicle subjected to the same torque at synchronous altitude would tumble about the pitch axis! To achieve the same error angle at synchronous altitude would require I_{yp} to be increased as follows:*

$$(I_{yp})_{sync.} = \frac{(\dot{\theta}_c^2)_{ref.}}{(\dot{\theta}_c^2)_{sync.}} (I_{yp})_{ref.} = 190(I_{yp})_{ref.}$$

Thus for Fig. 24 to be valid for synchronous orbits, the pitch moment of inertia must be 190 $(I_{yp})_{ref.}$ where the subscript ref. refers to the 625 mile reference orbit.

To be specific, let us consider the disturbance to be a force equal to 10^{-6} lb displaced from the center-of-mass by a distance of 1 ft. Thus for reference conditions I_{yp} is 10 slug-ft^2 and for synchronous orbits I_{yp} is 1900 slug-ft^2. All of the other inertias would scale according to the ratios of Table 1, where I_{yp}/I_z equals 1.15. Figures 25 and 26 show the attitude response when a disturbance torque of 10^{-6} lb-ft is applied first to the yaw axis of the vehicle, and then to the roll axis. An examination of Fig. 25 indicates that the satellite is

*I_{xp} and I_{zp} must be scaled in the same manner.

unstable in yaw, although the pitch and roll errors are reasonably small. Figure 26 shows that the steady-state responses to a constant roll torque of 10^{-6} lb-ft are small in amplitude, again with the exception of the yaw mode.

If the constant yaw-disturbing torque is reduced in magnitude from 10^{-6} to 10^{-7} lb-ft, the steady-state yaw angle response is approximately 0.1 radian. For pitch and roll disturbance torques, respectively, of 10^{-7} lb-ft, the steady-state pitch and roll responses are about 0.1 of those of Figs. 24 and 26.

Identical results to those of the preceding paragraph can be obtained with a 10^{-6} lb-ft disturbance if all of moments-of-inertia are increased by a factor of 10. Thus for synchronous orbits, I_{xp}, I_{yp} and I_{zp} must be increased to 3,300, 19,000 and 17,330 slug-ft, respectively.

Figures 27-29 show the vehicle attitude response for sinusoidal disturbances at orbital frequency about the pitch, yaw and roll axes, respectively. Figures 30-32 repeat Figs. 27-29 but at a frequency equal to twice orbital rate.

IV. CONCLUSIONS AND DISCUSSION

In the previous section, a representative selection of the digital computer results obtained to date has been presented. A large number of other cases has been investigated, including many different combinations of the various initial errors and/or disturbances. The conclusions drawn from all of the data concerning this specific passive stabilization concept can be summarized as follows:

1) The transient responses due to initial angle errors, singly or in combination, are rapidly damped, with three to five orbital periods being typical of the time required. (See Figs. 4,8,9.)

2) The transient responses due to initial angular rate errors are rapidly damped if the vehicle oscillates but does not rotate with respect to the local horizontal coordinates. Large yaw angular rates, e.g., five times orbital rate, will damp within five to six orbital periods, but comparable pitch angular rate errors may take 10 times as long to damp. (See Figs. 10,13,17.)

3) The magnitude of the responses due to orbital motion is a function of the eccentricity. The steady-state amplitude of the yaw response, which is the largest, is approximately $4e$ radians. (See Figs. 20-21.) The forcing due to orbital regression is negligible.

4) With respect to external disturbances the pitch and roll response have approximately the same steady-state magnitude for a given constant pitch or roll torque. The yaw response, however, is approximately 30 times larger for the same constant disturbance. The yaw mode is sensitive to sinusoidal disturbances at orbital frequency, while the roll mode is sensitive to sinusoidal disturbances at twice orbital frequency. (See Figs. 24-32.)

The basis on which the parameters of Table 1 were chosen was essentially an optimization of the transient response.[8] The time to damp was made as small as possible, and equal for the pitch, yaw and roll modes. (See Fig. 4.) Although the analytic approach of Merrick and Tinling was restricted to small angle and angular rate errors the results of the present study indicate that excellent transient responses can

be expected for large error angles and for relatively large initial rate errors.

It is doubtful that continuous limiting would be a real operational problem. To begin with it should not be too difficult to keep the pitch component of angular rate within $+4\dot{\theta}_c$ to $-6\dot{\theta}_c$. For pitch rates within this range, continuous limiting is not possible although the time to damp might be as long as 30 orbital periods. (See Fig. 17.) Also the limiting angle of $\pm 30^\circ$, which was a condition for most of the machine runs, could probably be increased to at least $\pm 60^\circ$ if necessary.*

One particular aspect of the transient response to large initial errors is that the vehicle can become stabilized in a backward or upside down position or both. The importance of the final attitude of the satellite depends to a great extent upon its particular mission. Thus, for a communication satellite, being backwards may be unimportant but being upside down could be disastrous. In the final analysis, considerations of this sort will determine the permissible limits on the initial attitude and attitude rate errors and thus the required sophistication of the orbit injection procedure.

The forced response due to orbital motion is small if the eccentricity is small. Thus for an e of 0.005, the steady-state yaw, pitch and roll amplitudes are 0.02, 0.01 and 0.002 radians, respectively. Unless very precise attitude control is required, the range of acceptable eccentricities is compatible with current injection guidance

*It is possible that soft limits, utilizing a nonlinear spring, might change the situation. This has been suggested in private conversations with D. Watson of Ames Research Center and R. Moyer of General Electric, Valley Forge, Pennsylvania.

capabilities.

When the influence of external disturbing torques is examined, the importance of the specific design and mission becomes evident. The following list is representative of the possible disturbing torques that can influence vehicle angular motion.

- Residual aerodynamic forces
- Magnetic and electric fields
- Solar radiation effects
- Micro-meteorite impact
- Uncompensated motion of internal mass
- Thrust line, center-of-mass deviations

Obviously the degree of importance of any one of the disturbance sources depends to a great extent on a specific vehicle design and the intended mission. Thus, aerodynamic effects would be of interest for only very low altitude orbits. Solar radiation pressure effects, on the other hand, become relatively more important at high orbit altitudes, since for a given vehicle the gradient-restoring torques decrease with increasing altitude.

As a concrete example, let us consider the stabilization requirements for a passive communication satellite operating in a 6000 mile orbit. If station keeping is not utilized, the requirements could readily be met by the Ames design concept. The transient response is more than adequate and the only problem that remains is to choose the moments of inertia so that the response to external disturbances is acceptable.

Of the possible external disturbances, solar radiation pressure effects would probably have the greatest potential for perturbing the

satellite. Since the yaw degree of freedom is the most sensitive to constant disturbing torques, overall performance will be adequate if the magnitudes of the moments of inertia are chosen to achieve a prescribed steady-state yaw response to the maximum yaw disturbance torque that could be expected.

In order to make this calculation, it is necessary to assume a configuration and certain physical properties for the satellite. (See Appendix D.) The main body of the satellite is an "X" formed by two rods with tip to tip lengths, L. The included angle has been selected to achieve the body inertia ratios of Table 1, p. 10.

Table 2 shows the yaw disturbance torques for various ratios of the yaw error to Δd (where Δd is the displacement of the center-of-pressure from the center-of-mass). To achieve these ratios the rods must have either the specified value of L or, if L is limited to 100 ft, the indicated mass, m, must be used to load the tips of the rods.

Table 2

STEADY-STATE YAW ERROR DUE TO RADIATION PRESSURE TORQUES
(6000 mile orbit)

$\delta\varphi_{ss}/\Delta d$ (rad/ft)	L (ft)	m (slugs)	I_{yp} (slug-ft^2)	$(M_D)_{xp}/\delta\varphi_{ss}$ (lb-ft/rad)
1	105	0	367	3.15×10^{-6}
1	100	~0	320	3×10^{-6}
0.1	332	0	11,700	9.96×10^{-5}
0.1	100	1.24	3,500	3×10^{-5}
0.01	1050	0	370,000	3.15×10^{-3}
0.01	100	13.5	35,000	3×10^{-4}

The first row of Table 2 indicates that if $\delta\varphi_{ss}$ is 0.1 rad, then a Δd of 0.1 ft will require rod lengths of 105 ft. If the Δd is 1 ft, then to achieve a $\delta\varphi_{ss}$ of 0.1 rad requires rods 332 ft long or, alternately, 100 ft rods loaded at the tips with 1.24 slugs, i.e., about 40 lb. If the longer rods are used, with m = 0, then the pitch moment of inertia is 11,700 slug ft^2, and the disturbing torque due to radiation pressure is approximately 10^{-5} lb-ft. With tip loading, shorter rods may be used thus reducing the radiation pressure torques and as a consequence I_{yp} for a given yaw error.

With no loading of the tips, the rod lengths vary from about 100 to 1000 ft. Although rods 300 to 1000 ft in overall length are quite feasible, the thermal bending of the longer rods is a serious problem.[7,12] By restricting the overall length of the rods to 100 ft the bending problem can be alleviated, so that a Δd of 1 ft or less should be possible. Thus the fourth line of Table 2, with tip loading, indicates the more feasible design.

If a synchronous communication satellite is desired, the yaw stabilization problem is much more severe. With overall rod lengths restricted to 100 ft, the radiation pressure torque from Table 2 is 3×10^{-6} lb-ft, independent of orbit altitude. However, synchronous orbits would most likely be confined to the earth's equatorial plane, resulting in a reduction of the above number to approximately 1.2×10^{-6} lb-ft. With a disturbance of this magnitude, and with $\delta\varphi_{ss}/\Delta d$ equal to 0.1, the required mass for loading is 10.05 slugs, or over 320 lb!

Furthermore, station-keeping would probably be required, introducing another source of disturbance.[15] Unless thrust levels are limited to 10^{-5} to 10^{-6} lb, yaw instability could be a serious problem.

The lack of stiffness about the yaw axis, due to the particular parameters of Table 1, leads to large weight penalties for the synchronous case. Thus it would appear to be desirable to alter the inertia ratios of Table 1 so that the yaw response is improved. For small constant disturbances, the steady-state yaw, pitch and roll angles are

$$\delta\varphi_{ss} = \frac{(M_D)_{xp}}{\dot{\theta}_c^2 (I_{yp} - I_{zp})}$$

$$\delta\alpha_{ss} = \frac{(M_D)_{yp}}{3\dot{\theta}_c^2 (I_{zp} - I_{xp})}$$

$$\delta\beta_{ss} = \frac{(M_D)_{zp}}{4\dot{\theta}_c^2 (I_{yp} - I_{xp})}$$

If the pitch and yaw errors are arbitrarily set equal, then for equal disturbing torques $I_{yp} = 4\, I_{zp} - 3\, I_{xp}$

and

$$\delta\beta_{ss} = \frac{3}{16}\,\delta\alpha_{ss} = \frac{3}{16}\,\delta\varphi_{ss}$$

Thus if the pitch and yaw errors are satisfactory the roll response is more than adequate, for the same disturbance.

For the above conditions, the limiting inertia ratios which are physically possible are (I_{yp}/I_{zp}) equal to 1.75 and (I_{xp}/I_{zp}) equal to 0.75. However these ratios correspond to a planar mass distribution

and thus would not permit the damper-rod to be skewed with respect to the body. By shifting the ratios such that (I_{yp}/I_{zp}) equals 1.666 and (I_{xp}/I_{zp}) equals 0.778, a three-dimensional mass distribution is assured and thus one rod can still damp all three rotational modes.

With this particular set of inertia ratios the pitch moment of inertia required for synchronous orbits, with the same $(M_D)_{xp}/\delta\varphi_{ss}$ as before, is 5680 slug-ft^2. The mass required for loading the tips of the 100 ft rods is now approximately 2.15 slugs or 70 lb.

Although the response to constant yaw torques has been markedly improved, the transient response has undoubtedly been degraded. The preceding example merely demonstrates one possible trade-off between the transient and forced responses. For many applications large yaw errors are of little importance. However if station keeping is required, then three-axis stabilization is necessary.

Appendix A

THE ROTATIONAL EQUATIONS OF MOTION

In terms of the principal axes, Euler's equations of motion for the body are:

$$\dot{\omega}_x - \omega_y \omega_z R_x = \left(\frac{M_x}{I_x}\right)_G + \left(\frac{M_x}{I_x}\right)_{dr} + \left(\frac{M_x}{I_x}\right)_D \qquad (a)$$

$$\dot{\omega}_y - \omega_z \omega_x R_y = \left(\frac{M_y}{I_y}\right)_G + \left(\frac{M_y}{I_y}\right)_{dr} + \left(\frac{M_y}{I_y}\right)_D \qquad (b) \quad (1)$$

$$\dot{\omega}_z - \omega_x \omega_y R_z = \left(\frac{M_z}{I_z}\right)_G + \left(\frac{M_z}{I_z}\right)_{dr} + \left(\frac{M_z}{I_z}\right)_D \qquad (c)$$

The equations pertaining to the damper-rod can be written in the same manner.

$$\dot{\omega}_{x1} - \omega_{y1} \omega_{z1} R_{x1} = \left(\frac{M_{x1}}{I_{x1}}\right)_G + \left(\frac{M_{x1}}{I_{x1}}\right)_b + \left(\frac{M_{x1}}{I_{x1}}\right)_D \qquad (a)$$

$$\dot{\omega}_{y1} - \omega_{z1} \omega_{x1} R_{y1} = \left(\frac{M_{y1}}{I_{y1}}\right)_G + \left(\frac{M_{y1}}{I_{y1}}\right)_b + \left(\frac{M_{y1}}{I_{y1}}\right)_D \qquad (b) \quad (2)$$

$$\dot{\omega}_{z1} - \omega_{x1} \omega_{y1} R_{z1} = \left(\frac{M_{z1}}{I_{z1}}\right)_G + \left(\frac{M_{z1}}{I_{z1}}\right)_b + \left(\frac{M_{z1}}{I_{z1}}\right)_D \qquad (c)$$

In Eqs. (1,a-c), the torques which act about the x y z axes are M_x, M_y, and M_z, respectively. The subscript G refers to torques arising from the gravitational gradient; dr refers to those torques applied to the body by the damper-rod, and D refers to arbitrary disturbing torques. The variables ω_x, ω_y, ω_z are the components of the bodies' instantaneous angular velocity with respect to inertial space. Finally the moment-of-inertia ratios are defined as follows:

$$R_x = (I_y - I_z) / I_x \qquad (a)$$

$$R_y = (I_z - I_x) / I_y \qquad (b) \quad (3)$$

$$R_z = (I_x - I_y) / I_z \qquad (c)$$

The same definitions apply to the corresponding terms of Eqs. (2,a-c), with the exception that the subscript dr is replaced by b, indicating torques acting on the damper-rod due to the body.

At this point it is convenient to introduce the fact that the rod is constrained to rotate about the y_1 axis. Thus, from Fig. 3

$$\omega_{x1} = (\omega_y \sin \rho_1 - \omega_z \cos \rho_1) \cos \rho_2 + \omega_x \sin \rho_2 \qquad (a)$$

$$\omega_{y1} = - \dot{\rho}_2 + \omega_y \cos \rho_1 + \omega_z \sin \rho_1 \qquad (b) \quad (4)$$

$$\omega_{z1} = \omega_x \cos \rho_2 - (\omega_y \sin \rho_1 - \omega_z \cos \rho_1) \sin \rho_2 \qquad (c)$$

By introducing Eqs. (4a) and (4c) into Eqs. (2a) and (2c), respectively, the constraint torques, $(M_{x1})_b$ and $(M_{z1})_b$ can be expressed in terms of the gradient torques acting on the rod, the angular motion of the body, and the angle ρ_2. The form of $(M_{y1})_b$ depends upon the manner in which the body and damper-rod are coupled together. If a linear spring-dashpot mechanism is used, then the torque about y_1, due to the body is

$$\left(M_{y1}\right)_b = c_2 \rho_2 + c_1 \dot{\rho}_2 \qquad (5)$$

The reaction torques, due to the damper-rod, which act on the body are, from Fig. 3

$$(M_x)_{dr} = - (M_{x1})_b \sin \rho_2 - (M_{z1})_b \cos \rho_2 \qquad (a) \quad (6)$$

$$(M_y)_{dr} = -(c_2 \rho_2 + c_1 \dot{\rho}_2) \cos \rho_1 + (M_{z1})_b \sin \rho_2 \sin \rho_1$$

$$- (M_{x1})_b \cos \rho_2 \sin \rho_1 \qquad (b)$$

$$(M_z)_{dr} = -(M_{z1})_b \sin \rho_2 \cos \rho_1 + (M_{x1})_b \cos \rho_2 \cos \rho_1 \qquad (6)$$

$$- (c_2 \rho_2 + c_1 \dot{\rho}_2) \sin \rho_1 \qquad (c)$$

The substitution of Eqs. (6,a-c) into Eqs. (1,a-c) yields another set of expressions for the unknown constraint torques, $(M_{x1})_b$ and $(M_{z1})_b$. By eliminating $\dot{\omega}_x$, $\dot{\omega}_y$, and $\dot{\omega}_z$ between the two sets of constraint torque equations, $(M_{x1})_b$ and $(M_{z1})_b$ can each be expressed in terms of the variables ω_x , ω_y , ω_z , $\dot{\rho}_2$, α , β , φ , and ρ_2. Thus, these two equations of constraint replace Eqs. (2,a) and (2,c).

In the design under study, the damper-rod has a negligible moment-of-inertia about x_1, as compared to those moments about y_1, z_1, or any of the body axes. The damper-rod is also symmetric about x_1, thus

$$I_{x1} \cong 0 \qquad (a)$$

$$(7)$$

$$I_{y1} = I_{z1} = I_{dr} \qquad (b)$$

Under these conditions Eq. (2a) does not exist, and the only constraint torque that can act is $(M_{z1})_b$.* As a result of the simplifying assumption of Eqs. (7,a-b) the equations pertaining to the damper-rod

*This is true unless $|\rho_2|$ is limited to some maximum value. If such is the case, a constraint torque about y_1 can exist.

motion are

$$\dot{\omega}_{y1} - \omega_{z1}\,\omega_{x1} = \left(\frac{M_{y1}}{I_{dr}}\right)_G + \frac{c_2}{I_{dr}}\,\rho_2 + \frac{c_1}{I_{dr}}\,\dot{\rho}_2 \qquad \text{(a) (8)}$$

$$\left(\frac{M_{z1}}{I_{dr}}\right)_b = \frac{1}{1+\Delta_1}\Bigg\{ \omega_y\,\omega_z\,R_x\cos\rho_2 - \omega_z\,\omega_x\,R_y\sin\rho_1\sin\rho_2$$

$$+ \omega_x\,\omega_y\,R_z\cos\rho_1\sin\rho_2 + \omega_{x1}\,\omega_{y1}$$

$$+ \frac{c_1}{I_{dr}}\,\dot{\rho}_2\left(\frac{I_{dr}}{I_y} - \frac{I_{dr}}{I_z}\right)\sin\rho_1\cos\rho_1\sin\rho_2 \qquad \text{(b)}$$

$$- \dot{\rho}_2\,(\omega_x\sin\rho_2 + \omega_y\sin\rho_1\cos\rho_2 - \omega_z\cos\rho_1\cos\rho_2)$$

$$+ \frac{c_2}{I_{dr}}\,\rho_2\left(\frac{I_{dr}}{I_y} - \frac{I_{dr}}{I_z}\right)\sin\rho_1\cos\rho_1\sin\rho_2 + \left(\frac{M_x}{I_x}\right)_G\cos\rho_2$$

$$- \left(\frac{M_y}{I_y}\right)_G\sin\rho_1\sin\rho_2 + \left(\frac{M_z}{I_z}\right)_G\cos\rho_1\sin\rho_2 - \left(\frac{M_{z1}}{I_{dr}}\right)_G$$

$$+ \left(\frac{M_x}{I_x}\right)_D\cos\rho_2 - \left(\frac{M_y}{I_y}\right)_D\sin\rho_1\sin\rho_2 + \left(\frac{M_z}{I_z}\right)_D\cos\rho_1\sin\rho_2$$

$$- \left(\frac{M_{z1}}{I_{dr}}\right)_D\Bigg\}$$

where

$$\Delta_1 = \frac{I_{dr}}{I_x}\cos^2\rho_2 + \frac{I_{dr}}{I_y}\sin^2\rho_2\sin^2\rho_1 + \frac{I_{dr}}{I_z}\sin^2\rho_2\cos^2\rho_1$$

In a previous RAND Memorandum, expressions have been derived for the gravitational gradient torques which act upon a rigid body with an arbitrary mass distribution.[13] Utilizing the notation of this Memorandum the gradient torques in Eqs. (1,a-c) and Eqs. (8,a-b) have the following form:

$$(M_x)_G = -\frac{3g_o r_E^2}{r^3} I_x R_x a_z a_y \qquad (a)$$

$$(M_y)_G = -\frac{3g_o r_E^2}{r^3} I_y R_y a_x a_z \qquad (b)$$

$$(M_z)_G = -\frac{3g_o r_E^2}{r^3} I_z R_z a_y a_x \qquad (c) \quad (9)$$

$$(M_{y1})_G = -\frac{3g_o r_E^2}{r^3} I_{dr} a_{x1} a_{z1} \qquad (d)$$

$$(M_{z1})_G = \frac{3g_o r_E^2}{r^3} I_{dr} a_{y1} a_{x1} \qquad (e)$$

where

$$a_x = \cos\alpha \cos\beta$$

$$a_y = \sin\alpha \sin\varphi - \cos\alpha \sin\beta \cos\varphi$$

$$a_z = \sin\alpha \cos\varphi + \cos\alpha \sin\beta \sin\varphi$$

The parameters a_{x1}, a_{y1}, and a_{z1} can be defined in terms of α, β, φ, ρ_1 and ρ_2. Considering Figs. 2 and 3 the following relationships can be deduced

$$\cos\alpha_1 \cos\beta_1 = \sin\rho_2 \cos\beta \cos\alpha - \cos\rho_2 \cos(\rho_1 + \varphi) \sin\alpha$$

$$- \cos\rho_2 \sin(\rho_1 + \varphi) \sin\beta \cos\alpha \qquad (a) \quad (10)$$

$$\sin\alpha_1 \sin\varphi_1 - \cos\alpha_1 \sin\beta_1 \cos\varphi_1 = \sin(\rho_1 + \varphi)\sin\alpha$$

$$- \cos(\rho_1 + \varphi)\sin\beta\cos\alpha \qquad \text{(b) (10)}$$

$$\sin\alpha_1 \cos\varphi_1 + \cos\alpha_1 \sin\beta_1 \sin\varphi_1 = \cos\rho_2 \cos\alpha\cos\beta$$

$$+ \sin\rho_2 \sin\alpha \cos(\rho_1 + \varphi) + \sin\rho_2 \cos\alpha \sin\beta \sin(\rho_1 + \varphi) \qquad \text{(c)}$$

Finally the relationship between the rates of change of the orientation angles and the body angular rates must be obtained. The angular velocity of the local horizontal coordinates with respect to the inertial axes can be determined from Fig. 1.

$$\omega_i = \dot{\theta}\sin\gamma - \dot{\psi}(\cos i_o \sin\gamma + \sin i_o \sin\theta\cos\gamma) \qquad \text{(a)}$$

$$\omega_j = \dot{\theta}\cos\gamma + \dot{\psi}(\sin i_o \sin\theta\sin\gamma - \cos i_o \cos\gamma) \qquad \text{(b) (11)}$$

$$\omega_k = \dot{\gamma} + \dot{\psi}\sin i_o \cos\theta \qquad \text{(c)}$$

The body angular rates, projected into the i j k axes, are

$$\omega_{bi} = \omega_x \cos\alpha\cos\beta + \omega_y(\sin\alpha\sin\varphi - \cos\alpha\cos\varphi\sin\beta)$$

$$+ \omega_z(\sin\alpha\cos\varphi + \cos\alpha\sin\varphi\sin\beta) \qquad \text{(a)}$$

$$\omega_{bj} = \omega_x \sin\beta + \omega_y \cos\beta\cos\varphi - \omega_z \cos\beta\sin\varphi \qquad \text{(b) (12)}$$

$$\omega_{bk} = -\omega_x \sin\alpha\cos\beta + \omega_y(\cos\alpha\sin\varphi - \sin\alpha\sin\beta\cos\varphi)$$

$$+ \omega_z(\cos\alpha\cos\varphi - \sin\alpha\sin\beta\sin\varphi) \qquad \text{(c)}$$

Since the vector sum of ω_{bi}, ω_{bj} and ω_{bk} is the total angular velocity of the body as seen in the local horizontal coordinates, the following

relationships must hold. (See Fig. 2.)

$$\omega_{bi} = \omega_i + \dot{\varphi} \cos\alpha \cos\beta + \dot{\beta} \sin\alpha \qquad \text{(a)}$$

$$\omega_{bj} = \omega_j + \dot{\alpha} + \dot{\varphi} \sin\beta \qquad \text{(b)} \quad (13)$$

$$\omega_{bk} = \omega_k + \dot{\beta} \cos\alpha - \dot{\varphi} \cos\beta \sin\alpha \qquad \text{(c)}$$

From Eqs. (13,a-c), the rates-of-change of the body orientation angles are

$$\dot{\alpha} = \omega_{bj} - \omega_j - \tan\beta \left[(\omega_{bi} - \omega_i) \cos\alpha - (\omega_{bk} - \omega_k) \sin\alpha\right] \qquad \text{(a)}$$

$$\dot{\beta} = (\omega_{bi} - \omega_i) \sin\alpha + (\omega_{bk} - \omega_k) \cos\alpha \qquad \text{(b)} \quad (14)$$

$$\dot{\varphi} = \frac{1}{\cos\beta} \left[(\omega_{bi} - \omega_i) \cos\alpha - (\omega_{bk} - \omega_k) \sin\alpha\right] \qquad \text{(c)}$$

The rotational motion of the body, damper-rod combination is described by eight nonlinear, first-order differential equations, Eqs. (1,a-c), Eq. (4,b), Eq. (8,a), Eqs. (14,a-c), and by one constraint equation, Eq. (8,b). In these nine equations, the variables r, θ, γ and $\dot{\psi}$ arise from the orbital motion, and are known functions of time. (See Appendix B.) The influence of disturbing torques which are known functions of time can be studied by including the D terms.

In any practical design the possibility would exist that the maximum value of ρ_2 might be limited by the body structure. The actual interaction of the damper-rod with the structure is a very complicated affair. For the purposes of this study, a "hard" limit will be assumed. This means that the damper-rod and structure are completely inelastic. At the instant of impact, there is a discontinuous change in the angular rates of the rod and the body. However, the total

angular momentum of the rod and the body must be conserved. Since the orientation angles are continuous in value before and after contact, each component of angular momentum in body axes must be invariant. Thus

$$(I_x\ \omega_x + I_{dr}\ \omega_{z1}\ \cos\rho_2)_+ = (I_x\ \omega_x + I_{dr}\ \omega_{z1}\ \cos\rho_2)_- \qquad \text{(a)}$$

$$(I_y\ \omega_y - I_{dr}\ \omega_{z1}\ \sin\rho_2\ \sin\rho_1 + I_{dr}\ \omega_{y1}\ \cos\rho_1)_+ = \qquad \text{(b)} \quad (15)$$

$$(I_y\ \omega_y - I_{dr}\ \omega_{z1}\ \sin\rho_2\ \sin\rho_1 + I_{dr}\ \omega_{y1}\ \cos\rho_1)_-$$

$$(I_z\ \omega_z + I_{dr}\ \omega_{z1}\ \sin\rho_2\ \cos\rho_1 + I_{dr}\ \omega_{y1}\ \sin\rho_1)_+ = \qquad \text{(c)}$$

$$(I_z\ \omega_z + I_{dr}\ \omega_{z1}\ \sin\rho_2\ \cos\rho_1 + I_{dr}\ \omega_{y1}\ \sin\rho_1)_-$$

The subscript, +, indicates that the quantities in the bracket exist at an infinitesimal time after contact, while the subscript, -, refers to quantities which exist at an infinitesimal time prior to contact. At impact $\dot{\rho}_2$ is zero and therefore $\omega_{y1}(+)$ and $\omega_{z1}(+)$ are functions of $\omega_x(+)$, $\omega_y(+)$ and $\omega_z(+)$. Thus Eqs. (15,a-c) can be solved to obtain the body angular rates which exist at the instant after the rod and the body come into contact.

Once the new initial conditions have been found, it is necessary to determine whether or not the damper-rod stays on the limit or immediately drops away. From Fig. 3 it can be seen that if the body exerts a constraint torque, $(M_{y1})_b$, upon the rod, the sign of $(M_{y1})_b$ and of ρ_2 must be identical. Also, when $(M_{y1})_b$ exists as a constraint torque, the damper-rod, body combination behaves as single rigid body.

Thus the differential equation, Eq. (8,a) is replaced by an equation of constraint. Expressions for the two constraint torques, $(M_{zl})_b$ and $(M_{yl})_b$ can be found by following the procedure outlined previously in this Appendix.

$$\left(\frac{M_{zl}}{I_{dr}}\right)_b = \left(\frac{M_{zl}}{I_{dr}}\right)_{bo} - \left(\frac{M_{yl}}{I_{dr}}\right)_b \frac{\cos\rho_1 \sin\rho_1 \sin\rho_2 \left(\frac{I_{dr}}{I_z} - \frac{I_{dr}}{I_y}\right)}{(1 + \Delta_1)} \qquad (a)$$

$$\left(\frac{M_{yl}}{I_{dr}}\right)_b = -\frac{c_2}{I_{dr}}\rho_2 + \frac{1}{(1+\Delta_2)} \left\{ -\left(\frac{M_{zl}}{I_{dr}}\right)_b \sin\rho_1 \cos\rho_1 \sin\rho_2 \left(\frac{I_{dr}}{I_z} - \frac{I_{dr}}{I_y}\right) \right. \qquad (16)$$

$$\cos\rho_1\, \omega_x\, \omega_z\, R_y + \sin\rho_1\, \omega_x\, \omega_y\, R_z - \omega_{zl}\, \omega_{xl} \qquad (b)$$

$$+ \left(\frac{M_y}{I_y}\right)_G \cos\rho_1 + \left(\frac{M_z}{I_z}\right)_G \sin\rho_1 - \left(\frac{M_{yl}}{I_{dr}}\right)_G$$

$$\left. + \left(\frac{M_y}{I_y}\right)_D \cos\rho_1 + \left(\frac{M_z}{I_z}\right)_D \sin\rho_1 - \left(\frac{M_{yl}}{I_{dr}}\right)_D \right\}$$

where $\left(\frac{M_{zl}}{I_{dr}}\right)_{bo}$ is the expression for $\left(\frac{M_{zl}}{I_{dr}}\right)_b$ prior to the limit, given by Eq. (8,b), and where

$$\Delta_2 = \frac{I_{dr}}{I_y}\cos^2\rho_1 + \frac{I_{dr}}{I_z}\sin^2\rho_1$$

In Eqs. (16,a-b) $\dot{\rho}_2$ is zero and ρ_2 is a constant, corresponding to plus or minus the maximum permissible value of the angle.

Thus when the damper-rod and the body come into contact, the first step is to determine the new body angular rates from Eqs. (15,a-c).

Next Eqs. (16,a-b) are solved for $(M_{z1})_{b+}$ and $(M_{y1})_{b+}$. If $(M_{y1})_{b+}$ has the same sign as ρ_2, then Eqs. (1,a-c), Eqs. (14,a-d), and Eqs. (16,a-b) describe the combined body, damper-rod angular motion where

$$(M_x)_{dr} = - (M_{z1})_b \cos \rho_2 \qquad (a)$$

$$(M_y)_{dr} = - (M_{y1})_b \cos \rho_1 + (M_{z1})_b \sin \rho_1 \sin \rho_2 - c_2 \rho_2 \cos \rho_1 \qquad (b) \quad (17)$$

$$(M_z)_{dr} = - (M_{z1})_b \cos \rho_1 \sin \rho_2 - (M_{y1})_b \sin \rho_1 - c_2 \rho_2 \sin \rho_1 \qquad (c)$$

When the magnitude of $(M_{y1})_b$ goes to zero, the rod leaves the limit and Eqs. (1,a-c), Eqs. (6,a-c), Eq. (4,b), Eqs. (8,a-b) and Eqs. (14, a-c) prevail again. There is no discontinuity in the angular rates when limiting ends.

If the solution of Eqs. (16,a-c) yields a value for $(M_{y1})_{b+}$ of opposite sign to that of ρ_2, then the conditions immediately after contact are such that the rod and body separate. Under these circumstances the solutions of the equations of motion are obtained in the same manner as was done before the limit. The only effect of the contact between the damper-rod and the body is the discontinuous change in the angular rates.

Appendix B

THE TRANSLATIONAL EQUATIONS OF MOTION

The center-of-mass motion of the body, damper-rod combination is described by the variables, r, θ, γ and ψ. (See Fig. 1.) Since only three variables are required to specify the position of the vehicle, one of the above quantities is redundant. Expressed in the local horizontal coordinate system, the three translational equations of motion are

$$\ddot{r} - r(\omega_j^2 + \omega_k^2) = -\frac{g_o r_E^2}{r^2} + \frac{1.5 J_2 g_o r_E^4}{r^4}\left[3(\sin\gamma\cos i_o + \cos\gamma\sin\theta\sin i_o)^2 - 1\right] \quad (a)$$

$$r\dot{\omega}_j - r\omega_i\omega_k + 2\dot{r}\omega_j = -\frac{3J_2 g_o r_E^4}{r^4}\sin i_o\cos\theta(\sin\gamma\cos i_o + \cos\gamma\sin\theta\sin i_o) \quad (b) \quad (18)$$

$$r\dot{\omega}_k + r\omega_i\omega_j + 2\dot{r}\omega_k = -\frac{3J_2 g_o r_E^4}{r^4}(\cos i_o\cos\gamma - \sin i_o\sin\theta\sin\gamma)(\sin\gamma\cos i_o + \cos\gamma\sin i_o\sin\theta) \quad (c)$$

The parameter J_2 in Eqs. (18,a-c) is a non-dimensional constant of the order of 10^{-3}, and is a measure of the earth's oblateness. The angular rates, ω_i, ω_j and ω_k are defined by Eqs. (11,a-c).

If the earth were not oblate, the solutions of Eqs. (18,a-c) could readily be found, and would be the well-known relationships of Kepler.[16] The orbit, which is in general an ellipse, lies in a plane fixed in inertial space. Thus, the only variables required are θ and r, since

the orientation of the orbital plane with respect to the inertial axes is specified by the constants, i_o and Ψ_o. For the unperturbed case, Eqs. (18,a-c) reduce to the following:

$$\ddot{r} - r\dot{\theta}^2 + \frac{g_o r_E^2}{r^2} = 0 \qquad \text{(a)}$$

$$\ddot{\theta} + \frac{2\dot{r}}{r}\dot{\theta} = 0 \qquad \text{(b)} \qquad (19)$$

Equation (19,b) integrates once directly, and then with a little manipulation, r can be found as a function of θ.

$$r^2\dot{\theta} = C \qquad \text{(a)}$$

$$\frac{1}{r} = \frac{1}{r_c}\left[1 + e\cos(\theta - \epsilon)\right] \qquad \text{(b)} \qquad (20)$$

$$\dot{\theta} = \dot{\theta}_c\left[1 + e\cos(\theta-\epsilon)\right]^2 \qquad \text{(c)}$$

where e is the eccentricity, ϵ is the argument of perigee, and

$$\frac{1}{r_c} = \frac{g_o r_E^2}{C^2} \qquad \text{(a)}$$

$$\dot{\theta}_c = \frac{(g_o r_E^2)^2}{C^3} \qquad \text{(b)} \qquad (21)$$

The integration of Eq. (20,c) yields θ as a function of time.

When J_2 is included as a perturbing disturbance, the equations of motion are

$$\ddot{\delta r} - (\dot{\theta}^2 + \frac{2g_o r_E^2}{r^3})\,\delta r - 2r\dot{\theta}\,\delta\omega_j = \frac{1.5\,J_2\,g_o\,r_E^4}{r^4}(3\sin^2\theta\sin^2 i_o - 1) \qquad \text{(a)} \qquad (22)$$

$$\frac{1}{r}\frac{d}{dt}\left(r^2\,\delta\omega_j + 2r\,\dot{\theta}\,\delta r\right) = -\frac{1.5\,J_2\,g_o\,r_E^4}{r^4}\sin^2 i_o \sin 2\theta \qquad \text{(b)} \quad (22)$$

$$\frac{1}{r}\frac{d}{dt}\left(r^2\,\delta\omega_k\right) + r\dot{\theta}\,\delta\omega_i = -\frac{1.5\,J_2\,g_o\,r_E^4}{r^4}\sin 2i_o \sin\theta \qquad \text{(c)}$$

where

$$\delta\omega_i = \dot{\theta}\,\delta\gamma - \delta\dot{\psi}\sin i_o \sin\theta \qquad \text{(a)}$$

$$\delta\omega_j = \delta\dot{\theta} - \delta\dot{\psi}\cos i_o \qquad \text{(b)} \quad (23)$$

$$\delta\omega_k = \delta\dot{\gamma} + \delta\dot{\psi}\sin i_o \cos\theta \qquad \text{(c)}$$

The δ indicates that the term in question is a differential quantity. An examination of Eqs.(22,a-c) reveals that the first two equations are coupled and independent of the third.

Let us first consider Eqs. (22,a-b). Since r is known explicitly as a function of θ, it is convenient to change the independent variable from t to θ by means of Eq. (20,a). Equation (22,b) can be integrated once to yield an expression for $\delta\omega_j$.

$$\delta\omega_j = -2\frac{C}{r^2}\,\delta u + \frac{1}{r^2}\left[\delta C + \frac{1.5\,J_2\,g_o\,r_E^4}{r_c C}\sin^2 i_o\left(\frac{\cos 2\theta}{2} + \frac{e}{2}\cos\theta + \frac{e}{6}\cos 3\theta\right)\right] \qquad (24)$$

where δC is a constant of integration and

$$\delta u = \frac{\delta r}{r}$$

$$\epsilon = 0$$

By employing Eq. (24), $\delta\omega_j$ may be eliminated from Eq. (22,a)

$$\delta u'' + \left(\frac{1 + 4e\cos\theta}{1 + e\cos\theta}\right)\delta u = \frac{1.5\, J_2\, g_o\, r_E^4}{r_c C^2}\left[\frac{3}{2}\sin^2 i_o - 1 - \frac{\sin^2 i_o}{2}\cos 2\theta + \left(\frac{7}{4}\sin^2 i_o - 1\right)e\cos\theta - \frac{5e}{12}\sin^2 i_o \cos 3\theta\right] + \frac{2\delta C}{C} \tag{25}$$

where the prime notation indicates differentiation with respect to θ. Since the unperturbed solutions provide the necessary constants of integration, only a particular solution of Eq. (25) is required. Neglecting terms in e^2, a particular solution which satisfies Eq. (25) is

$$\delta u = \frac{1.5\, J_2\, g_o\, r_E^4}{r_c C^2}\left[\frac{1}{3}\left(\frac{3}{2}\sin^2 i_o - 1\right) + \frac{\sin^2 i_o}{6}\cos 2\theta + \frac{e\sin^2 i_o}{12}\cos 3\theta\right] \tag{26}$$

where

$$\frac{2\delta C}{C} = -\frac{J_2\, g_o\, r_E^4}{r_c C^2}\left(\frac{3}{2}\sin^2 i_o - 1\right) \tag{27}$$

The substitution of Eqs. (26), (27) and (23,b) into Eq. (24) yields

$$\delta\dot{\theta} = -\frac{C}{r_c^2}(1 + e\cos\theta)^2 \frac{1.5\, J_2\, g_o\, r_E^4}{r_c C^2}\left[\left(\frac{3}{2}\sin^2 i_o - 1\right) - \frac{e\sin^2 i_o}{2}\cos\theta - \frac{\sin^2 i_o}{6}\cos 2\theta\right] + \delta\dot{\psi}\cos i_o \tag{28}$$

We must now consider the solution of Eq. (22,c). Again using θ as the independent variable and utilizing Eqs. (23,a) and (23,c),

we find

$$\delta\gamma'' + \delta\gamma + \delta\psi'' \sin i_o \cos\theta - 2\,\delta\psi' \sin i_o \sin\theta =$$

$$-\frac{1.5\, J_2\, g_o\, r_E^4}{r_c C^2} \sin 2i_o \sin\theta\,(1 + e\cos\theta) \qquad (29)$$

Since there is one equation and two variables, one of the two variables may be specified. Thus

$$\delta\psi' = \frac{1.5\, J_2\, g_o\, r_E^4}{r_c C^2} \cos i_o \qquad \text{(a)}$$

$$\delta\psi'' = 0 \qquad \text{(b)} \qquad (30)$$

The substitution of Eqs. (30,a-b) into Eq. (29) yields

$$\delta\gamma'' + \delta\gamma = -\frac{1.5\, J_2\, g_o\, r_E^4}{2 r_c C^2} \sin 2i_o\, e \sin 2\theta \qquad (31)$$

An examination of Eqs. (30,a-b) and (31) indicates that without eccentricity, the out-of-plane motion is zero. It should be noted that Eq. (30,a) is <u>not</u> the standard definition of the orbital regression rate.[16] Thus

$$\dot{\delta\psi} = \frac{1.5\, J_2\, g_o\, r_E^4}{r_c^3 C} \cos i_o\,(1 + e\cos\theta)^2 \qquad \text{(a)}$$

$$\delta\gamma = \frac{1.5\, J_2\, g_o\, r_E^4}{6\, r_c C^2} \sin 2i_o\, e \sin 2\theta \qquad \text{(b)} \qquad (32)$$

By introducing Eq. (32,a) into Eq. (28) and simplifying, an expression for $\delta\dot{\theta}$ can be found.

$$\delta\dot{\theta} = -\frac{1.5\, J_2\, g_o\, r_E^4}{r_c^3 C}\,(1 + e\cos\theta)^2\left[\left(\frac{5}{2}\sin^2 i_o - 2\right)\right.$$

$$\left. -\frac{e\sin^2 i_o}{2}\cos\theta - \frac{\sin^2 i_o}{6}\cos 2\theta\right] \qquad (33)$$

The perturbed orbital variables as a function of θ are thus

$$r(\theta,J_2) = \frac{C_o^2}{g_o\, r_E^2\,(1 + e_o\cos\theta)} + \frac{1.5\, J_2\, r_E^2}{r_c\,(1 + e\cos\theta)}\left[\frac{1}{2}\sin^2 i_o - \frac{1}{3}\right.$$

$$\left. +\frac{\sin^2 i_o}{6}\cos 2\theta + \frac{e\sin^2 i_o}{12}\cos 3\theta\right] \qquad (a)$$

$$\dot{\theta}(\theta,J_2) = \frac{\left(g_o\, r_E^2\right)^2}{C_o^3}\,(1 + e_o\cos\theta)^2 + \frac{1.5\, J_2\, \dot{\theta}_c\, r_E^2}{r_c^2}\,(1 + e\cos\theta)^2\left[2\right.$$

$$\left. -\frac{5}{2}\sin^2 i_o + \frac{e\sin^2 i_o}{2}\cos\theta + \frac{\sin^2 i_o}{6}\cos 2\theta\right] \qquad (b) \quad (34)$$

$$\delta\gamma = \frac{1.5\, J_2\, r_E^2}{6 r_c^2}\, e\sin 2i_o\sin 2\theta \qquad (c)$$

$$\delta\dot{\psi} = \frac{1.5\, J_2\, \dot{\theta}_c\, r_E^2}{r_c^2}\cos i_o\,(1 + e\cos\theta)^2 \qquad (d)$$

where C_o and e_o are new constants of integration.* Since θ is a known function of time, the perturbed variables, Eqs. (34,a-d), can be found

*Since ϵ is zero, $\dot{r}(\theta,J_2)$ must be zero at θ equal to zero.

as functions of time. The integration of Eq. (34,b) gives $\theta(\theta,J_2)$ as a function of time. The difference between θ and $\theta(\theta,J_2)$ is due to the shift of perigee with time.

Appendix C

CONDITIONS FOR CONTINUOUS LIMITING

It is possible, with certain initial conditions, for the damper-rod to remain at the limiting value of ρ_2. In order to demonstrate this behavior, let us assume that the damper-rod is on the limit. Under these circumstances the damper-rod and body act as a single rigid body. Due to the simple mass distribution of the rod, it is convenient to express the moments and cross-products of inertia with respect to the x y z axes. Thus

$$I_{brx} = I_x + I_{dr} \cos^2\rho_L \qquad (a)$$

$$I_{bry} = I_y + I_{dr}(\cos^2\rho_1 + \sin^2\rho_1 \sin^2\rho_L) \qquad (b)$$

$$I_{brz} = I_z + I_{dr}(\sin^2\rho_1 + \cos^2\rho_1 \sin^2\rho_L) \qquad (c)$$

$$(J_{br})_{xy} = \frac{1}{2} \sin 2\rho_L \sin \rho_1 I_{dr} \qquad (d) \qquad (35)$$

$$(J_{br})_{yz} = -\frac{1}{2} \sin 2\rho_1 \cos^2\rho_L I_{dr} \qquad (e)$$

$$(J_{br})_{zx} = -\frac{1}{2} \sin 2\rho_L \cos \rho_1 I_{dr} \qquad (f)$$

where ρ_L is the limit value of ρ_2 and the subscript br refers to the combination of the body and the rod.

A set of central principal axes, x_p, y_p, z_p, are related to x, y and z by the angles η_1, η_2 and η_3.

$$\begin{bmatrix} x_p \\ y_p \\ z_p \end{bmatrix} = \begin{bmatrix} A \end{bmatrix} \begin{bmatrix} x \\ y \\ z \end{bmatrix} \qquad (36)$$

where

$$A = \begin{bmatrix} a_{11} & a_{12} & a_{13} \\ a_{21} & a_{22} & a_{23} \\ a_{31} & a_{32} & a_{33} \end{bmatrix}$$

and

$$a_{11} = \cos \eta_1 \cos \eta_2$$

$$a_{12} = \sin \eta_2$$

$$a_{13} = - \sin \eta_1 \cos \eta_2$$

$$a_{21} = \sin \eta_1 \sin \eta_3 - \cos \eta_1 \cos \eta_3 \sin \eta_2$$

$$a_{22} = \cos \eta_2 \cos \eta_3$$

$$a_{23} = \cos \eta_1 \sin \eta_3 + \sin \eta_1 \sin \eta_2 \cos \eta_3$$

$$a_{31} = \sin \eta_1 \cos \eta_3 + \cos \eta_1 \sin \eta_2 \sin \eta_3$$

$$a_{32} = - \sin \eta_3 \cos \eta_2$$

$$a_{33} = \cos \eta_1 \cos \eta_3 - \sin \eta_1 \sin \eta_2 \sin \eta_3$$

To find the angles η_1, η_2 and η_3, one can make use of the fact that $J_{x_p y_p}$, $J_{y_p z_p}$ and $J_{z_p x_p}$ are, by the definition of principal axes, zero.

For example

$$\int x_p\, y_p\, dm = \int dm \Big\{ \big[x \cos \eta_1 \cos \eta_2 + y \sin \eta_2 - z \sin \eta_1 \cos \eta_2 \big] \big[x (\sin \eta_1 \sin \eta_3 - \cos \eta_1 \cos \eta_3 \sin \eta_2) + y \cos \eta_2 \cos \eta_3 + z (\cos \eta_3 \cos \eta_1 - \sin \eta_1 \sin \eta_2 \sin \eta_3) \big] \Big\} \tag{37}$$

$$= J_{x_p y_p} = 0$$

The expansion and simplification of the terms within the brackets of Eq. (37) leads to the following expression:

$$(I_{brz} - I_{brx})\, f_1(\eta_{1,2,3}) + (I_{brx} - I_{bry})\, f_2(\eta_{1,2,3}) + (J_{br})_{xy}\, f_3(\eta_{1,2,3}) + (J_{br})_{yz}\, f_4(\eta_{1,2,3}) + (J_{br})_{zx}\, f_5(\eta_{1,2,3}) = 0 \tag{38}$$

where the f's are various combinations of the trigonometric functions of η_1, η_2 and η_3. Two more equations, similar in form, can be obtained by equating $J_{y_p z_p}$ and $J_{z_p x_p}$ to zero. Thus there are three equations in terms of functions of the three unknown angles.

Once the η's have been found, the principal moments of inertia of the rod, body combination can be determined from the equation of the momental ellipsoid. For example

$$I_{xp} = I_{brx}\, a_{11}^2 + I_{bry}\, a_{12}^2 + I_{brz}\, a_{13}^2 - 2(J_{br})_{yz}\, a_{12}\, a_{13} - 2(J_{br})_{zx}\, a_{11}\, a_{13} - 2(J_{br})_{xy}\, a_{11}\, a_{12} \tag{39}$$

where the a's are the elements of the first row of the matrix, A. The values of I_{yp} and I_{zp} can be found in a similar manner.

For this body, the motion about y_p, the pitch axis, is independent of the roll-yaw motion. Thus let us assume that the initial conditions are such that only the pitch mode is excited. Restricting the center-of-mass motion to a circular orbit without external disturbances, the pitch equation of motion is

$$\ddot{\alpha}_p + 1.5\,\dot{\theta}_c^{\,2}\,R_{yp}\sin 2\alpha_p = 0 \tag{40}$$

where

$$\dot{\alpha}_p = \omega_{yp} - \dot{\theta}_c$$

The orientation angle, α_p, corresponds to α of Fig. 2 and it is assumed that β_p and φ_p are zero. By utilizing α_p as the independent variable Eq. (40) can be integrated once.

$$\omega_{yp} = \dot{\theta}_c\left(1 \pm \sqrt{(n-1)^2 + 1.5\,R_{yp}\left[\cos 2\alpha_p - \cos 2\alpha_p(0)\right]}\right) \tag{41}$$

where the initial pitch rate is defined as

$$\omega_{yp}(0) = n\dot{\theta}_c \tag{42}$$

If n is negative, the negative sign of the radical of Eq. (41) must be used. It can be easily shown that, for positive values of $\omega_{yp}(0)$, n must be equal to or larger than 2.73 for unidirectional rotation to occur. If $\omega_{yp}(0)$ is negative then n must be equal to or less than -0.73.*

*In obtaining the above values of n, it is assumed that the maximum value of R_{yp} is 1.

Otherwise, oscillatory motion about the local vertical will take place.

When the damper-rod is on the limit, an expression for $(M_{yl}/I_{dr})_b$ can be deduced from Eqs. (4,a-c) and Eq. (2b).

$$\left(\frac{M_{yl}}{I_{dr}}\right)_b = \dot{\omega}_y \cos \rho_l + \dot{\omega}_z \sin \rho_l - \frac{c_2}{I_{dr}} \rho_L - \left(\frac{M_{yl}}{I_{dr}}\right)_G \qquad (43)$$

$$- \left[(\omega_y \sin \rho_l - \omega_z \cos \rho_l) \cos \rho_L + \omega_x \sin \rho_L \right] \left[\omega_x \cos \rho_L \right.$$

$$\left. - (\omega_y \sin \rho_l - \omega_z \cos \rho_l) \sin \rho_L \right]$$

Since the total angular rate of the rod, body combination is ω_{yp}, then ω_x, and ω_z are functions of ω_{yp}. Thus if ω_{yp} is non-oscillatory and sufficiently large, $(M_{yl})_b$ must exist due to the cross-product term of Eq. (43). This so-called gyroscopic term will not reverse sign as will the gradient-torques and the angular accelerations, $\dot{\omega}_y$ and $\dot{\omega}_z$. The constraint torque will oscillate in magnitude but will not reverse sign if the parameter, n, of Eq. (42) is large enough. As might be expected, the required value of n for continuous limiting depends upon ρ_L but must always, of course, exceed 2.73 or be less than -0.73 depending upon the sign of $\omega_{yp}(0)$.

In terms of the x y z axes, ω_{yp} has the following components:

$$\omega_x = a_{21} \omega_{yp} \qquad (a)$$

$$\omega_y = a_{22} \omega_{yp} \qquad (b) \qquad (44)$$

$$\omega_z = a_{23} \omega_{yp} \qquad (c)$$

where the a's are the elements of the second row of A or of the second column of A^{-1}. The angular accelerations are

$$\dot{\omega}_y = \dot{\omega}_{yp}\, a_{22} = -\,1.5\, \dot{\theta}_c^2\, R_{yp} \sin 2\alpha_p\, a_{22} \qquad (a)$$

$$\dot{\omega}_z = \dot{\omega}_{yp}\, a_{23} = -\,1.5\, \dot{\theta}_c^2\, R_{yp} \sin 2\alpha_p\, a_{23} \qquad (b) \qquad (45)$$

Finally the relationship between α_p and a_x, a_y and a_z must be established so that the gradient torque, $(M_{yl})_G$, can be evaluated.

$$\cos \alpha_p = a_{11}\, a_x + a_{12}\, a_y + a_{13}\, a_z \qquad (a)$$

$$0 = a_{21}\, a_x + a_{22}\, a_y + a_{23}\, a_z \qquad (b) \qquad (46)$$

$$\sin \alpha_p = a_{31}\, a_x + a_{32}\, a_y + a_{33}\, a_z \qquad (c)$$

From Eqs. (10,a-c) and the definitions of a_x, a_y and a_z, Eq. (9):

$$a_{xl} = a_x \sin \rho_L + a_y \sin \rho_l \cos \rho_L - a_z \cos \rho_l \cos \rho_L \qquad (a)$$

$$a_{zl} = a_x \cos \rho_L - a_y \sin \rho_l \sin \rho_L + a_z \cos \rho_l \sin \rho_L \qquad (b) \qquad (47)$$

The solution of Eqs. (46,a-c) yields the direction cosines, a_x, a_y and a_z as a function of the variable α_p. Equation (47,a-b) can then be used to find $(M_{yl}/I_{dr})_G$ as a function of α_p.

For a given value of n and ρ_L, $(M_{yl}/I_{dr})_b$ can be found as a function of α_p from Eq. (43). Thus the minimum value of n which will result in continuous limiting can be determined for a given limit angle, ρ_L.

The procedure outlined in the preceding paragraphs has been followed for the design under consideration. Since the determination of the η's and I_{xp}, I_{yp} and I_{zp} is a tedious process, only one limit angle was considered: ρ_L equal to $\pm 30^\circ$. The solutions of Eqs. (43) and (41) indicate that, for positive pitch rates, an n of 4.121 is sufficient for continuous limiting. This is true for the damper-rod at + 30° or - 30° initially. For negative pitch rates an n of -5.99 is required to limit continuously at $\pm 30^\circ$.

For small values of $|\rho_L|$, the gyroscopic term of Eq. (43) approaches zero. Thus for $(M_{yl})_b$ to exist, ω_{yp} must be very large. The same sort of behavior occurs as $|\rho_L|$ approaches 90°. Thus a minimum initial pitch rate must exist for which continuous limiting will prevail.

Appendix D

RADIATION PRESSURE TORQUES

It is necessary to select a nominal vehicle design before the effects of radiation pressure torques can be evaluated. The assumption is made that the main body consists of a "small" sphere at the center of an "X." The X is formed by rods which have diameters of 0.1 ft, and tip to tip lengths of L. Located at the tips of the rods are four equal masses. The moments of inertia of the body are

$$I_x = m\left(\frac{L}{2}\sin\angle\right)^2 + \frac{m_r}{6}\left(L\sin\angle\right)^2 \qquad (a)$$

$$I_y = m\frac{L^2}{4} + \frac{m_r}{6}L^2 \qquad (b) \quad (48)$$

$$I_z = m\left(\frac{L}{2}\cos\angle\right)^2 + \frac{m_r}{6}\left(L\cos\angle\right)^2 \qquad (c)$$

where m is the total tip mass, m_r is the mass of one rod and $2\angle$ is the acute angle of the X. The moment of inertia of the "small" sphere has been neglected. If it is assumed that the rods are Be Cu, then, based on Ref. 12

$$m_r \simeq \frac{6 \times 10^{-2}}{32.2} \text{ L (slugs)}$$

From Table 1, and Eqs. (48,a-c)

$$(I_x/I_z) = 0.12 = \tan^2\angle$$

Thus the angle $2\angle$ is approximately 38.2°.

For small disturbances, the yaw response to a constant torque is

$$\delta\varphi_{ss} = \frac{(M_D)_x}{\dot{\theta}_c^2 (I_{yp} - I_{zp})} \tag{49}$$

At an altitude of 6000 mi, and assuming a circular orbit, $\dot{\theta}_c^2$ is approximately $10^{-7}(\text{rad/sec})^2$. The principal moments of inertia of the damper-rod, body combination are

$$I_{xp} = 0.2\ I_z \qquad \text{(a)}$$

$$I_{yp} \cong 1.15\ I_z \qquad \text{(b)} \tag{50}$$

$$I_{zp} \cong 1.05\ I_z \qquad \text{(c)}$$

Finally $(M_D)_x$ for the worst case is

$$(M_D)_x = P_s\ A\ \Delta d = 1.5 \times 10^{-7}(0.2L)\ \Delta d \tag{51}$$

where the area of one rod is 0.1L, Δd is the separation between the center-of-pressure and the center-of-mass, and 1.5×10^{-7} is the average radiation pressure, P_s, in lb/ft^2. The area of the damper-rod has been neglected.

Thus, from Eqs. (48), (50) and (51)

$$\frac{\delta\varphi_{ss}}{\Delta d} = \frac{1.1 \times 10^4}{805\ m\ L + L^2} \tag{52}$$

Equation (52) has been solved for L as a function of $(\delta\varphi_{ss}/\Delta d)$, with $m = 0$, and for m as a function of $(\delta\varphi_{ss}/\Delta d)$ with $L = 100$ ft. (See Table 2.)

Appendix E

SOME REPRESENTATIVE DIGITAL COMPUTER SOLUTIONS

In this Appendix plots of α, β, φ, and ρ_2 as functions of the orbital period are presented. The particular initial conditions, orbital forcing, or external disturbances which pertain to a given case are indicated below. All unspecified conditions are standard. (See pg. 11, Section III)

Linearized and Exact Solutions

Fig. 4, $\alpha(0) = 10^\circ$

Transient Response to Attitude Errors

Fig. 5 $\alpha(0) = 45^\circ$; $\rho_L = \pm 30^\circ$

Fig. 6 $\alpha(0) = -45^\circ$; $\rho_L = \pm 30^\circ$

Fig. 7 $\alpha(0) = \beta(0) = \Delta\varphi(0) = 45^\circ$; $\rho_L = \pm 90^\circ$

Fig. 8 $\alpha(0) = \beta(0) = \Delta\varphi(0) = -45^\circ$; $\rho_L = \pm 30^\circ$

Fig. 9 $\alpha(0) = \beta(0) = \Delta\varphi(0) = 45^\circ$; $\rho_L = \pm 30^\circ$

Transient Response to Yaw Angular Rate Errors

Fig. 10 $\omega_{xp}(0) \equiv \omega_x(0) = 5\dot{\theta}_c$; $\rho_L = \pm 30^\circ$

Fig. 11 $\alpha(0) = 45^\circ$; $\omega_x(0) = 5\dot{\theta}_c$; $\rho_L = \pm 30^\circ$

Fig. 12 $\alpha(0) = -45^\circ$; $\omega_x(0) = 5\dot{\theta}_c$; $\rho_L = \pm 30^\circ$

Transient Response to Pitch Angular Rate Errors

Fig. 13 $\omega_{yp}(0) \equiv \omega_y(0) \cos \varphi_{ss} - \omega_z(0) \sin \varphi_{ss} = 2.5\dot{\theta}_c$; $\rho_L = \pm 30^\circ$

Fig. 14 $\omega_{yp}(0) = -0.5\dot{\theta}_c$; $\rho_L = \pm 30^\circ$

Fig. 15 $\omega_{yp}(0) = 3\dot{\theta}_c$; $\rho_L = \pm 30^\circ$

Fig. 16 $\omega_{yp}(0) = 3\dot{\theta}_c$; $\rho_L = \pm 90^\circ$ (no limit)

Fig. 17 $\omega_{yp}(0) = -3\dot{\theta}_c$; $\rho_L = \pm 30^\circ$

Fig. 18 $\beta(0) = -1.95^\circ$; $\varphi(0) = -14.1^\circ$; $\rho_2(0) = 30^\circ$

Fig. 18 $\beta(0) = -1.95^{\circ}$; $\varphi(0) = -14.1^{\circ}$; $\rho_2(0) = 30^{\circ}$

$\omega_{yp}(0) = 4.1\dot{\theta}_c$; $\omega_x(0) = -0.1411\dot{\theta}_c$; $\rho_L = \pm 30^{\circ}$

Fig. 19 $\beta(0) = -1.95^{\circ}$; $\varphi(0) = -14.1^{\circ}$ $\rho_2(0) = 30^{\circ}$

$\omega_{yp}(0) = -6\dot{\theta}_c$; $\omega_x(0) = -0.204 \times 10^{-3}$; $\rho_L = 30^{\circ}$

Forced Response due to Orbital Motion

Fig. 20 $e = 0.05$; $\rho_L = \pm 30^{\circ}$

Fig. 21 $e = 0.01$; $\rho_L = \pm 30^{\circ}$

Fig. 22 $J_2 = 1.082 \times 10^{-3}$; $i_o = 45^{\circ}$; $\rho_L = \pm 30^{\circ}$

Fig. 23 $e = 0.05$; $J_2 = 1.082 \times 10^{-3}$; $i_o = 45^{\circ}$; $\rho_L = \pm 30^{\circ}$

Forced Response due to Constant Disturbing Torques

Fig. 24 $(M_D)_{yp} = 10^{-6}$ lb-ft ; $\rho_L = \pm 30^{\circ}$

Fig. 25 $(M_D)_{xp} = 10^{-6}$ lb-ft ; $\rho_L = \pm 30^{\circ}$

Fig. 26 $(M_D)_{zp} = 10^{-6}$ lb-ft ; $\rho_L = \pm 30^{\circ}$

Forced Response due to Sinusoidal Disturbing Torques

Fig. 27 $(M_D)_{yp} = 10^{-6} \sin \dot{\theta}_c t$ lb-ft ; $\rho_L = \pm 30^{\circ}$

Fig. 28 $(M_D)_{xp} = 10^{-6} \sin \dot{\theta}_c t$ lb-ft ; $\rho_L = \pm 30^{\circ}$

Fig. 29 $(M_D)_{zp} = 10^{-6} \sin \dot{\theta}_c t$ lb-ft ; $\rho_L = \pm 30^{\circ}$

Fig. 30 $(M_D)_{yp} = 10^{-6} \sin 2\dot{\theta}_c t$ lb-ft ; $\rho_L = \pm 30^{\circ}$

Fig. 31 $(M_D)_{xp} = 10^{-6} \sin 2\dot{\theta}_c t$ lb-ft ; $\rho_L = \pm 30^{\circ}$

Fig. 32 $(M_D)_{zp} = 10^{-6} \sin 2\dot{\theta}_c t$ lb-ft ; $\rho_L = \pm 30^{\circ}$

NOTE:

If any one of the angles exceeds π radians in magnitude, then π is subtracted from (or added to) the function and the plot is then continued from zero. Due to the granularity of the data, the function does not always restart at exactly zero.

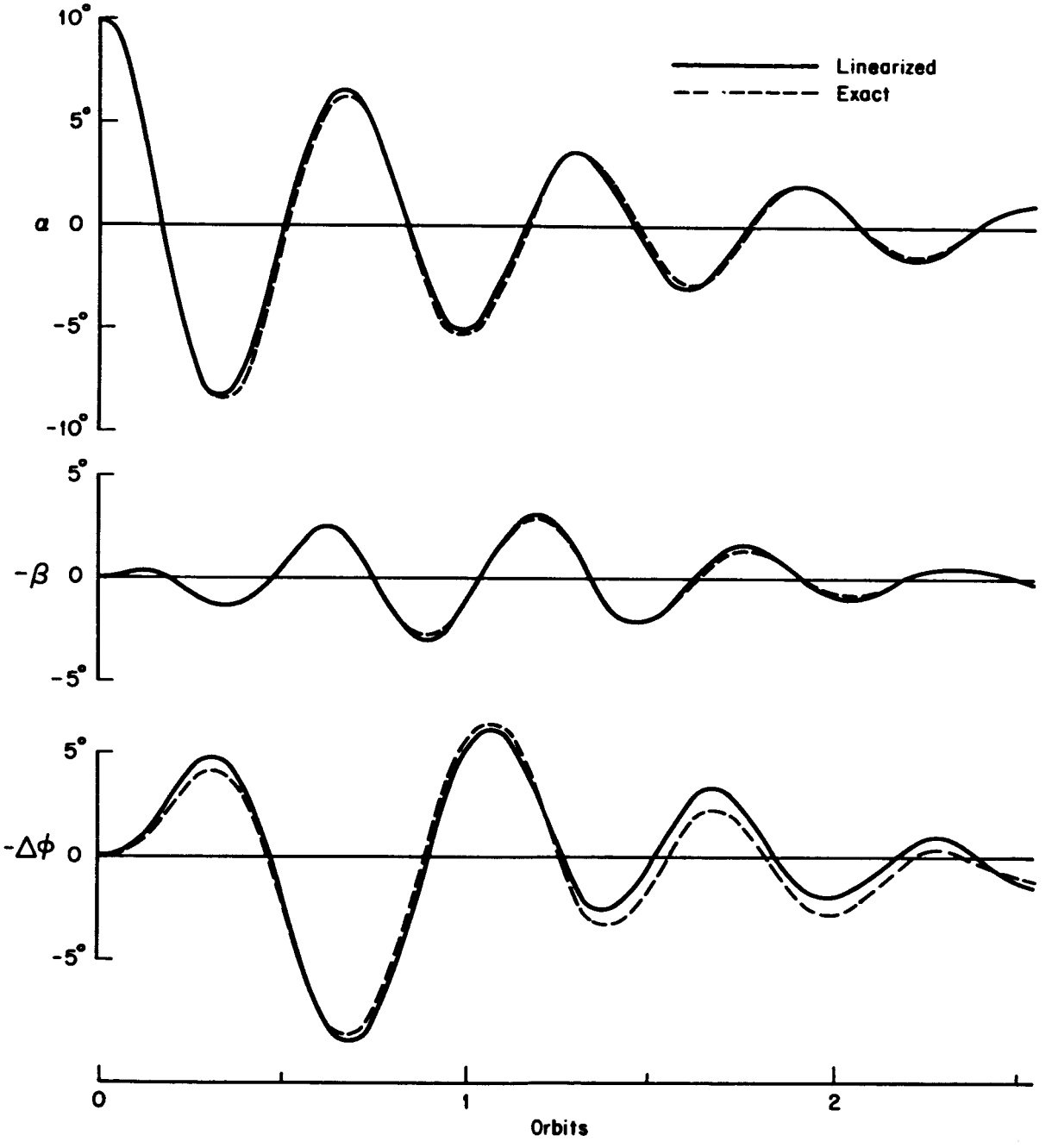

Fig. 4—Linearized and exact solutions

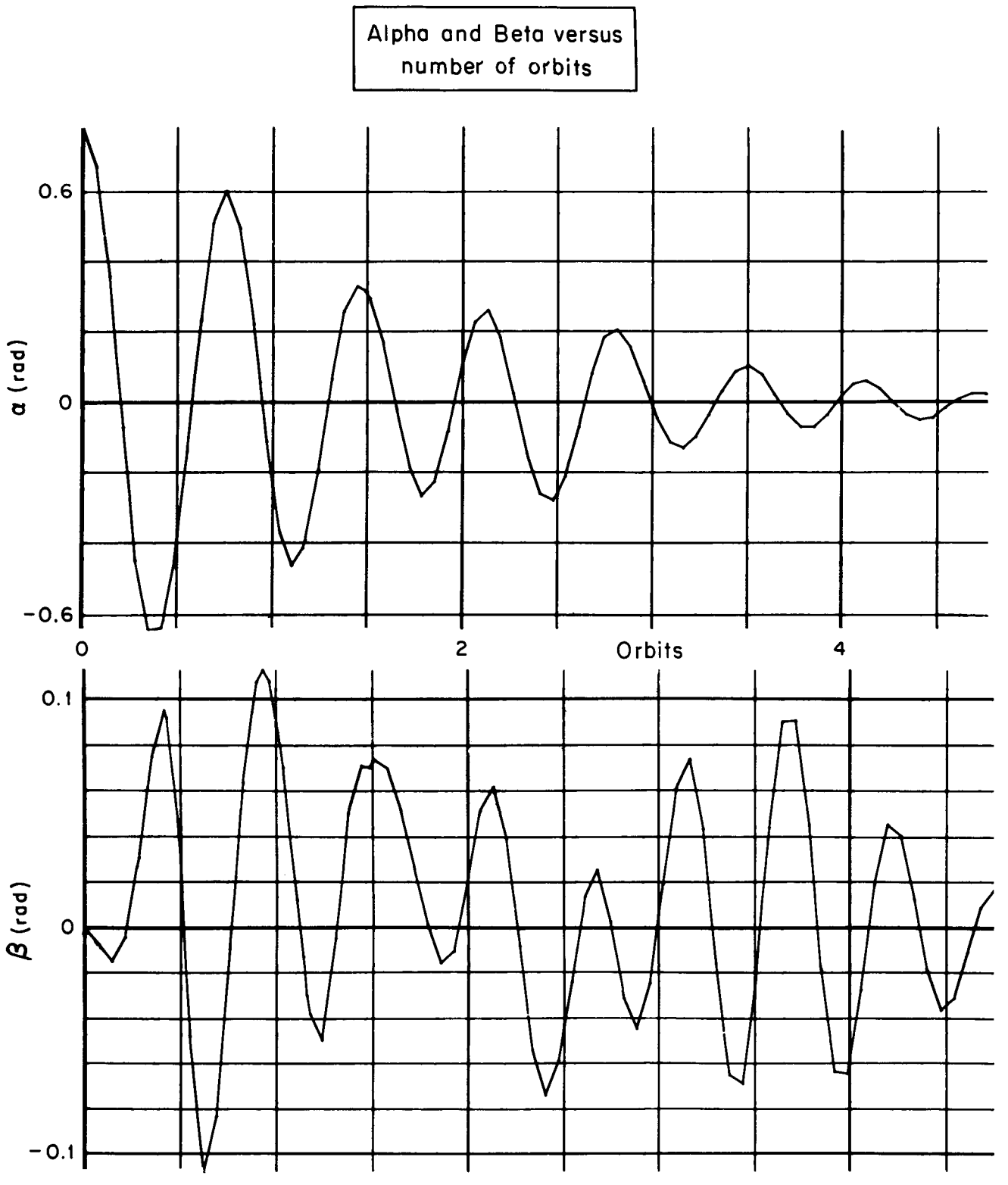

Fig. 5 — Transient response to attitude errors

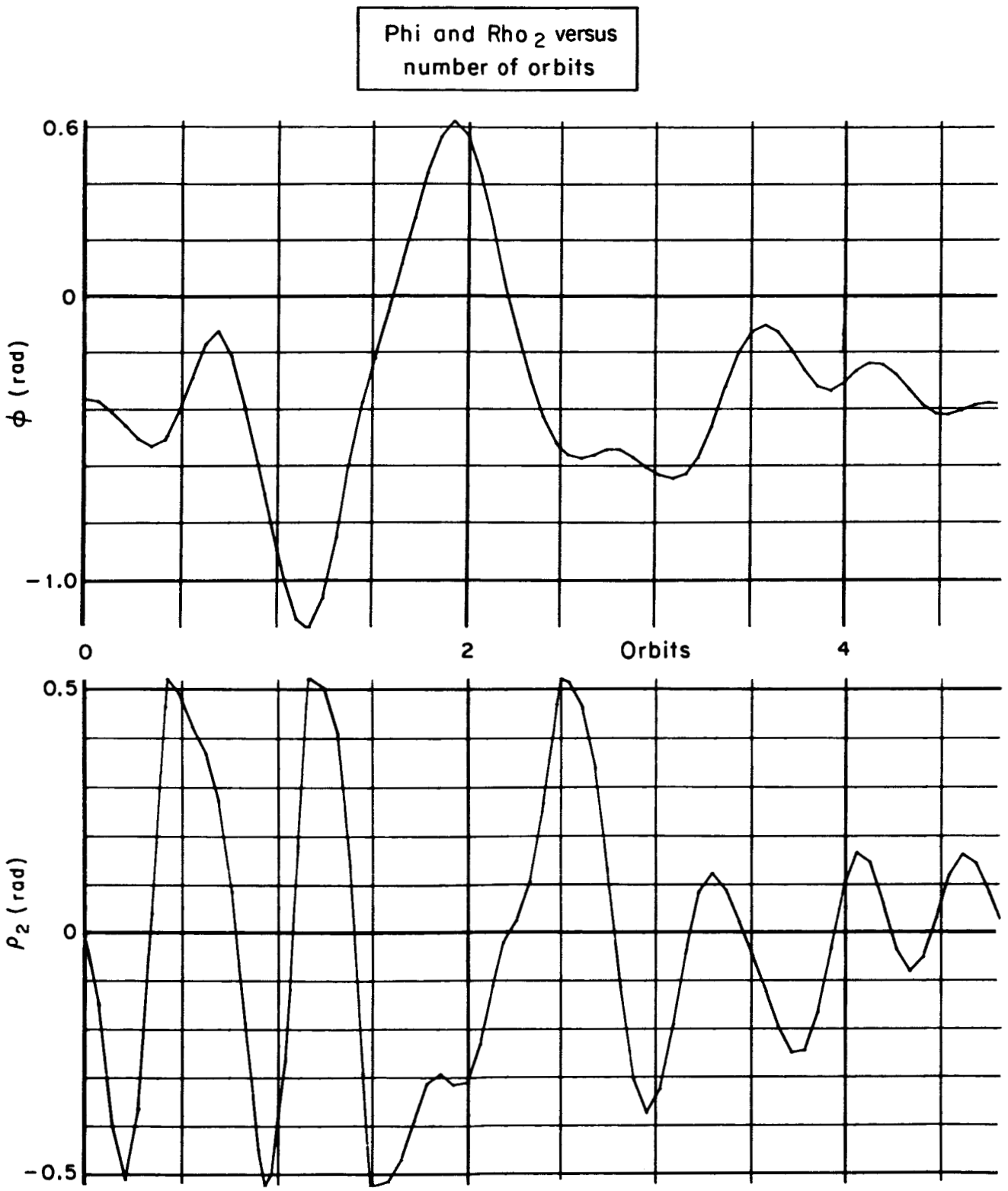
Phi and Rho 2 versus number of orbits
0.6
0
-1.0
ϕ (rad)
0
2
Orbits
4
0.5
0
-0.5
ρ2 (rad)

Fig. 5 (cont.)

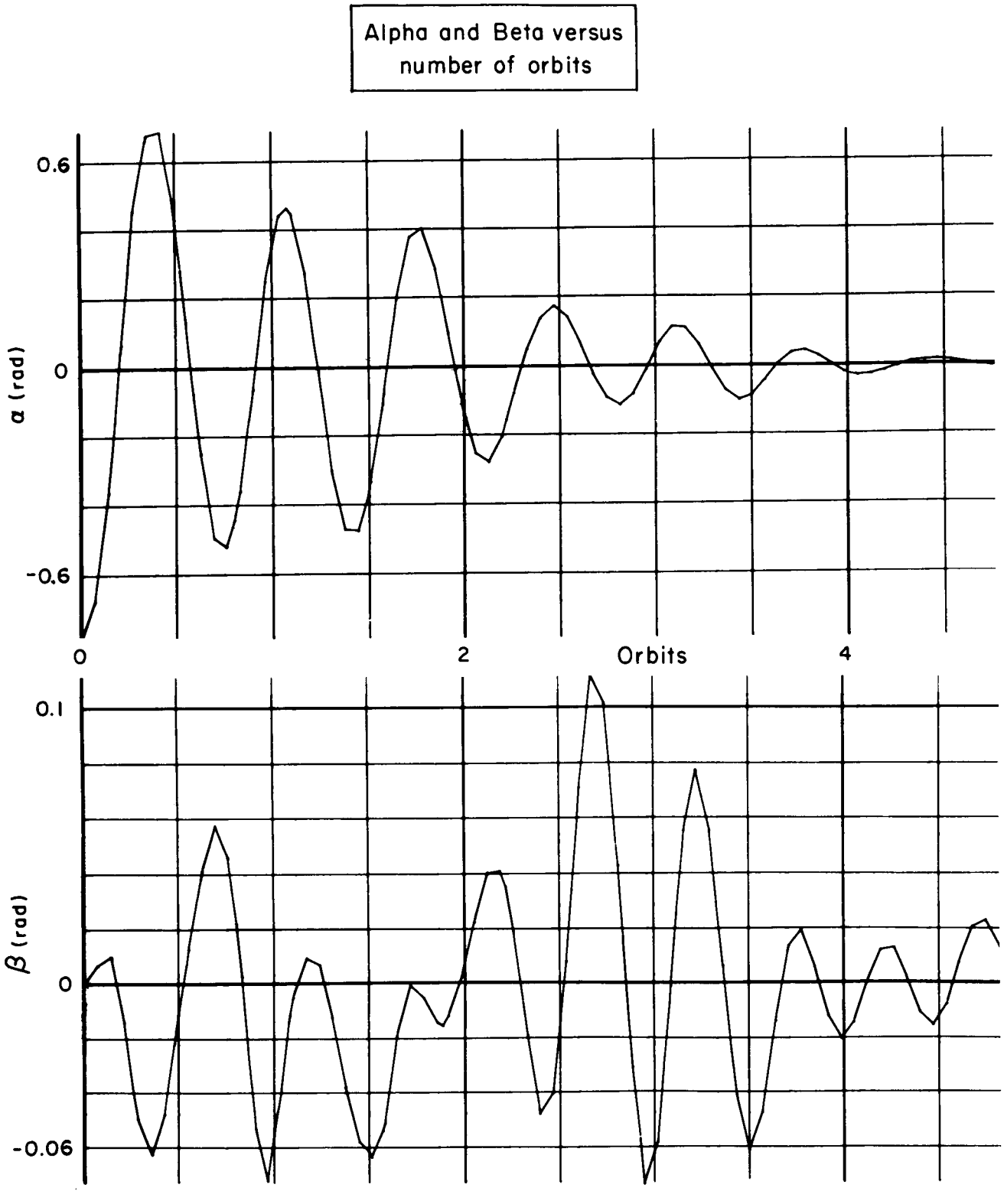

Fig. 6 — Transient response to attitude errors

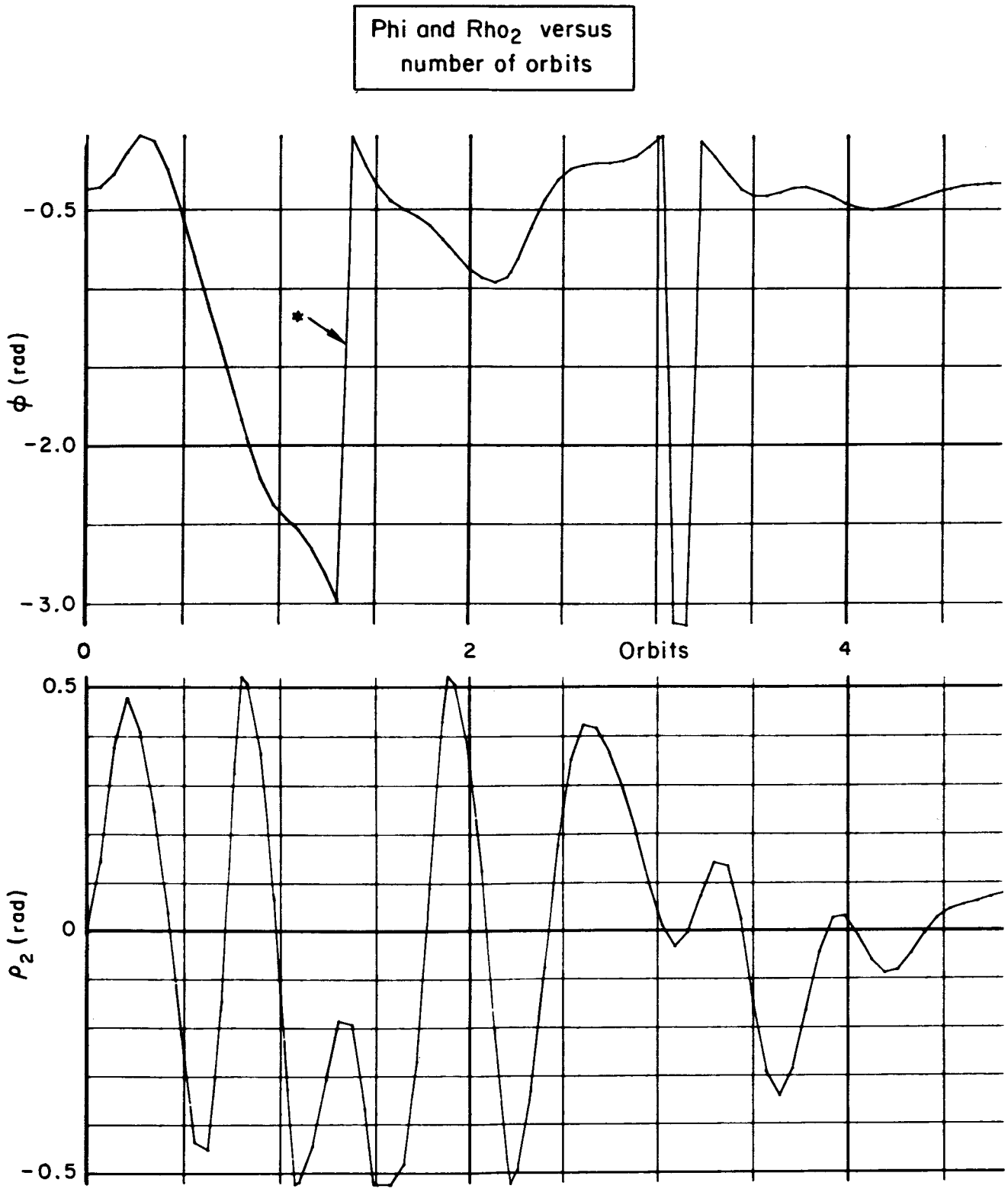

Fig. 6 (cont.)

*See note, p. 53.

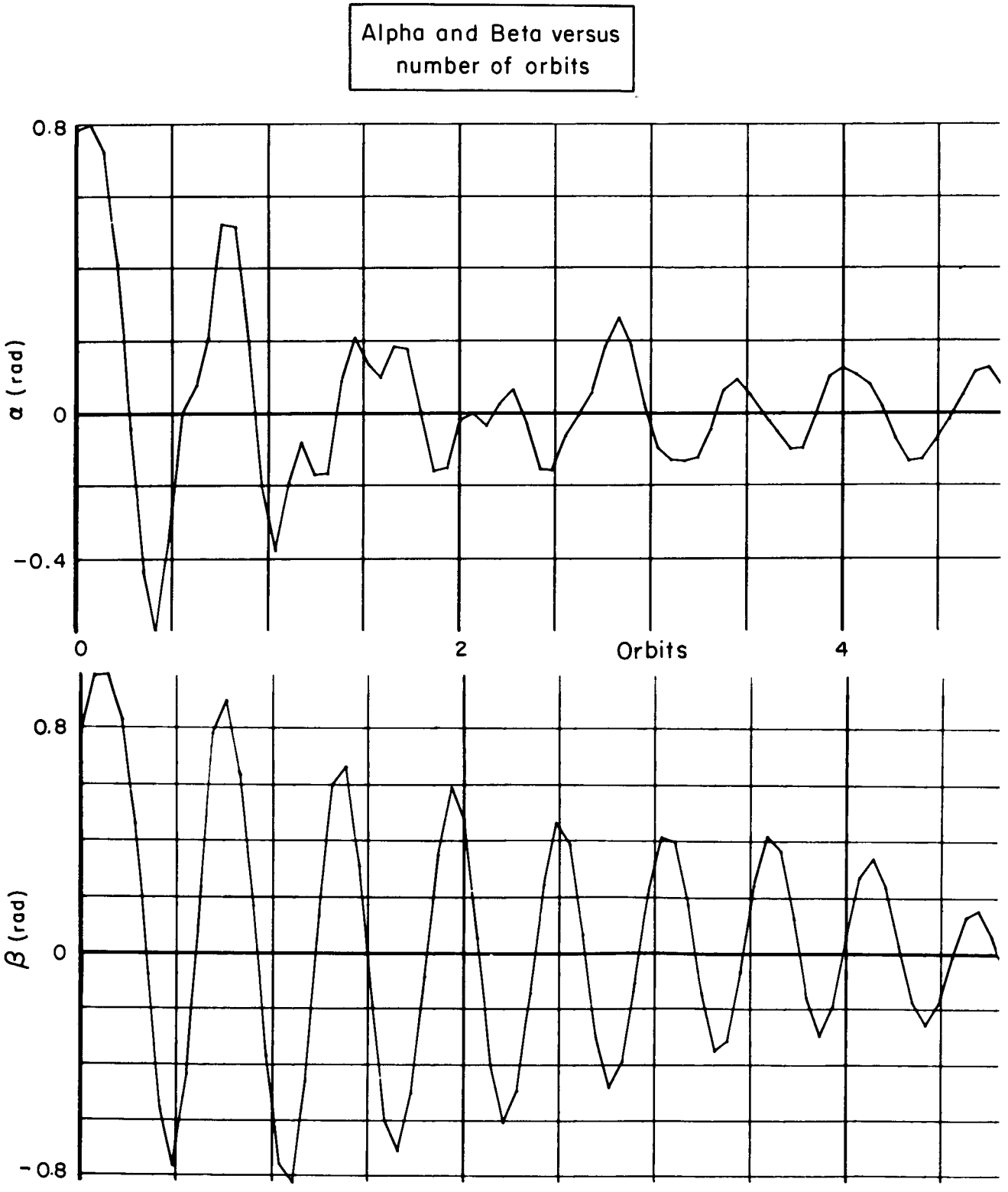

Fig. 7 — Transient response to attitude errors

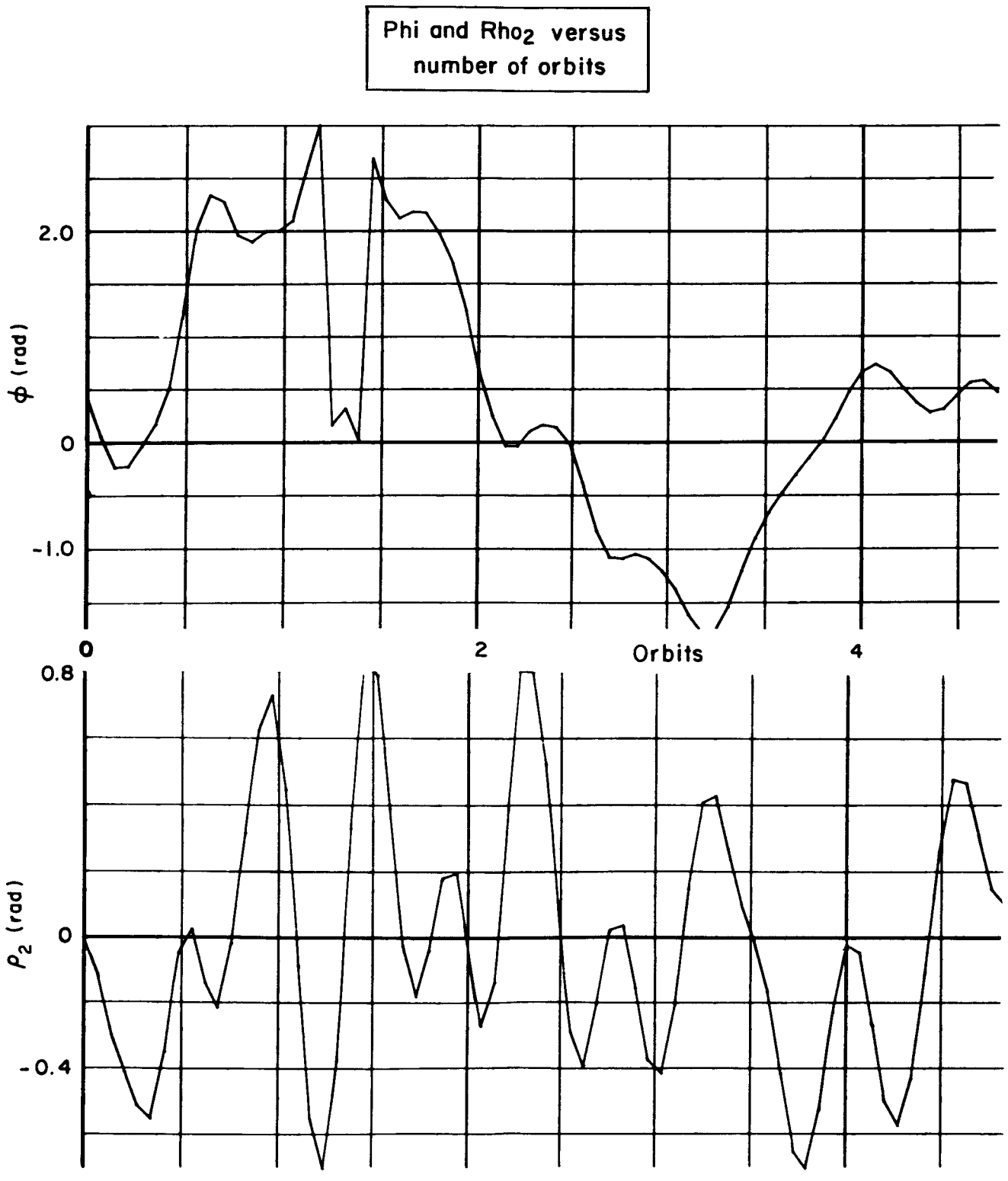
Phi and Rho2 versus number of orbits
2.0
0
-1.0
ϕ (rad)
0
2
Orbits
4
0.8
0
-0.4
ρ2 (rad)

Fig. 7 (cont.)

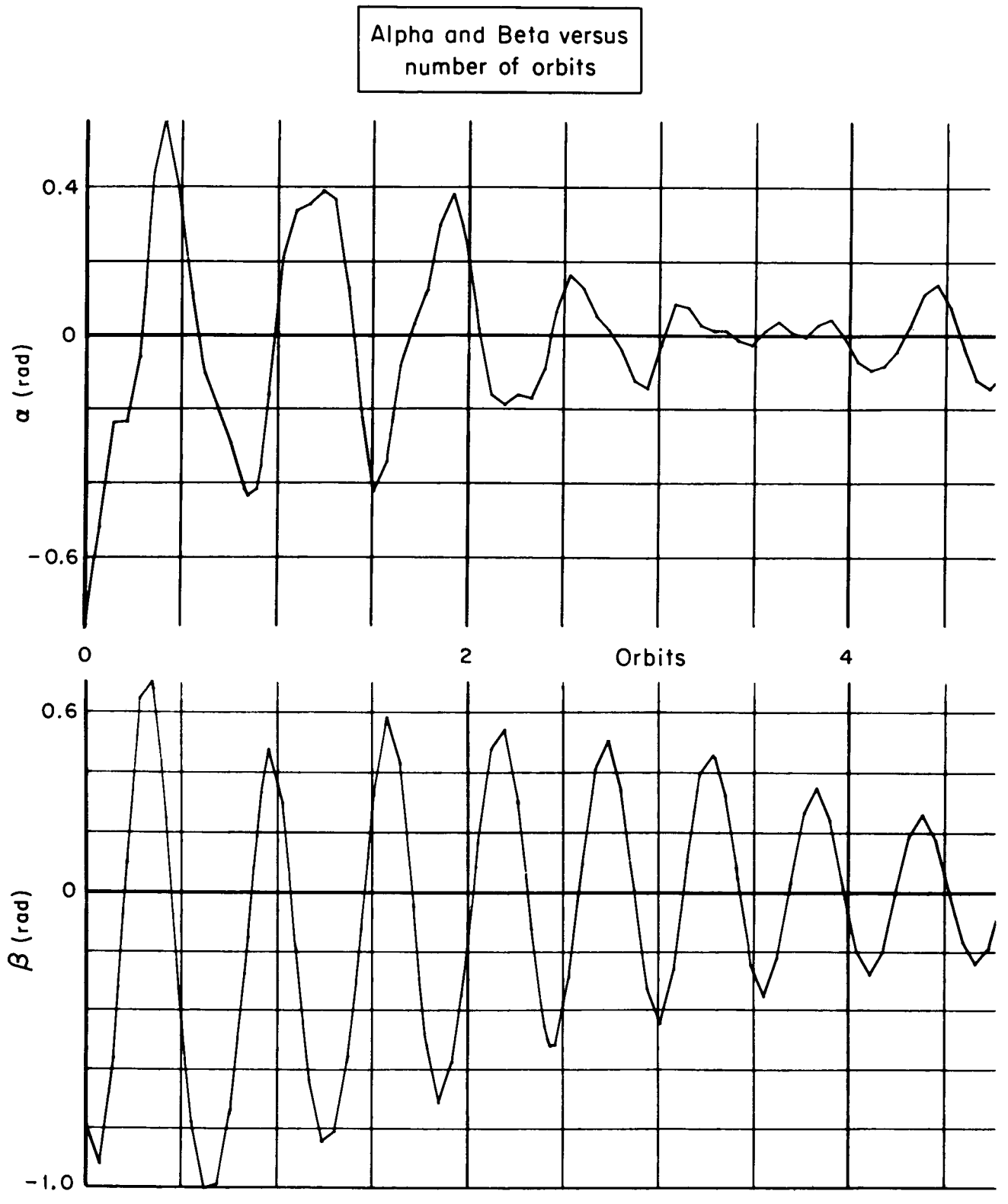

Fig. 8 — Transient response to attitude errors

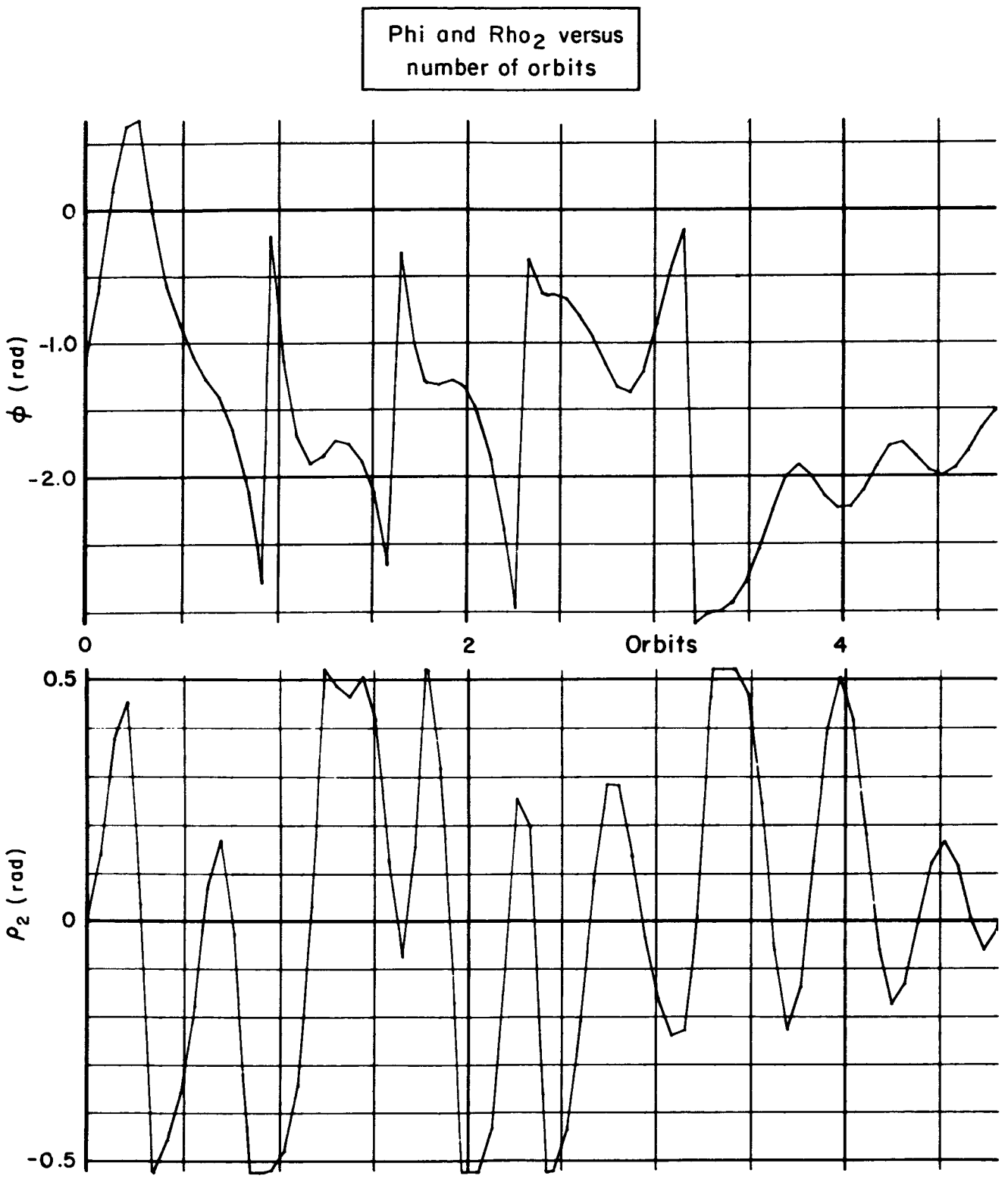
Phi and Rho2 versus number of orbits
0
-1.0
-2.0
φ (rad)
0
2
Orbits
4
0.5
0
-0.5
ρ2 (rad)

Fig. 8 (cont.)

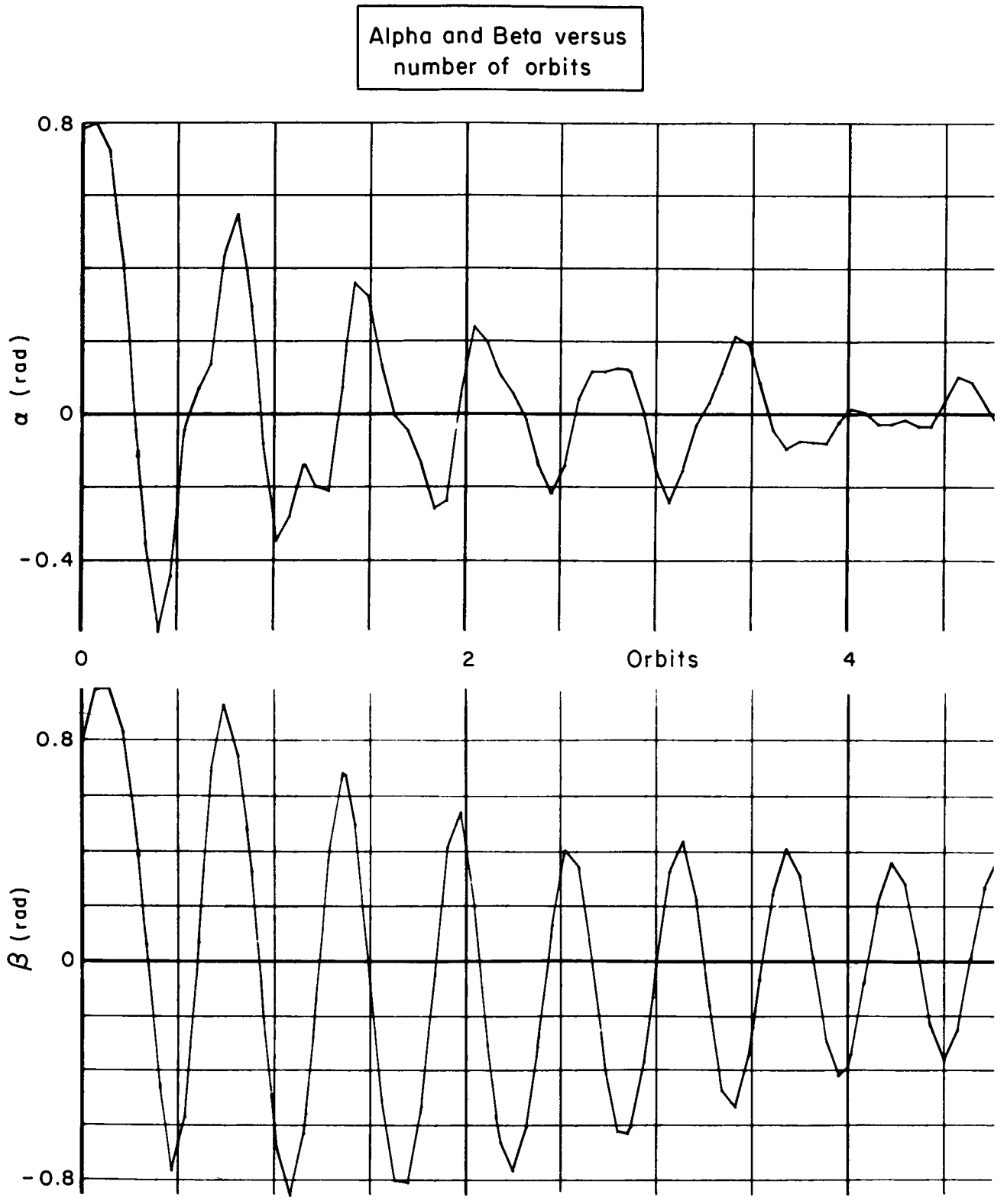

Fig. 9 — Transient response to attitude errors

Phi and Rho_2 versus number of orbits

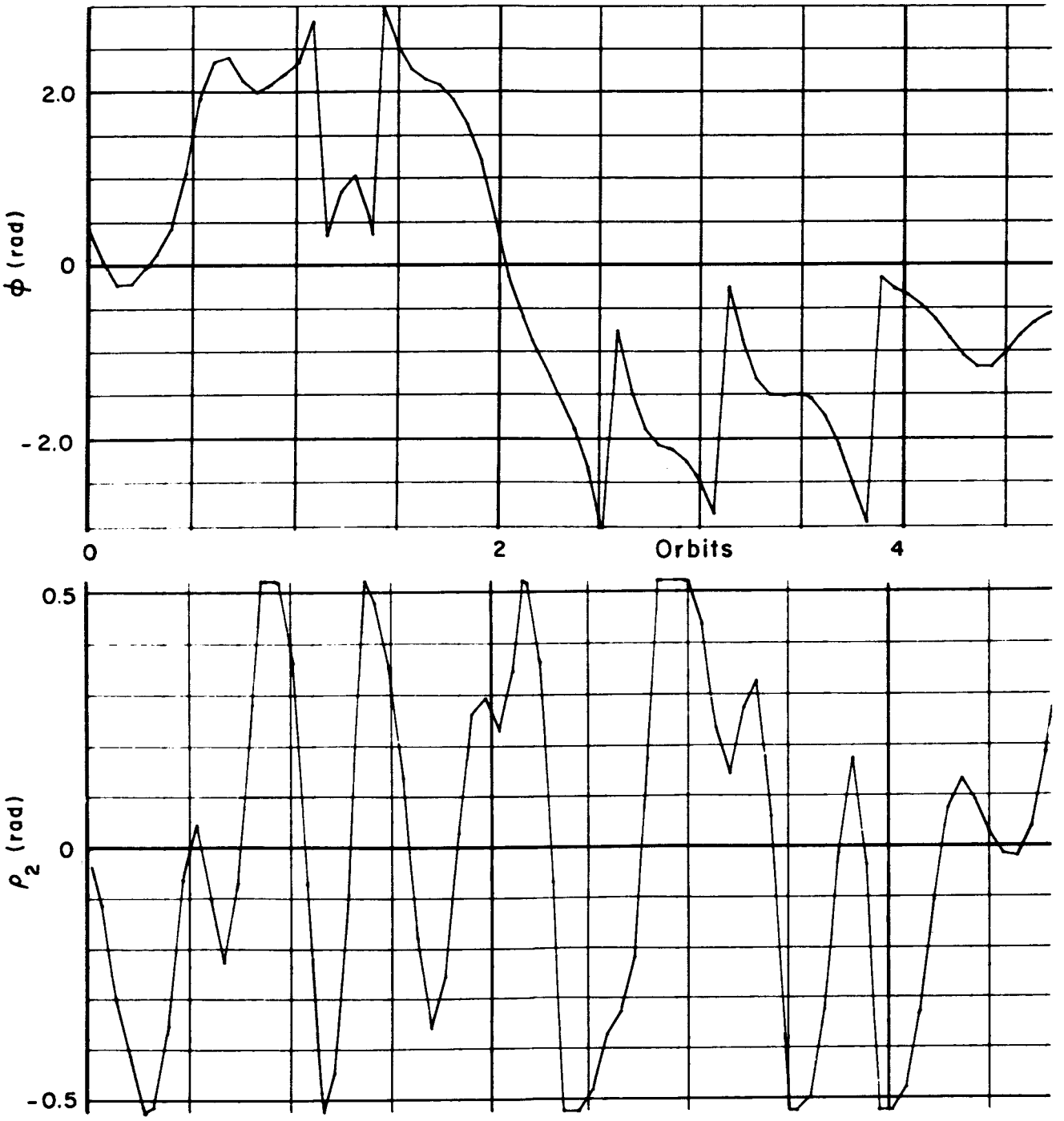

Fig. 9 (cont.)

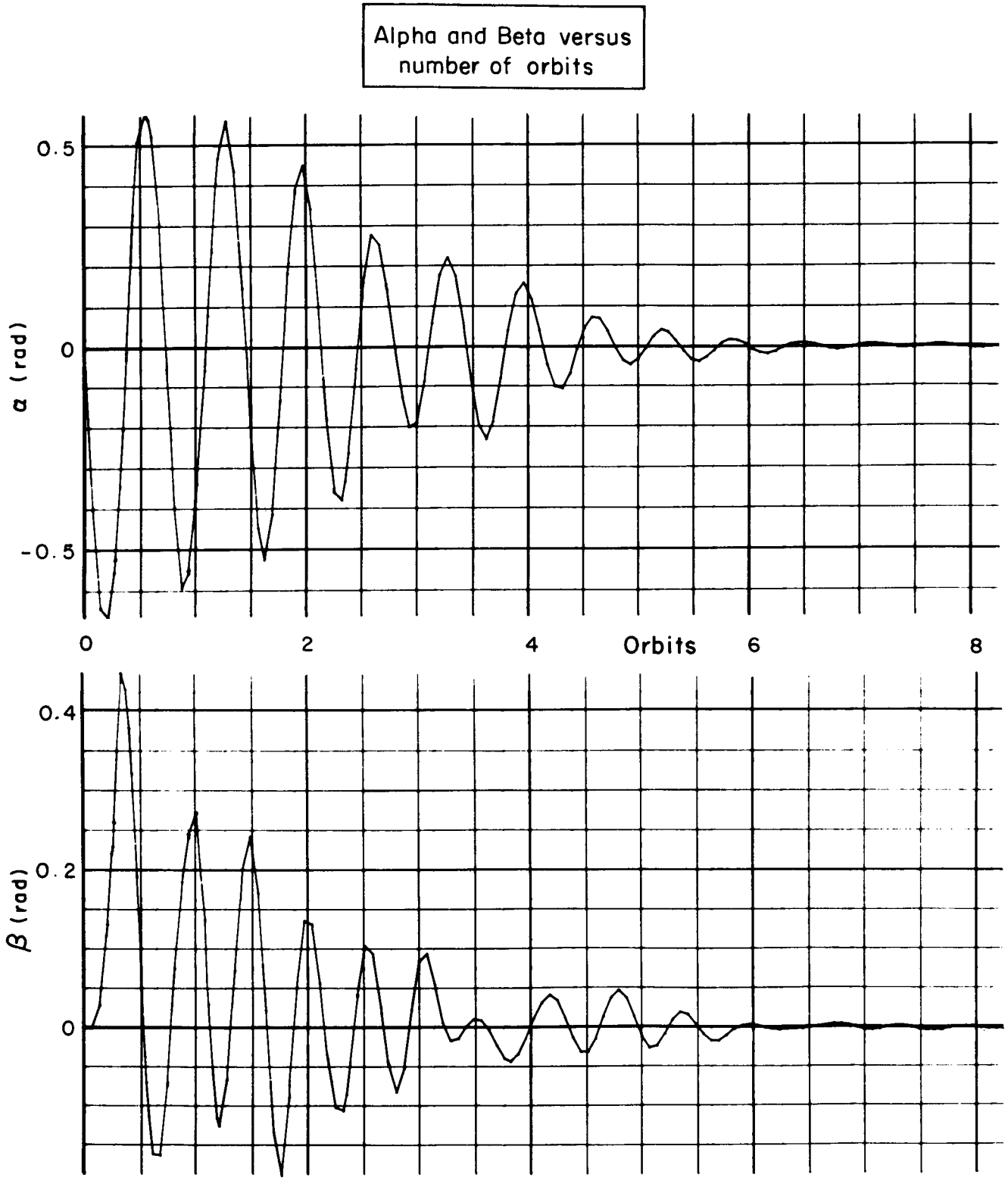

Fig. 10 — Transient response to initial yaw angular rate error

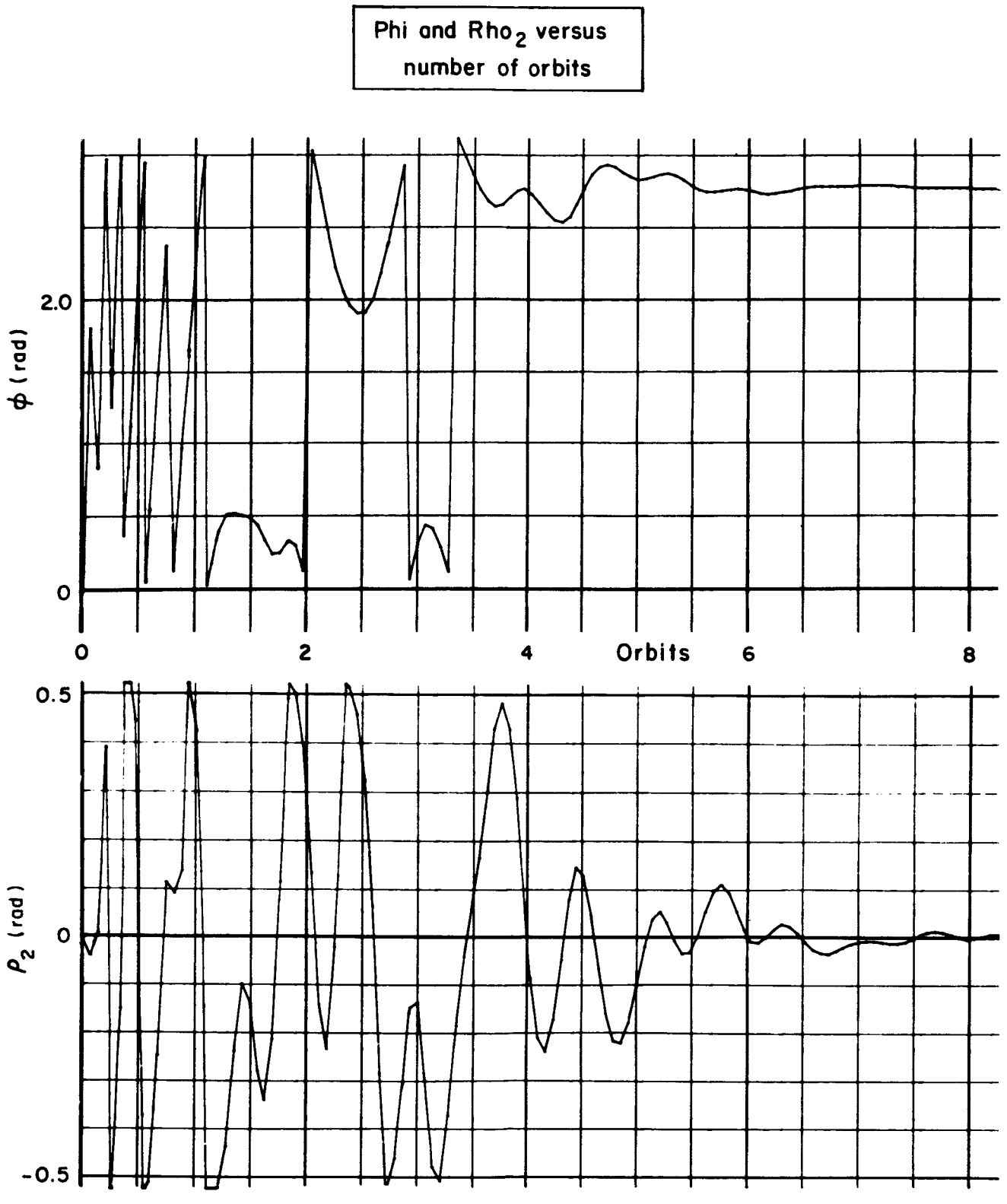
Phi and Rho$_2$ versus number of orbits
2.0
0
ϕ (rad)
0
2
4
Orbits
6
8
0.5
0
-0.5
ρ_2 (rad)

Fig. 10 (cont.)

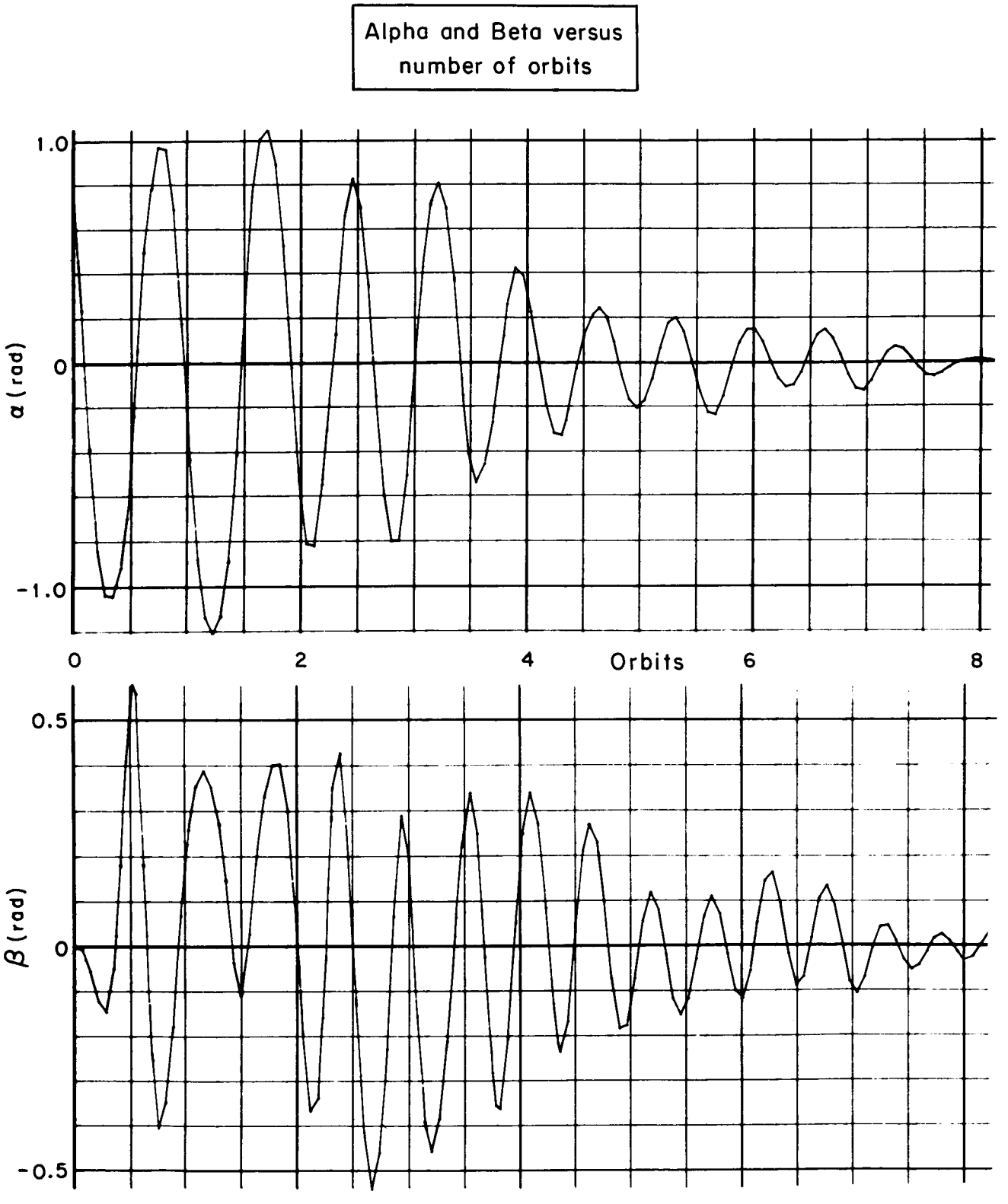

Fig. 11 — Transient response to initial yaw angular rate error

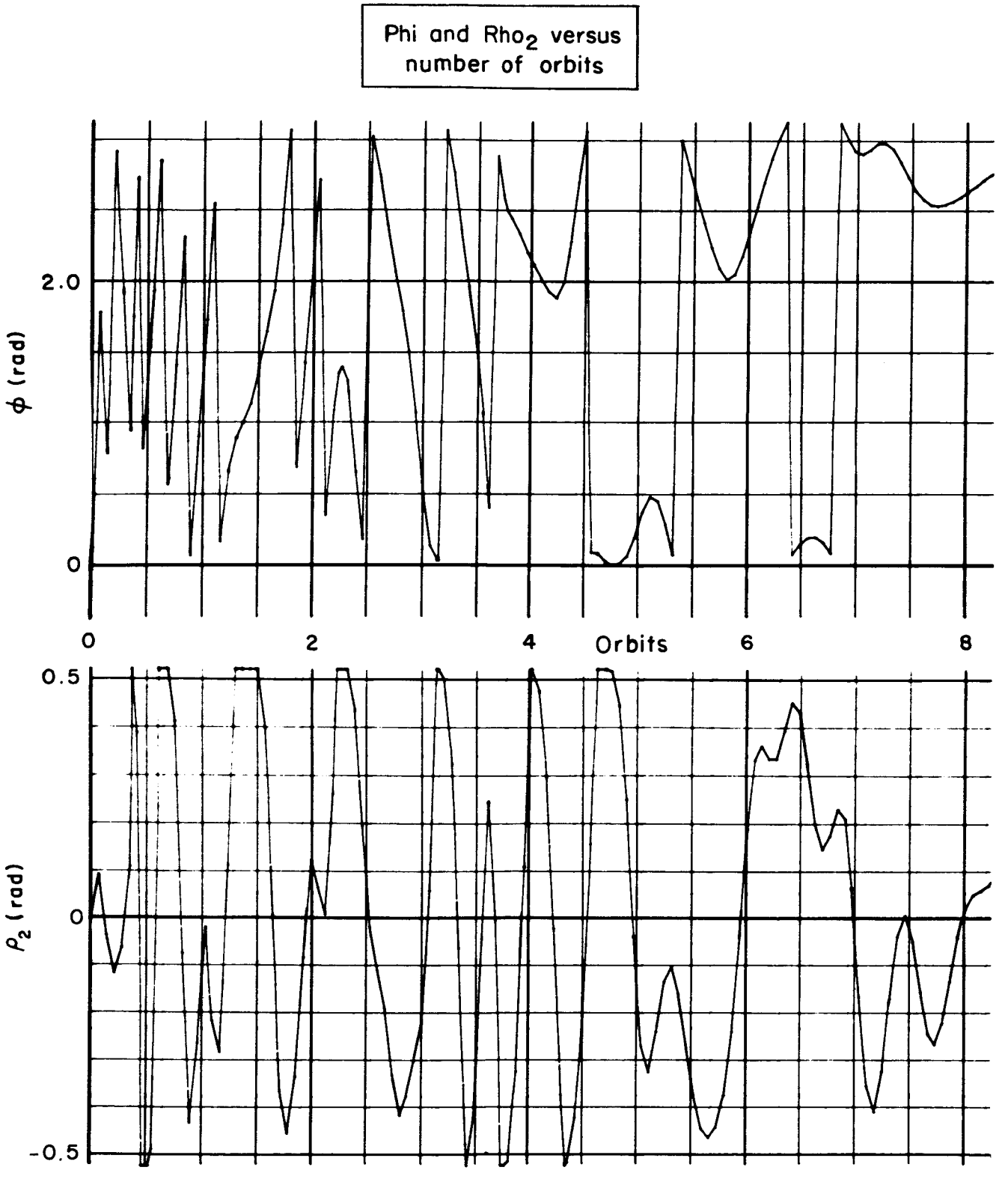
Phi and Rho2 versus number of orbits
2.0
0
φ (rad)
0
2
4
Orbits
6
8
0.5
0
-0.5
ρ2 (rad)

Fig. 11 (cont.)

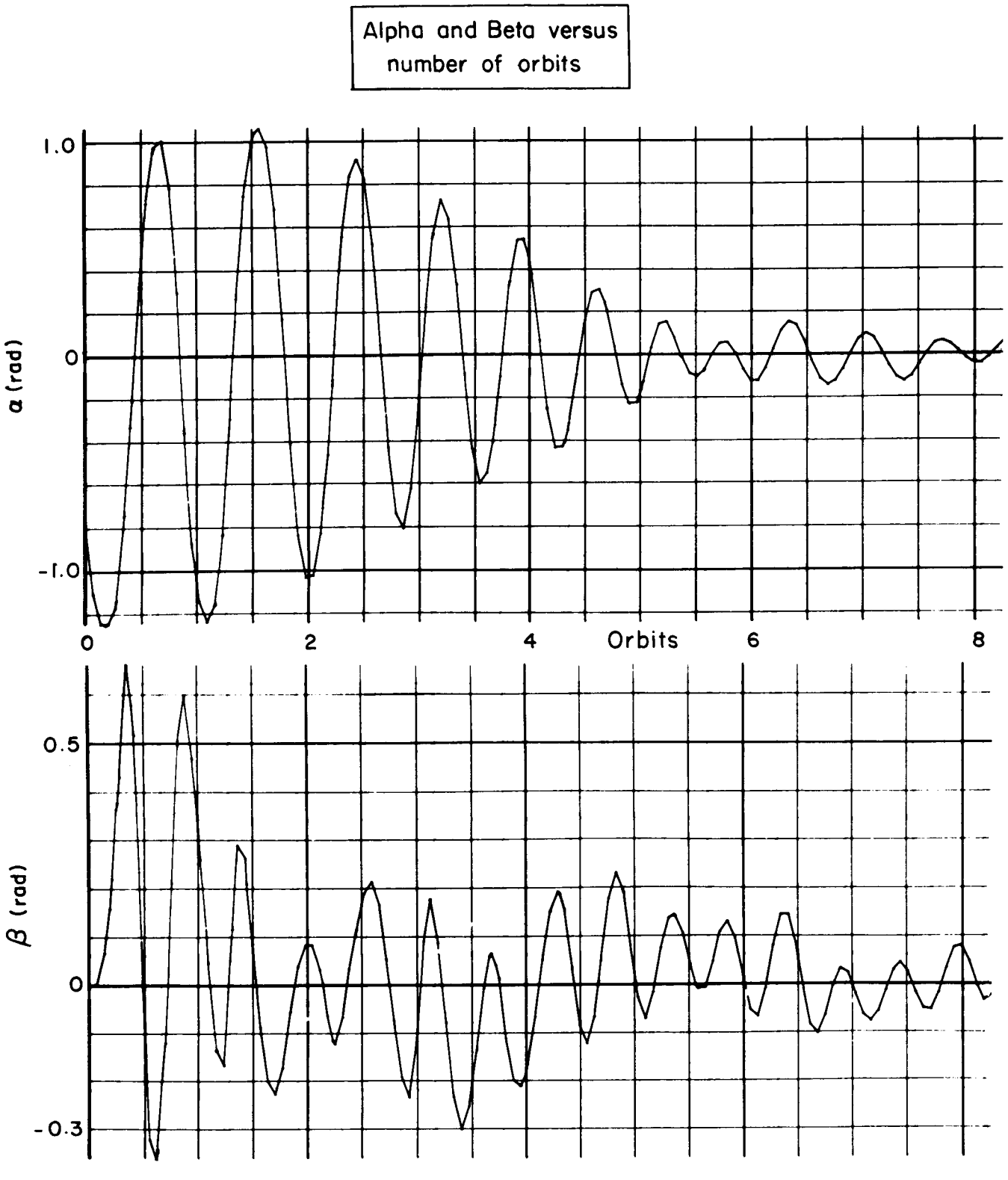

Fig. 12 — Transient response to initial yaw angular rate error

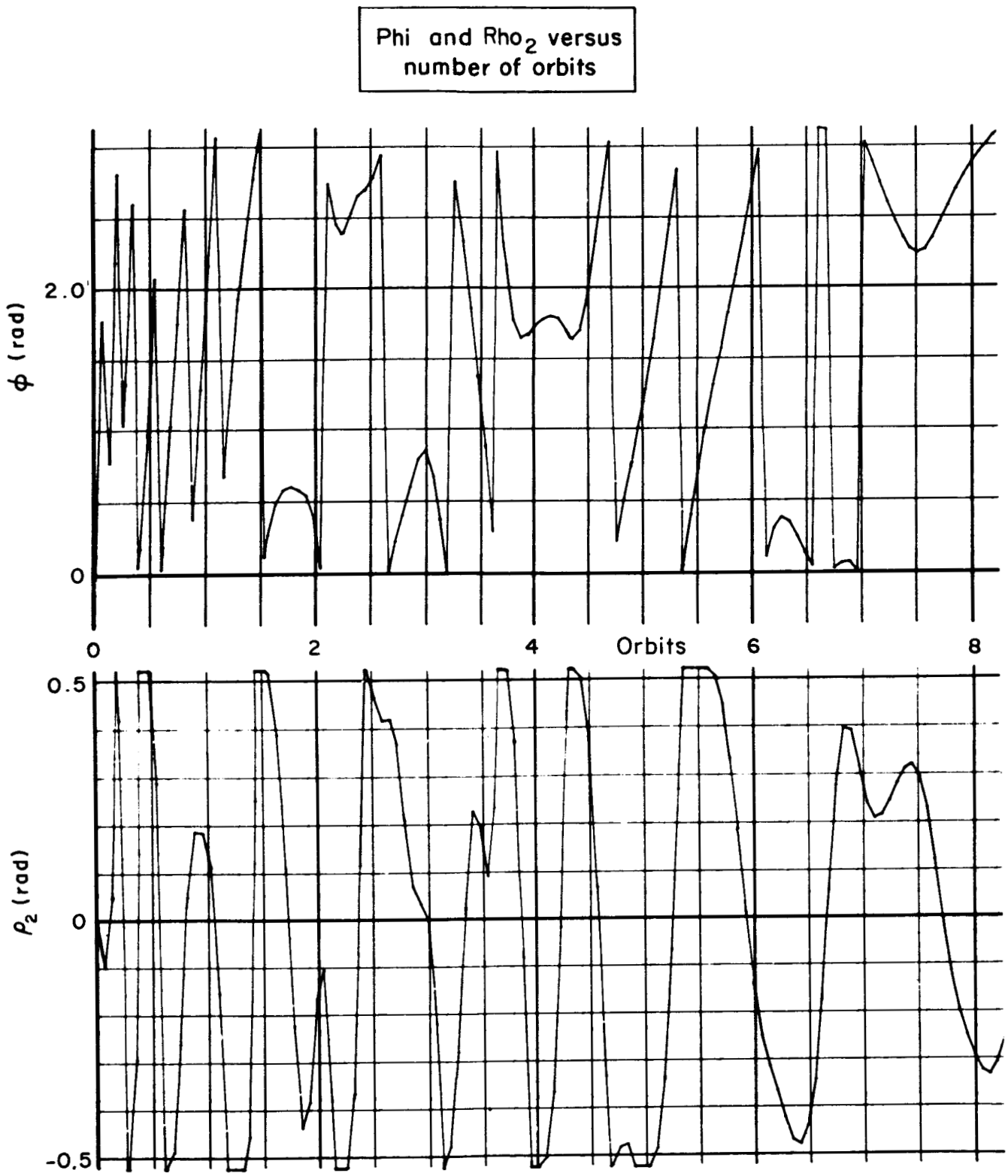
Phi and Rho$_2$ versus number of orbits
2.0
0
ϕ (rad)
0
2
4
Orbits
6
8
0.5
0
-0.5
ρ_2 (rad)

Fig. 12 (cont.)

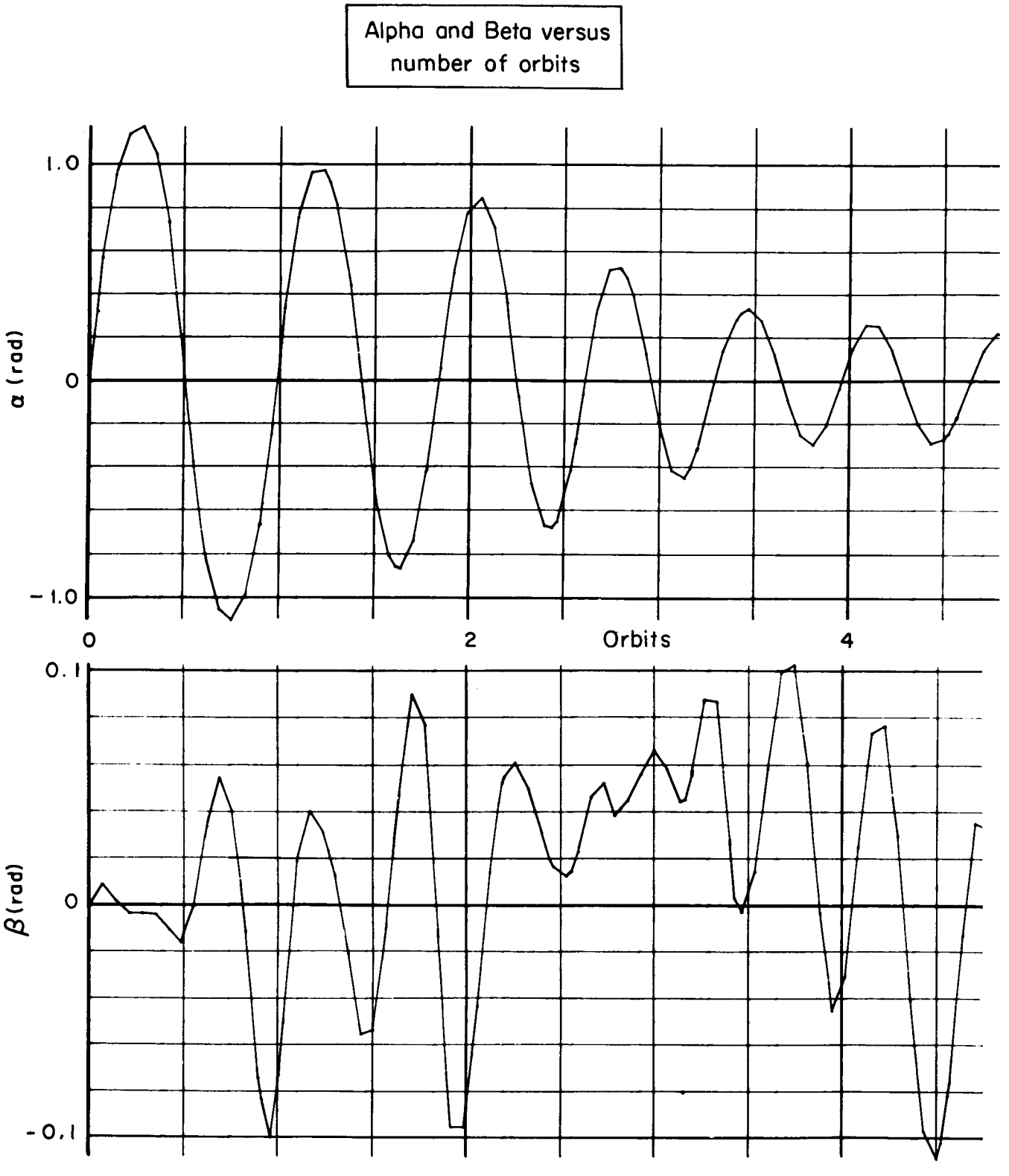

Fig. 13 — Transient response to initial pitch angular rate error

Phi and Rho_2 versus number of orbits

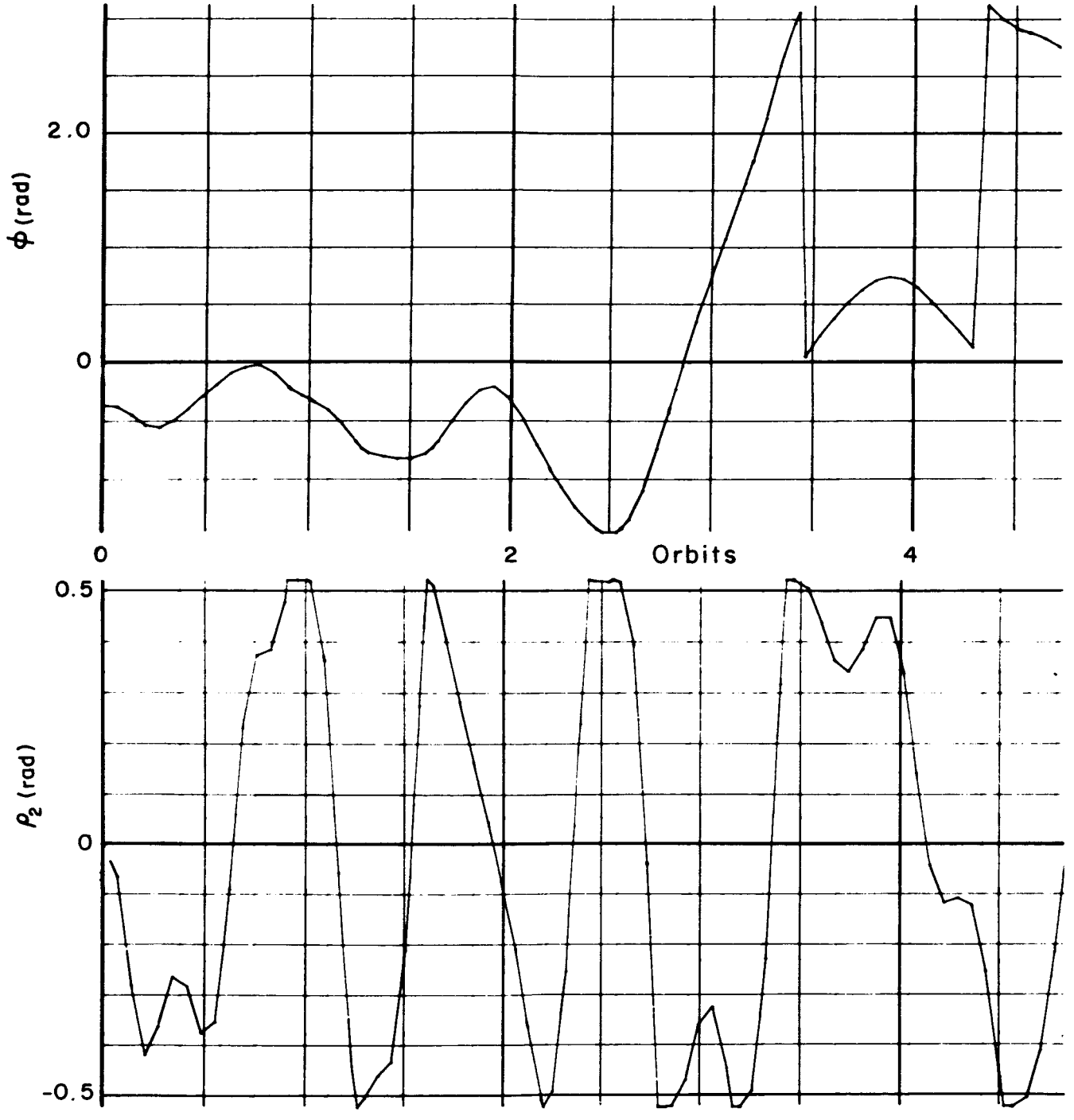

Fig. 13 (cont.)

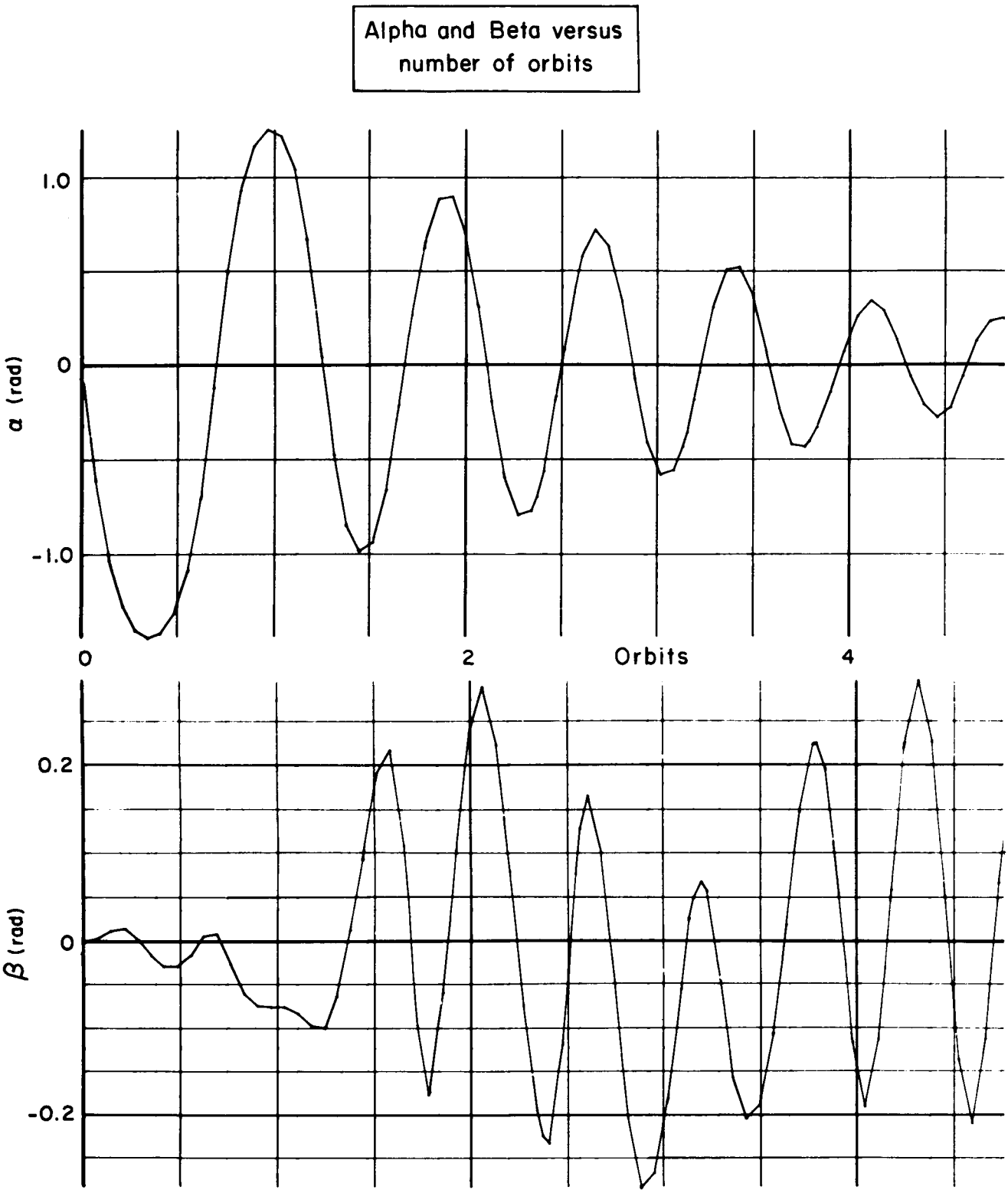

Fig. 14 — Transient response to initial pitch angular rate error

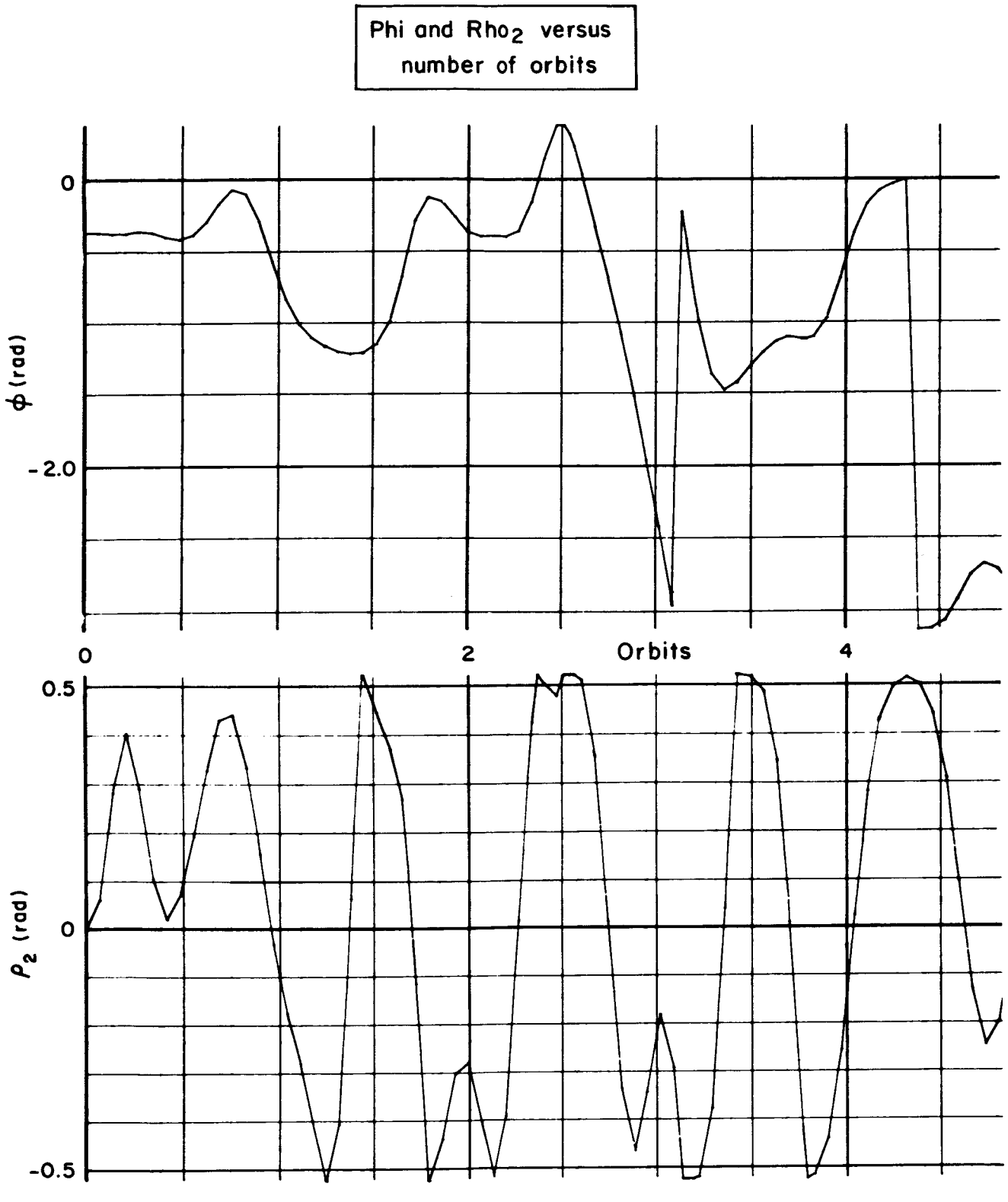
Phi and Rho2 versus number of orbits
0
-2.0
φ (rad)
0
2
Orbits
4
0.5
0
-0.5
ρ2 (rad)

Fig. 14 (cont.)

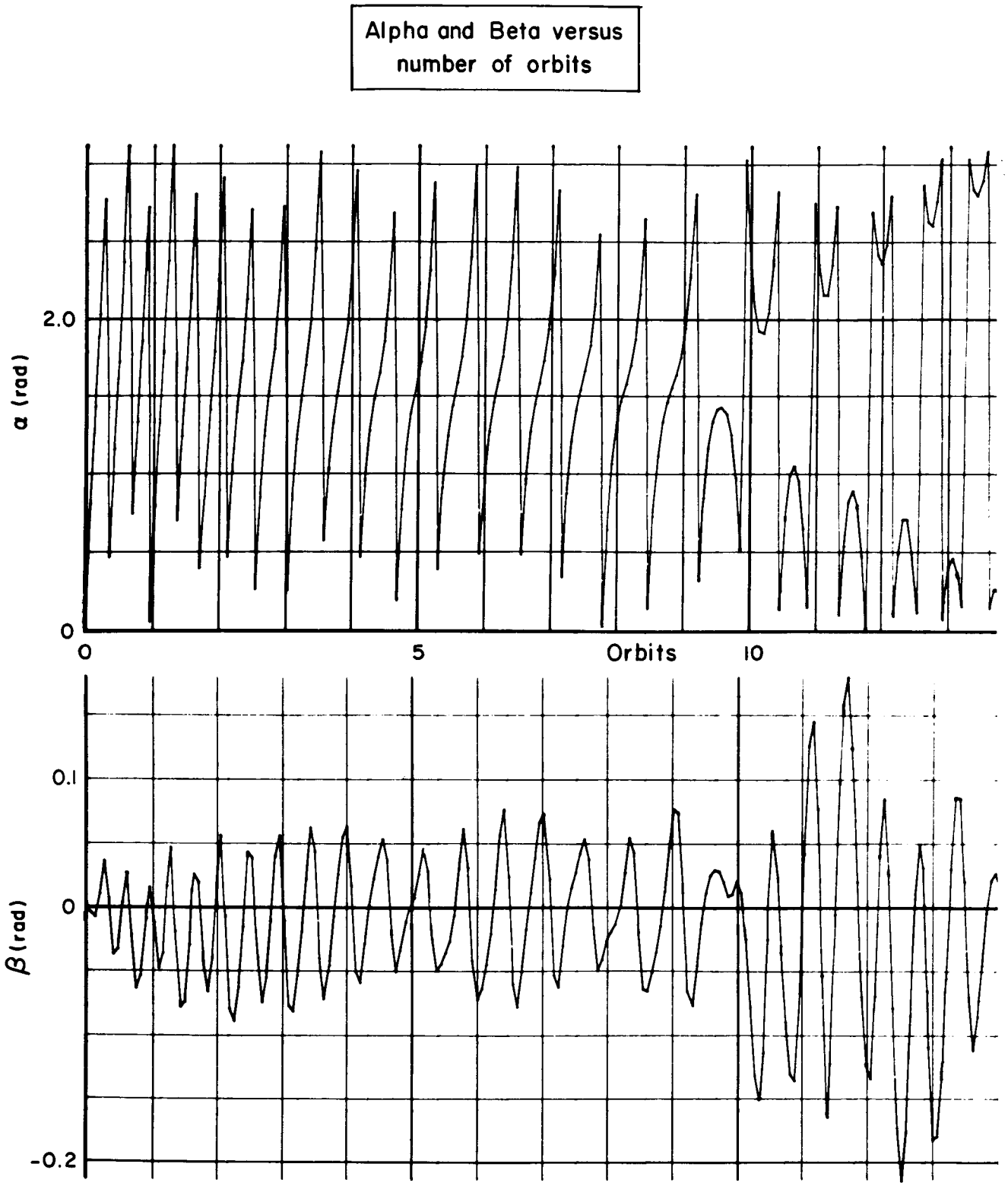

Fig. 15 — Transient response to initial pitch angular rate error

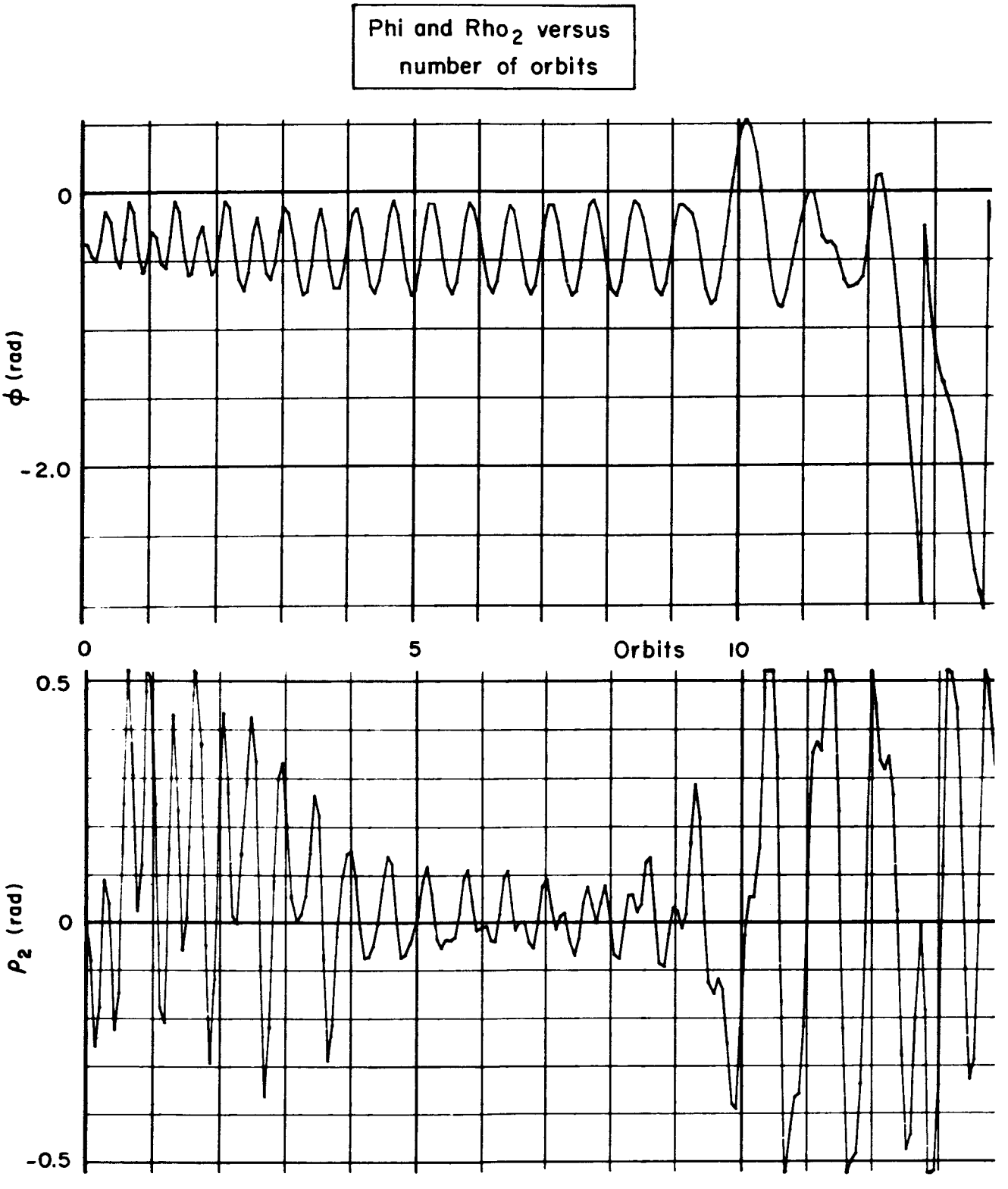
Phi and Rho$_2$ versus number of orbits
0
-2.0
ϕ (rad)
0
5
Orbits
10
0.5
0
-0.5
ρ_2 (rad)

Fig. 15 (cont.)

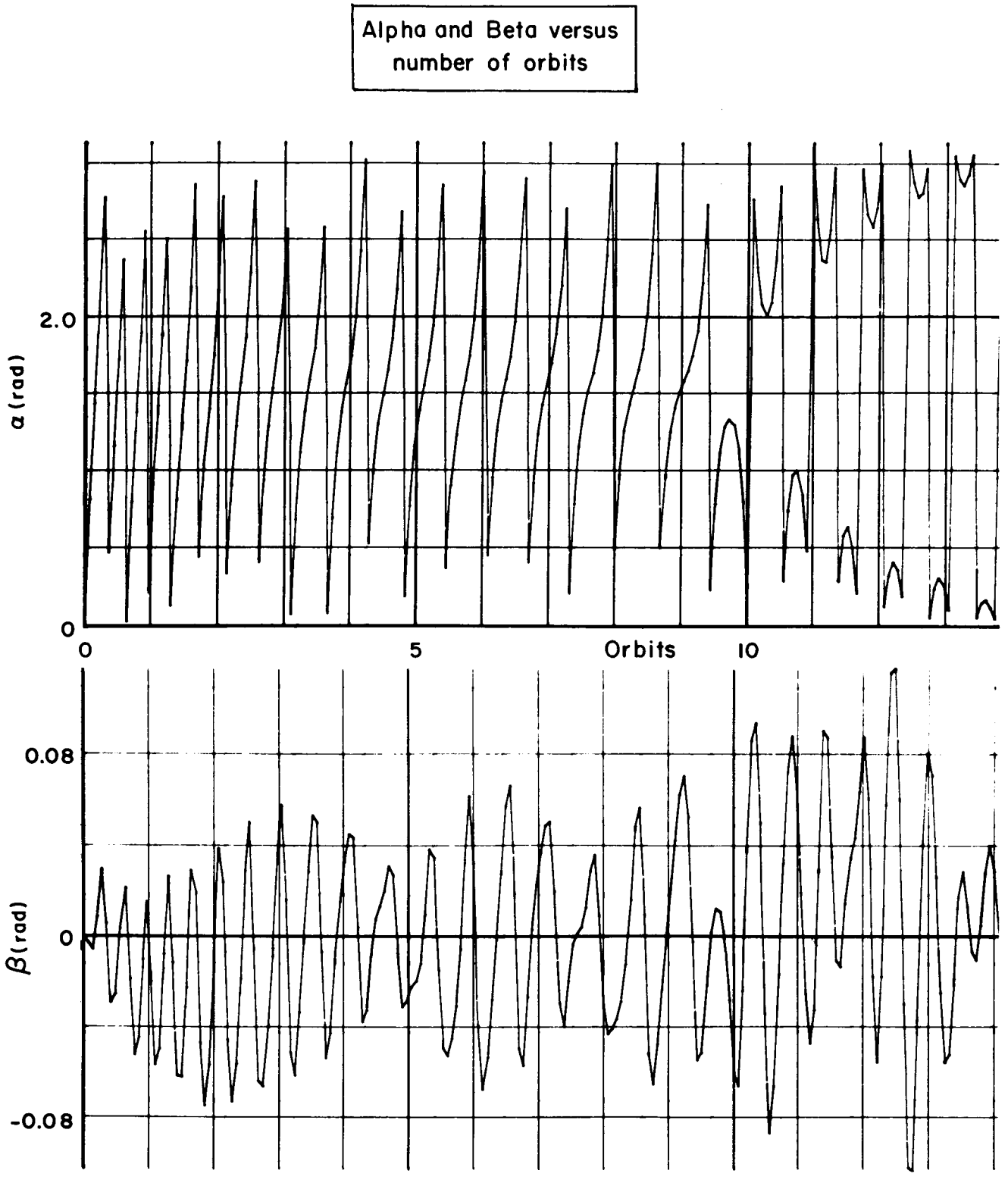

Fig. 16 — Transient response to initial pitch angular rate error

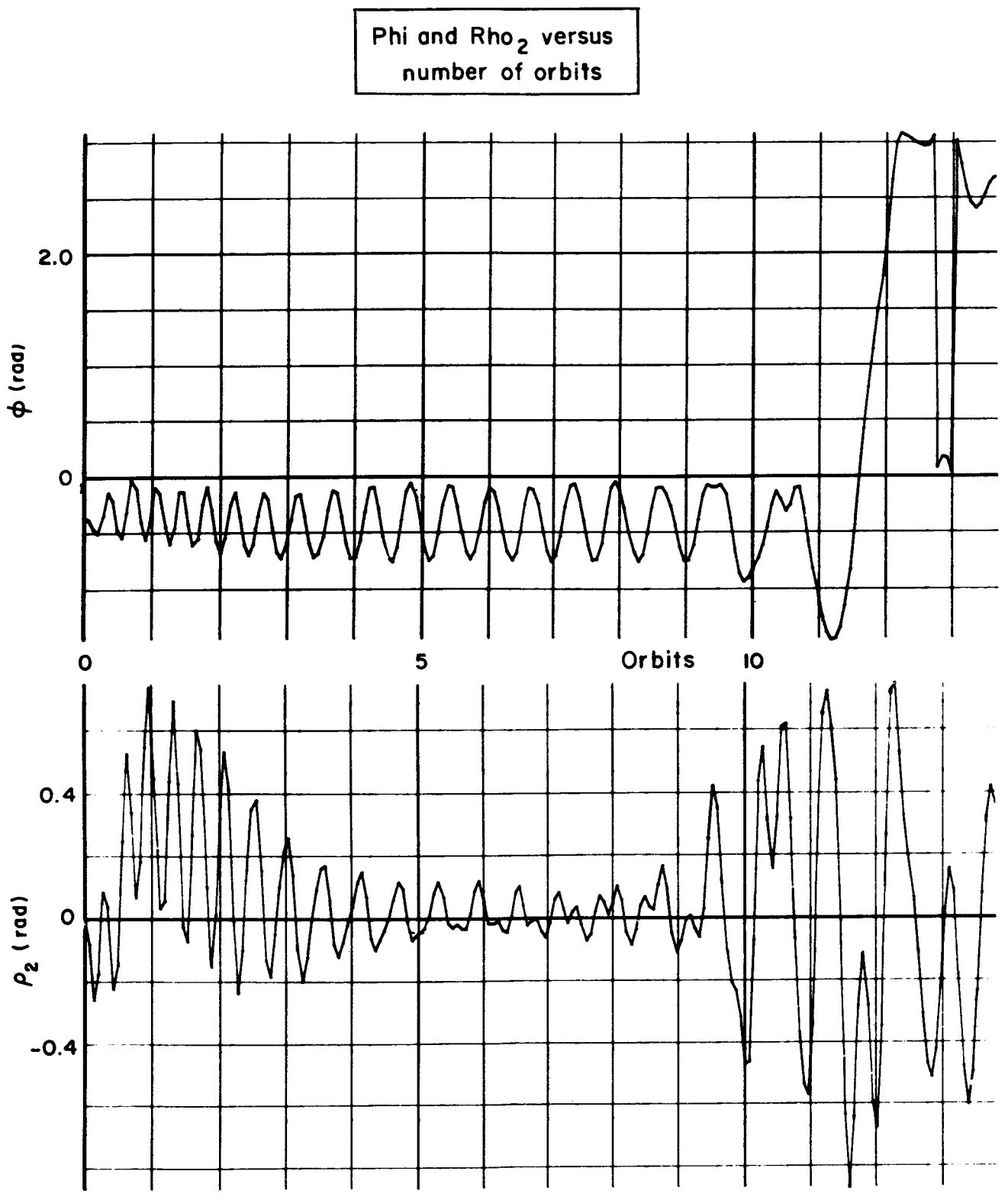
Phi and Rho 2 versus number of orbits
2.0
0
φ (rad)
0
5
Orbits
10
0.4
0
-0.4
ρ2 (rad)

Fig. 16 (cont.)

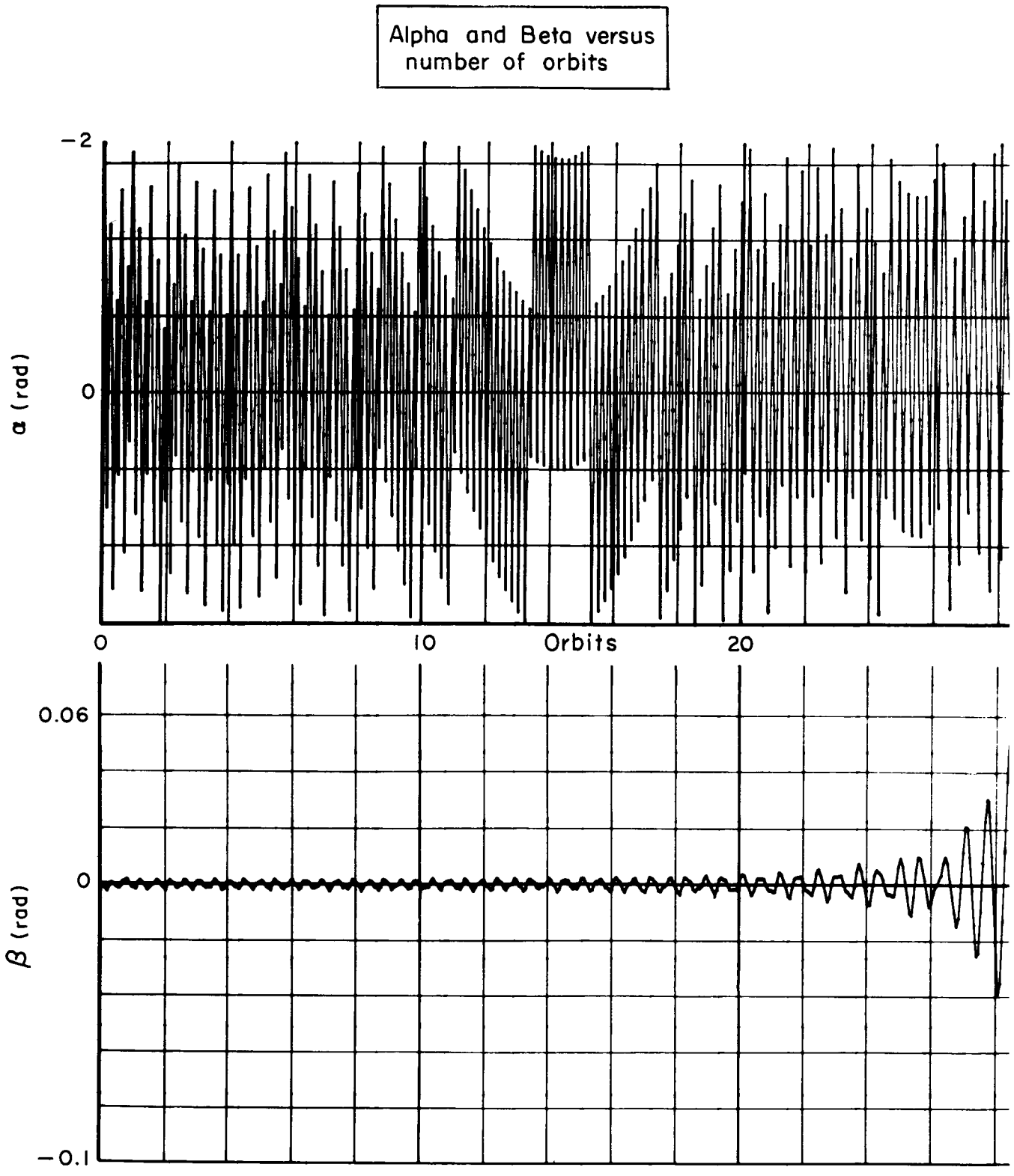

Fig.17 — Transient response to initial pitch angular rate error

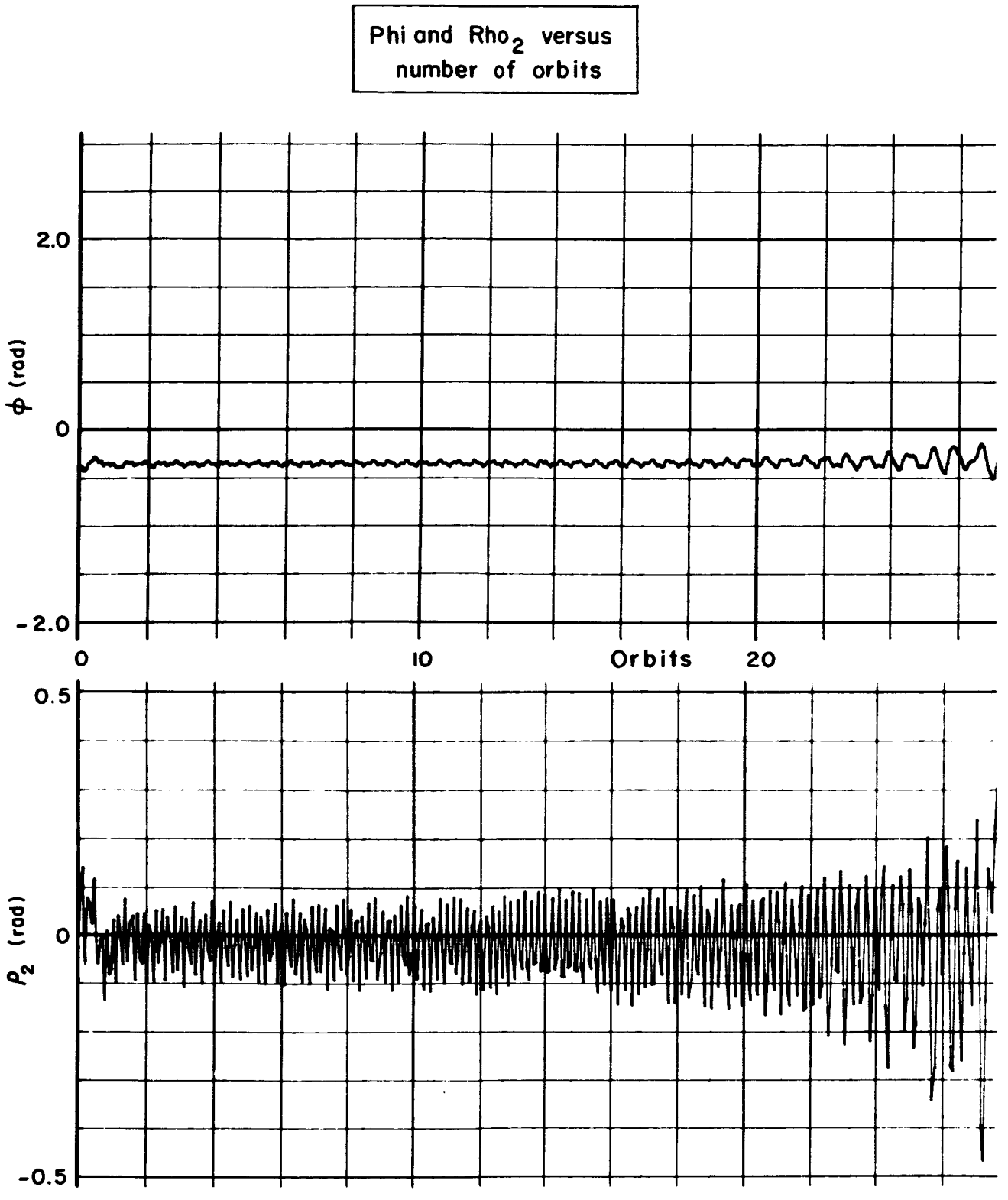
Phi and Rho$_2$ versus number of orbits
2.0
0
-2.0
ϕ (rad)
0
10
Orbits
20
0.5
0
-0.5
ρ_2 (rad)

Fig. 17 (cont.)

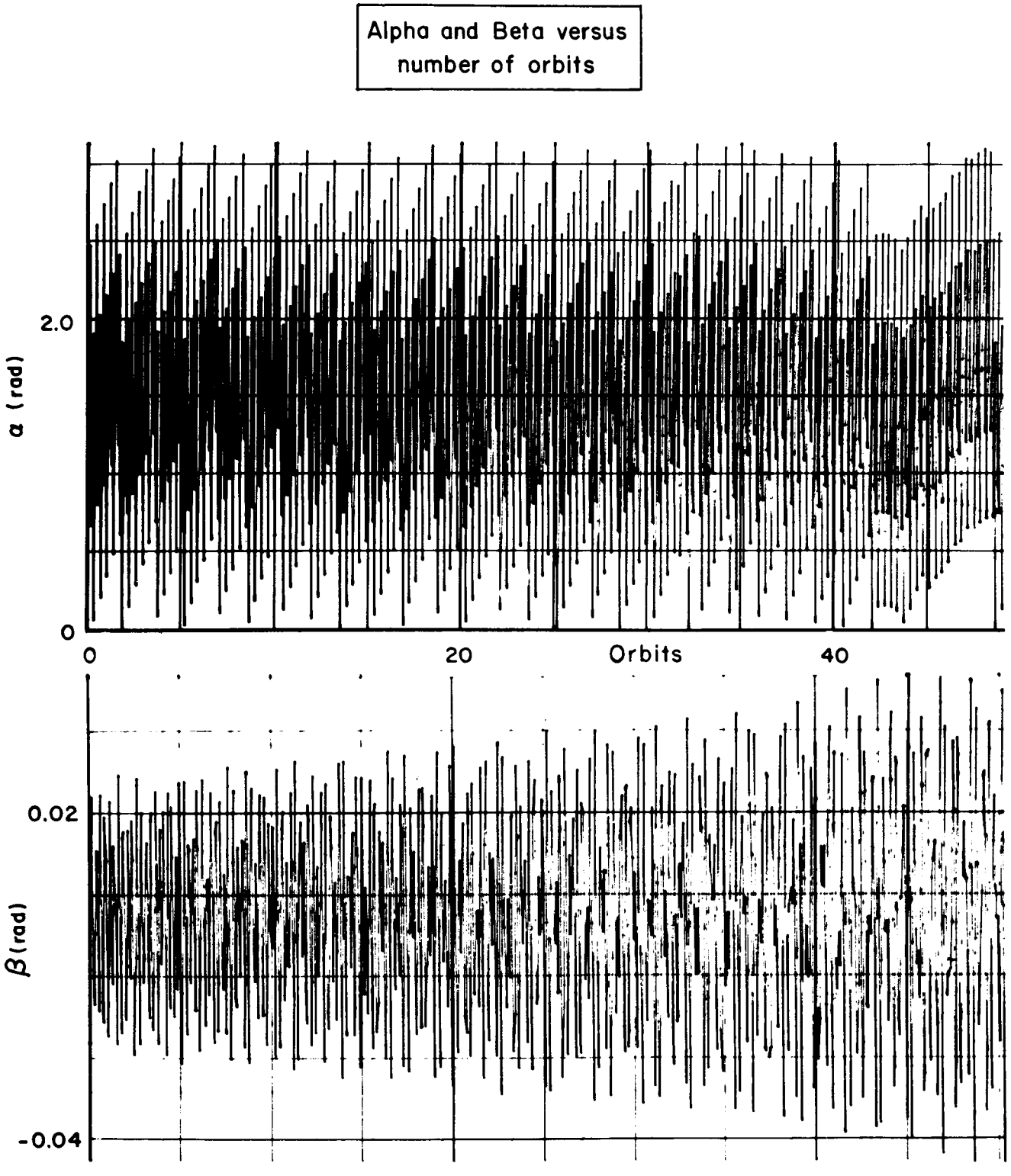

Fig. 18 — Transient response to initial pitch angular rate error

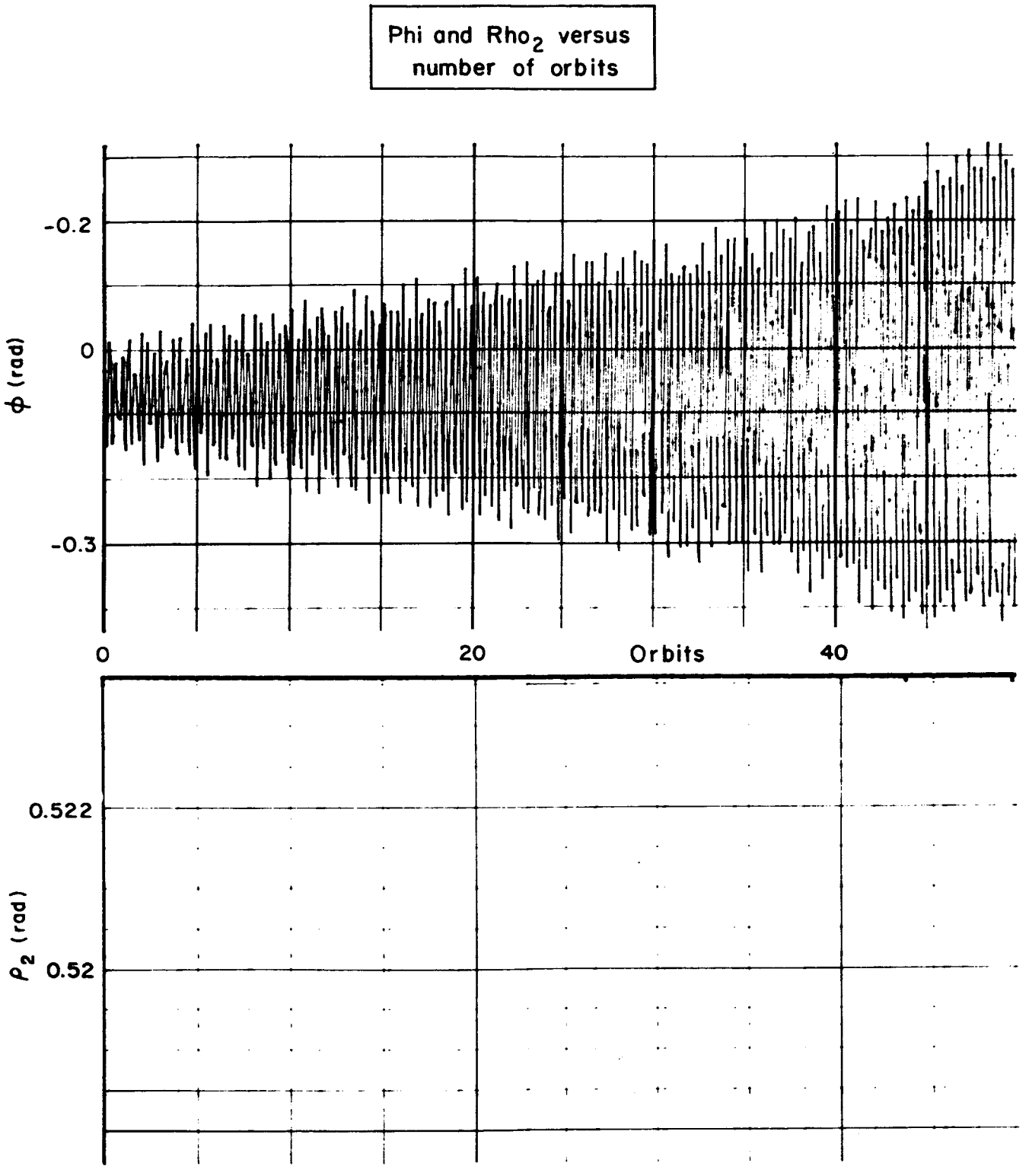
Phi and Rho$_2$ versus number of orbits
-0.2
0
-0.3
ϕ (rad)
0
20
Orbits
40
0.522
0.52
ρ_2 (rad)

Fig. 18 (cont.)

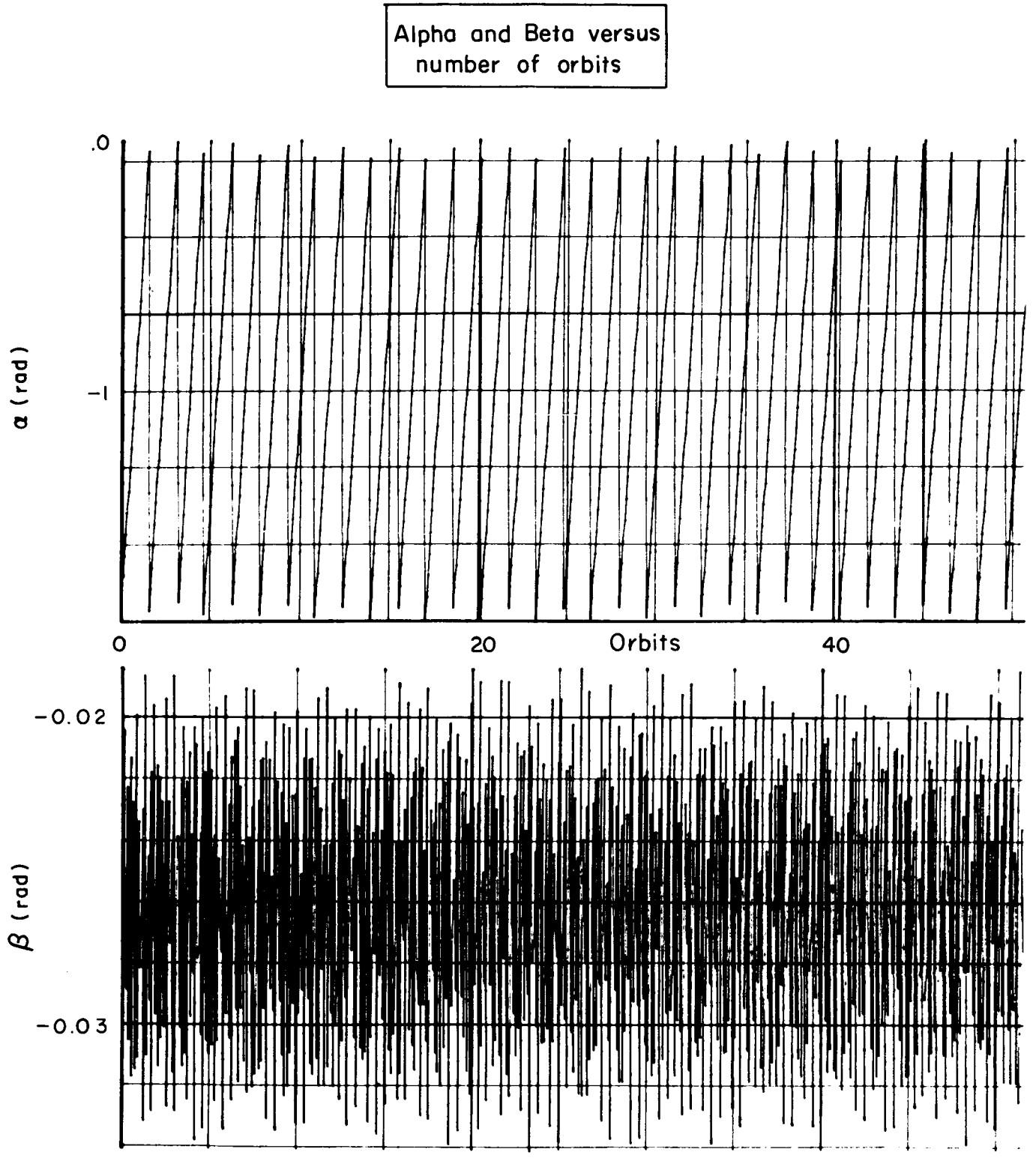

Fig. 19 — Transient response to initial pitch angular rate error

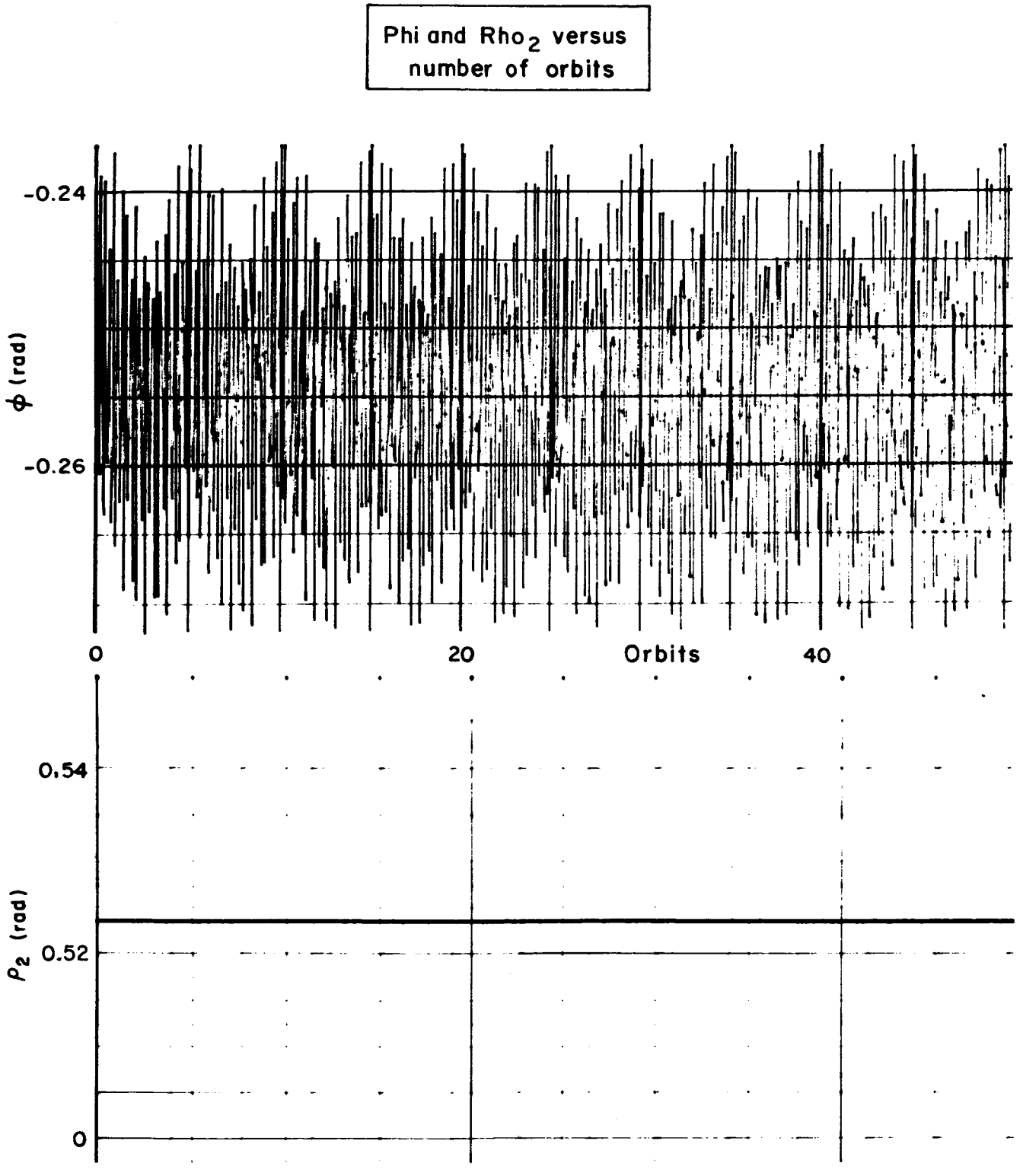
Phi and Rho$_2$ versus number of orbits
-0.24
-0.26
ϕ (rad)
0
20
Orbits
40
0.54
0.52
0
ρ_2 (rad)

Fig. 19 (cont.)

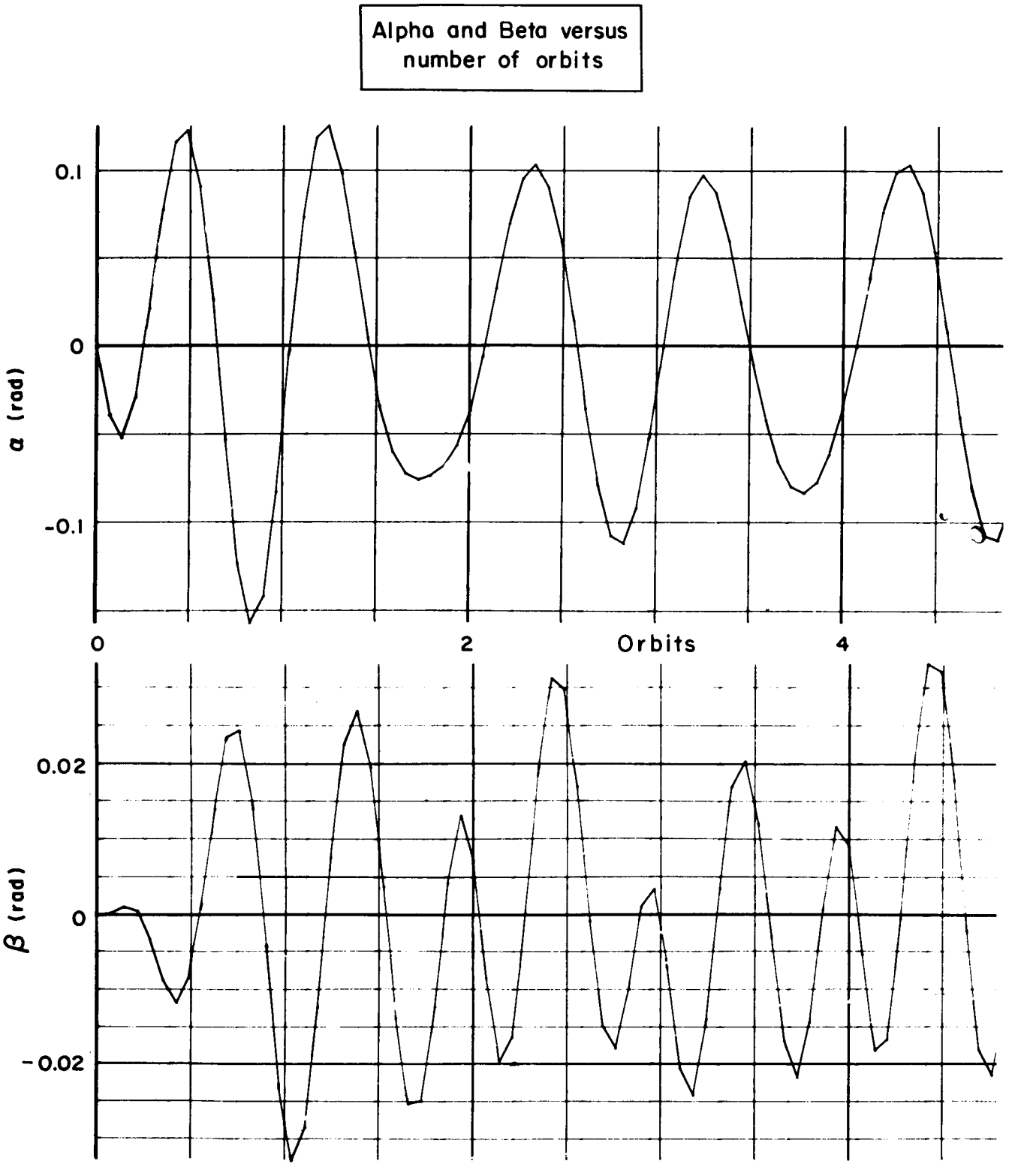

Fig. 20 — Forced response due to orbital motion

Phi and Rho_2 versus number of orbits

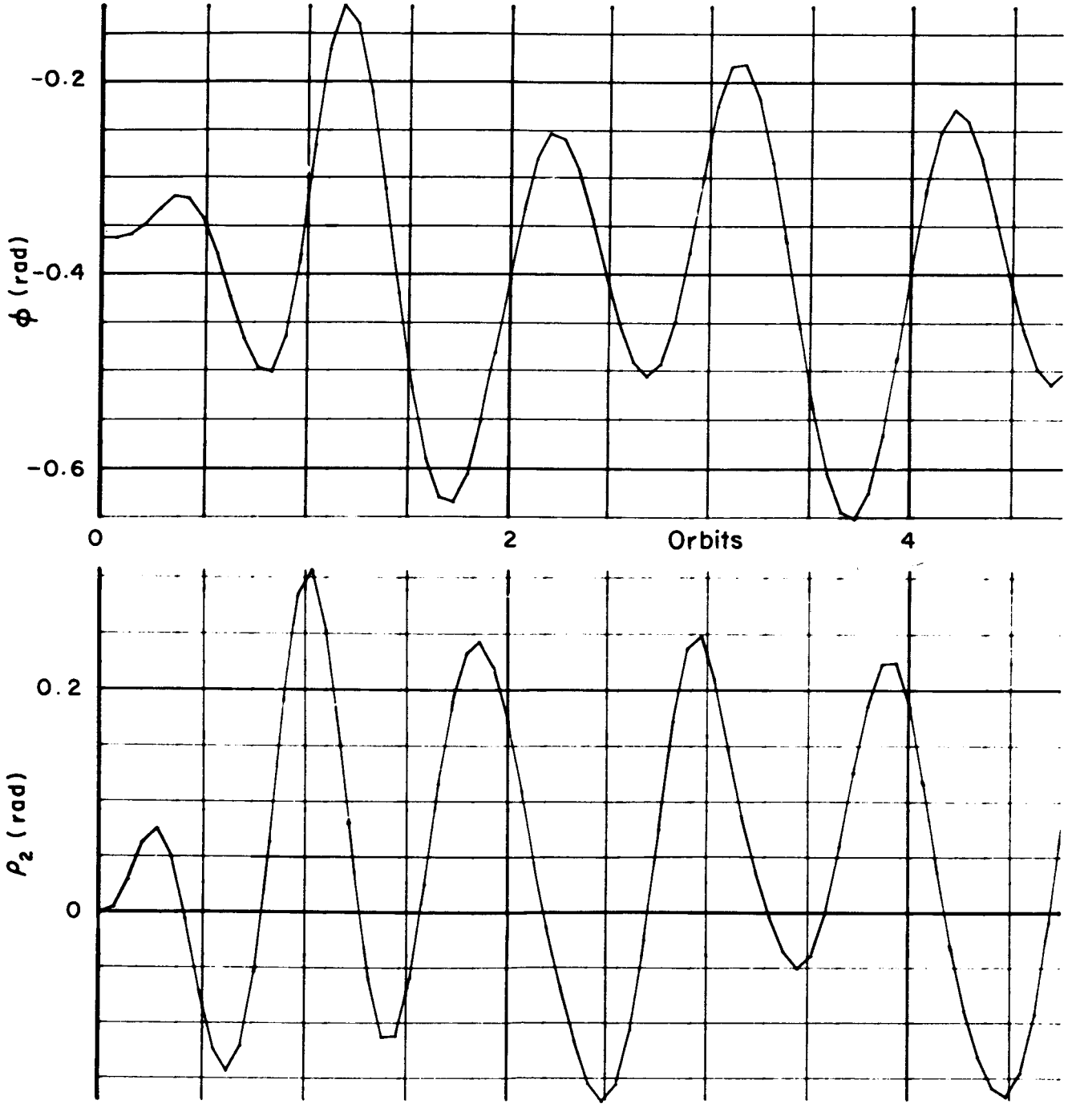

Fig. 20 (cont.)

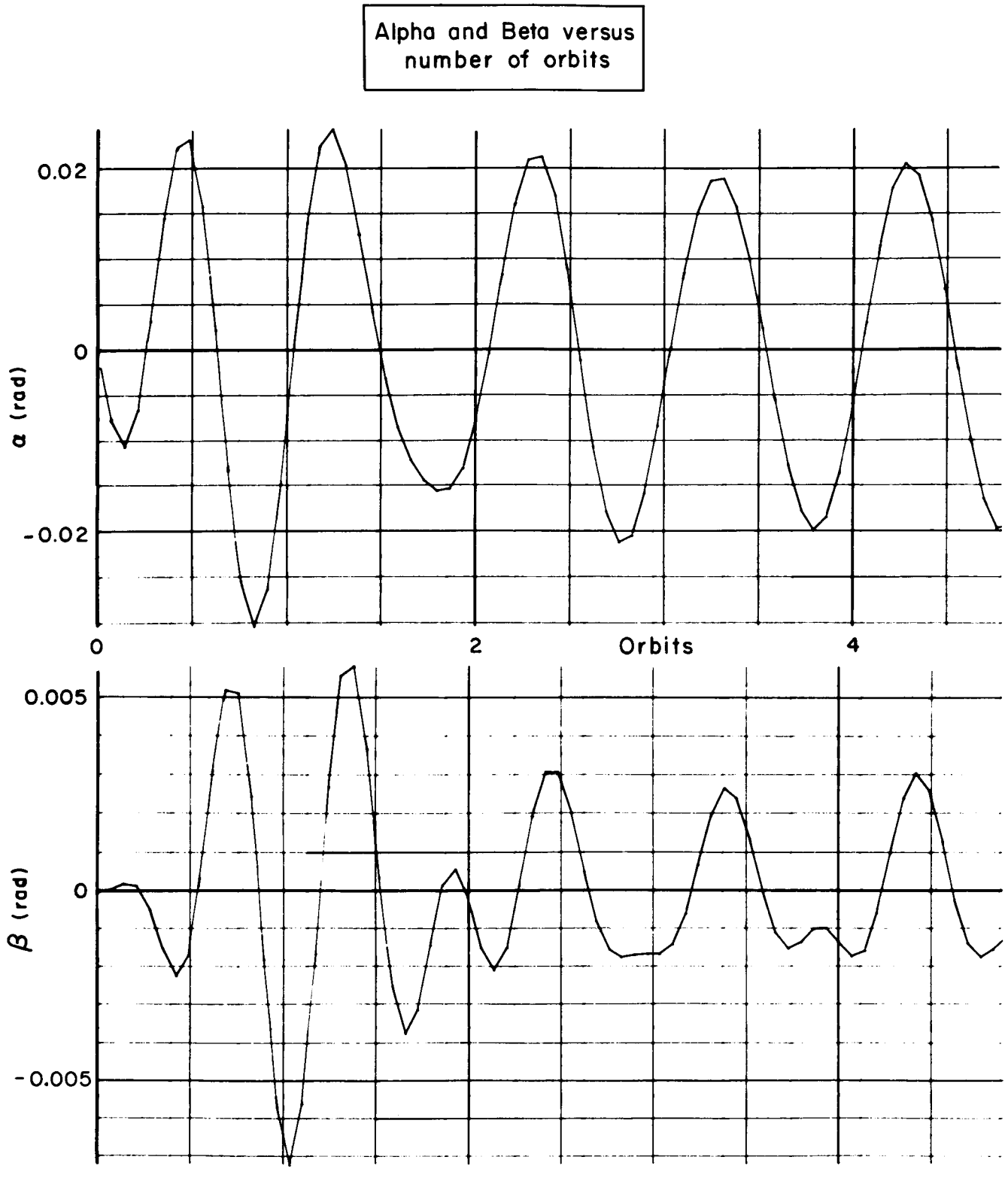

Fig. 21 — Forced response due to orbital motion

Phi and Rho_2 versus number of orbits

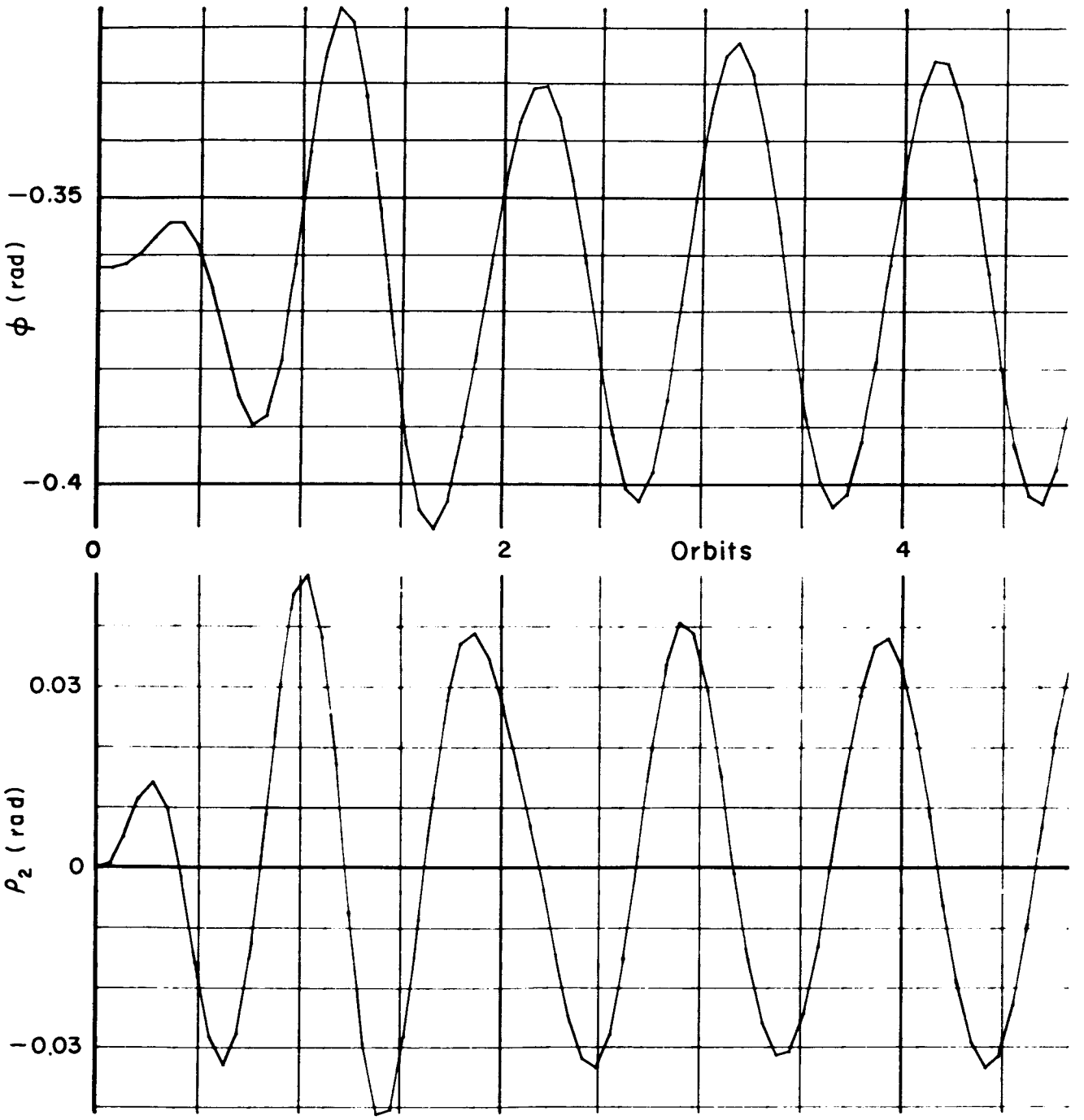

Fig. 21 (cont.)

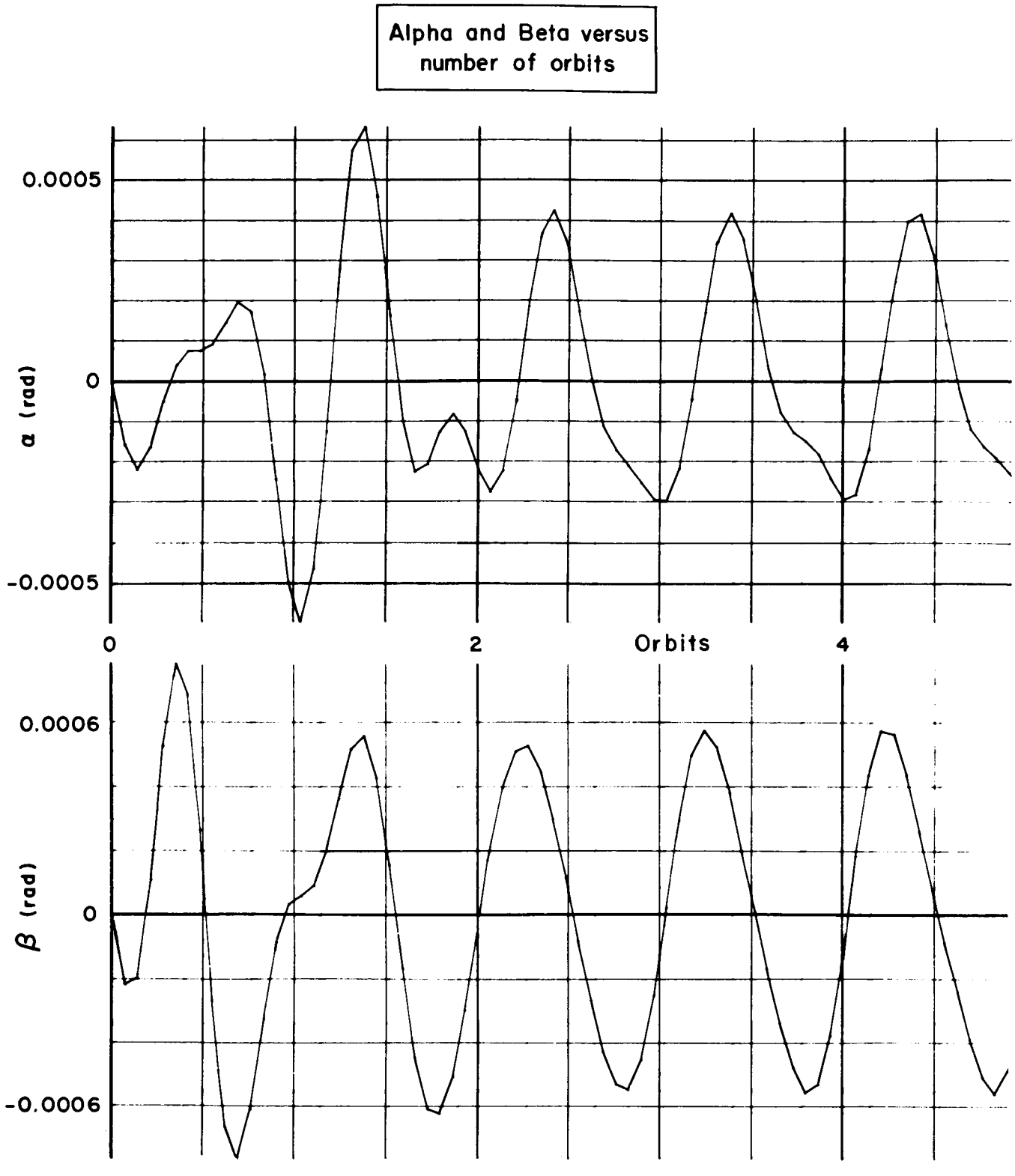

Fig. 22 — Forced response due to orbital motion

Phi and Rho_2 versus number of orbits

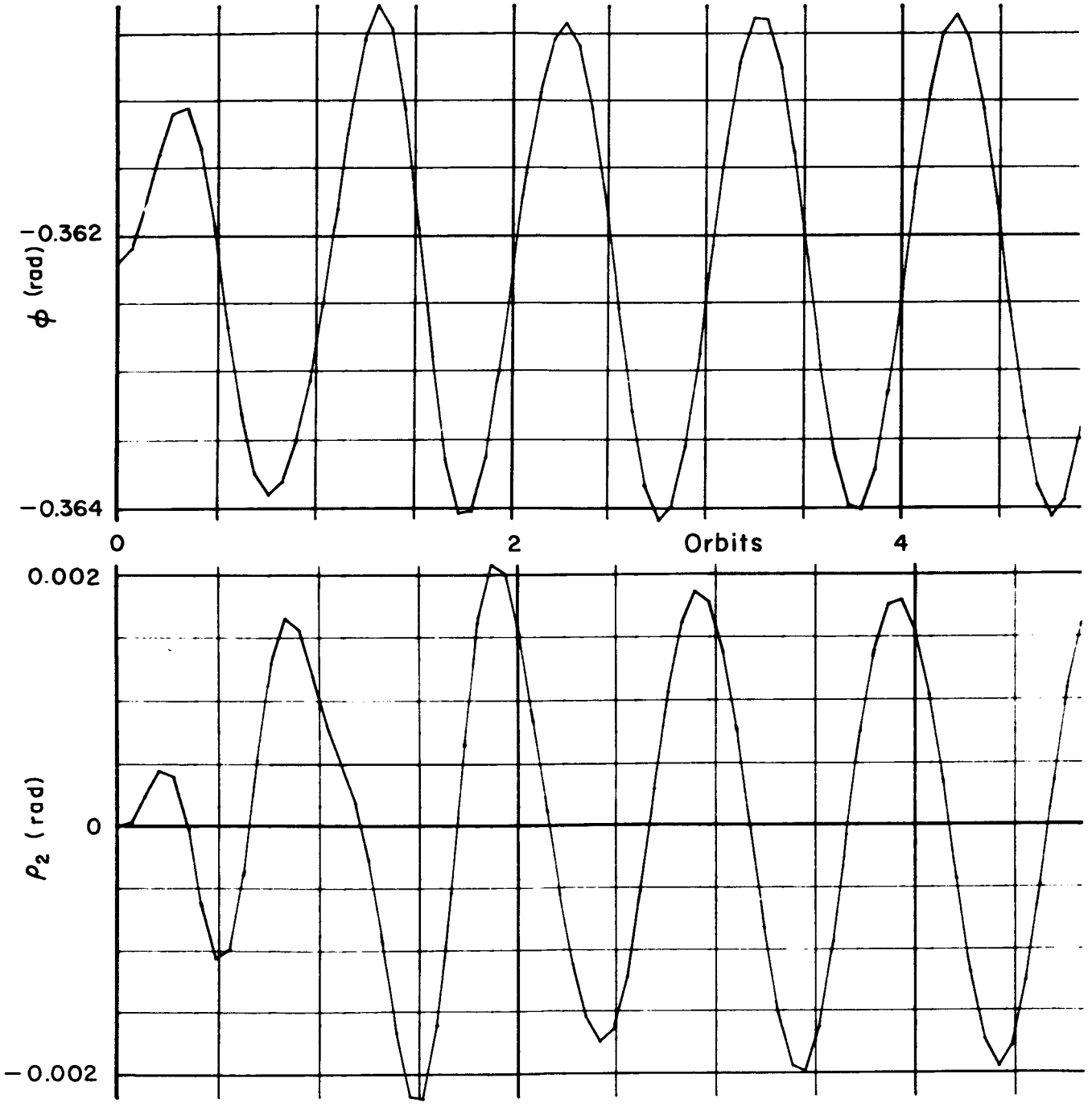

Fig. 22 (cont.)

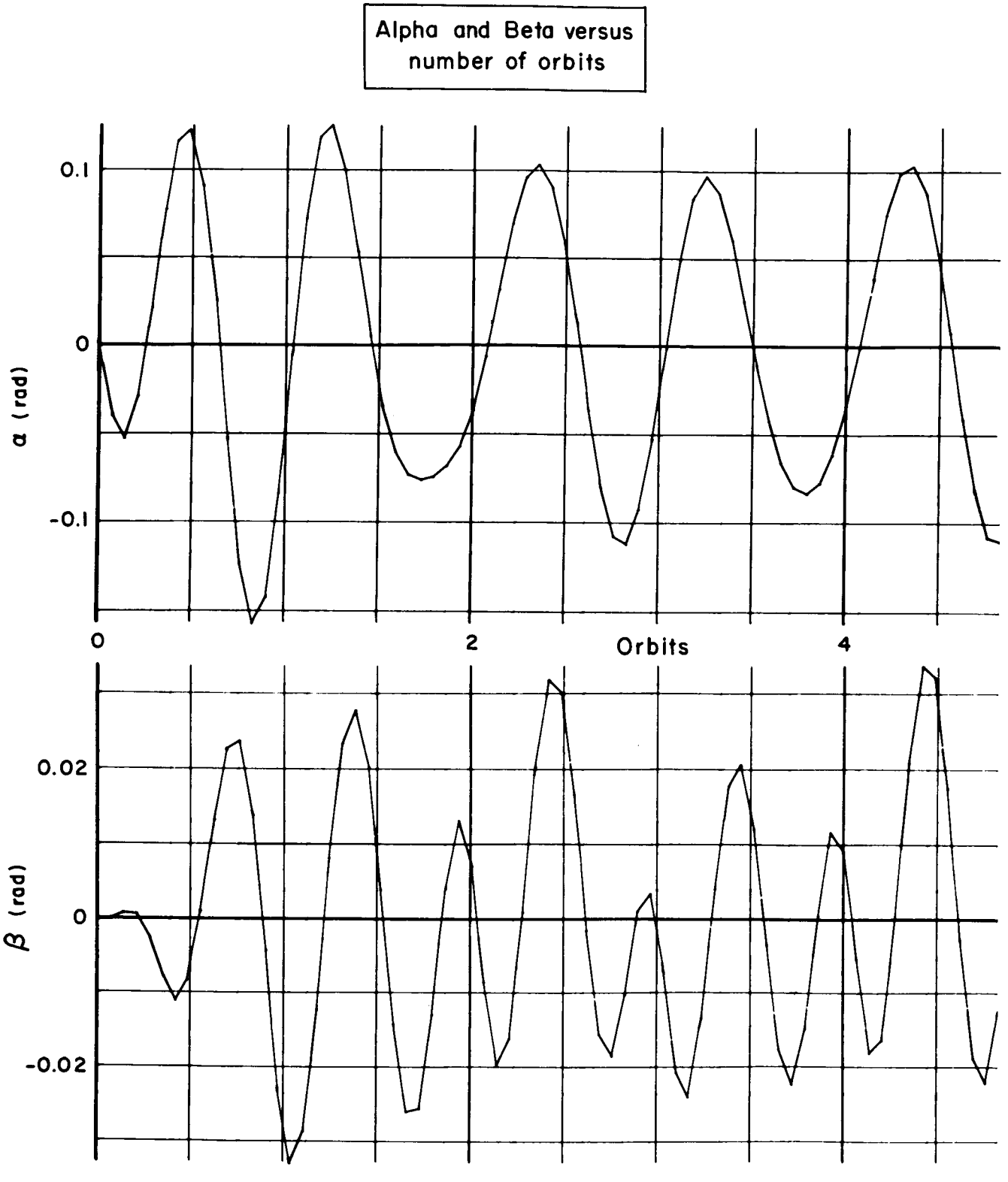

Fig. 23 — Forced response due to orbital motion

Phi and Rho_2 versus number of orbits

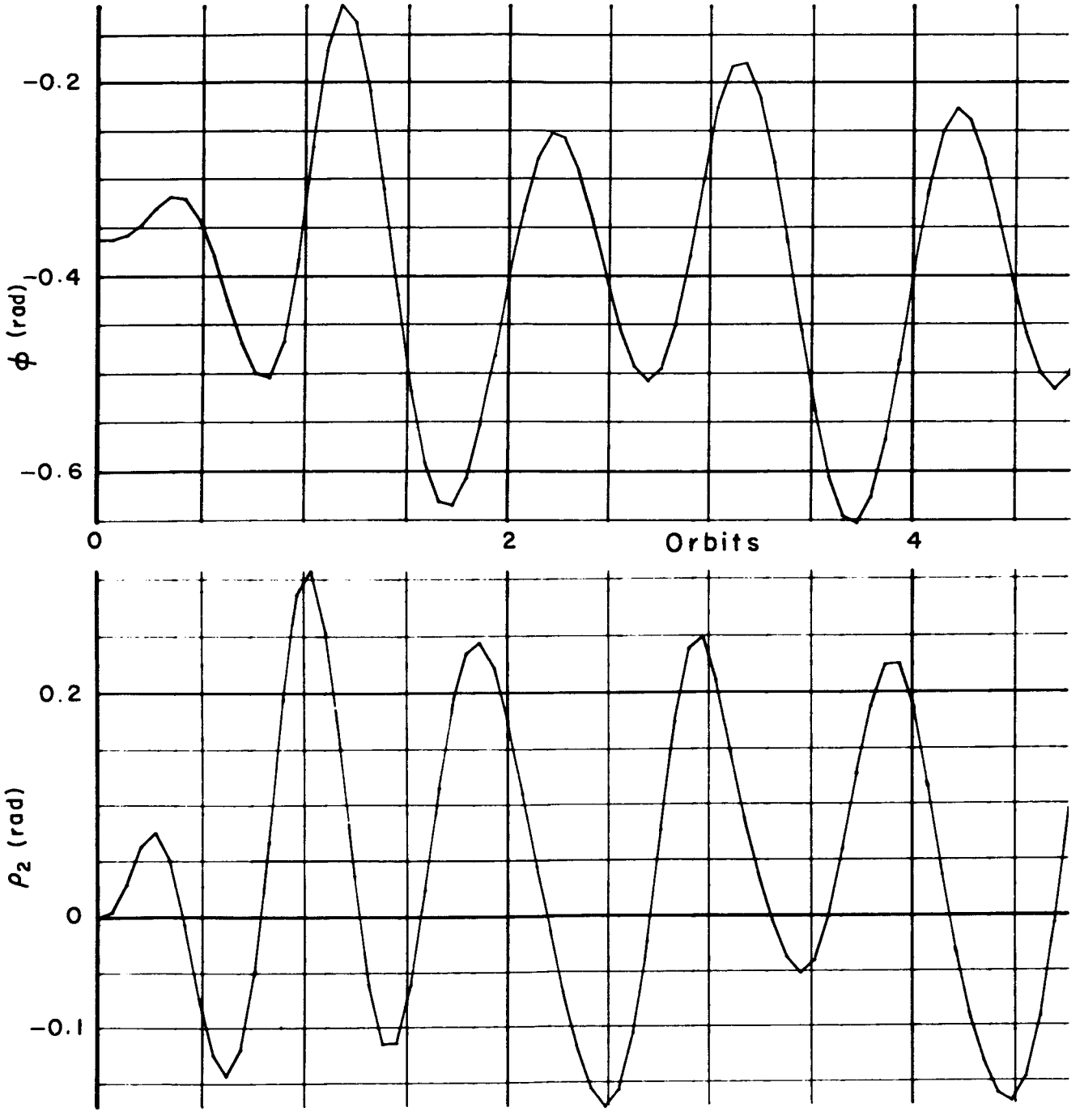

Fig. 23 (cont.)

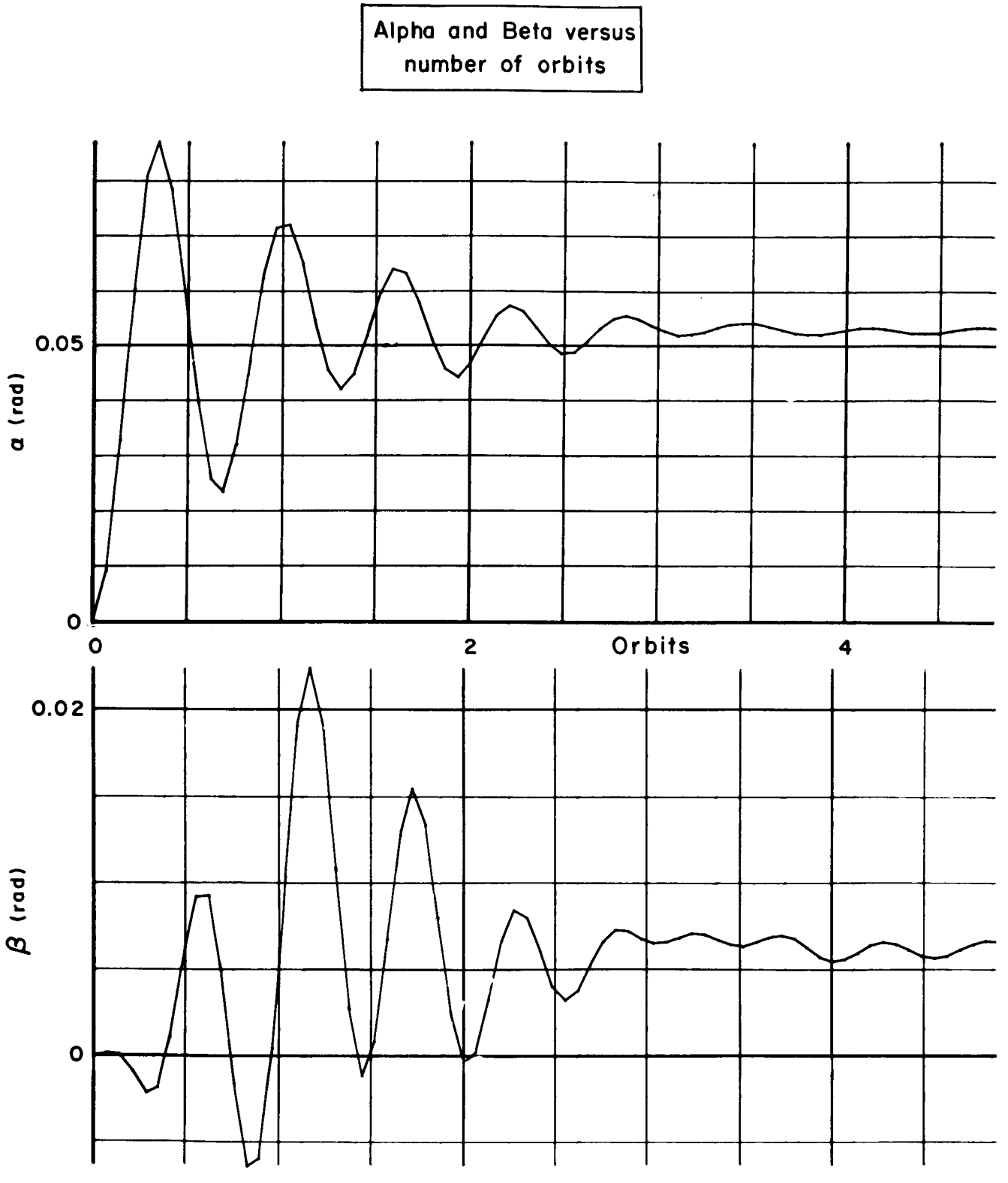

Fig. 24 — Forced response due to constant disturbing torques

Phi and Rho_2 versus number of orbits

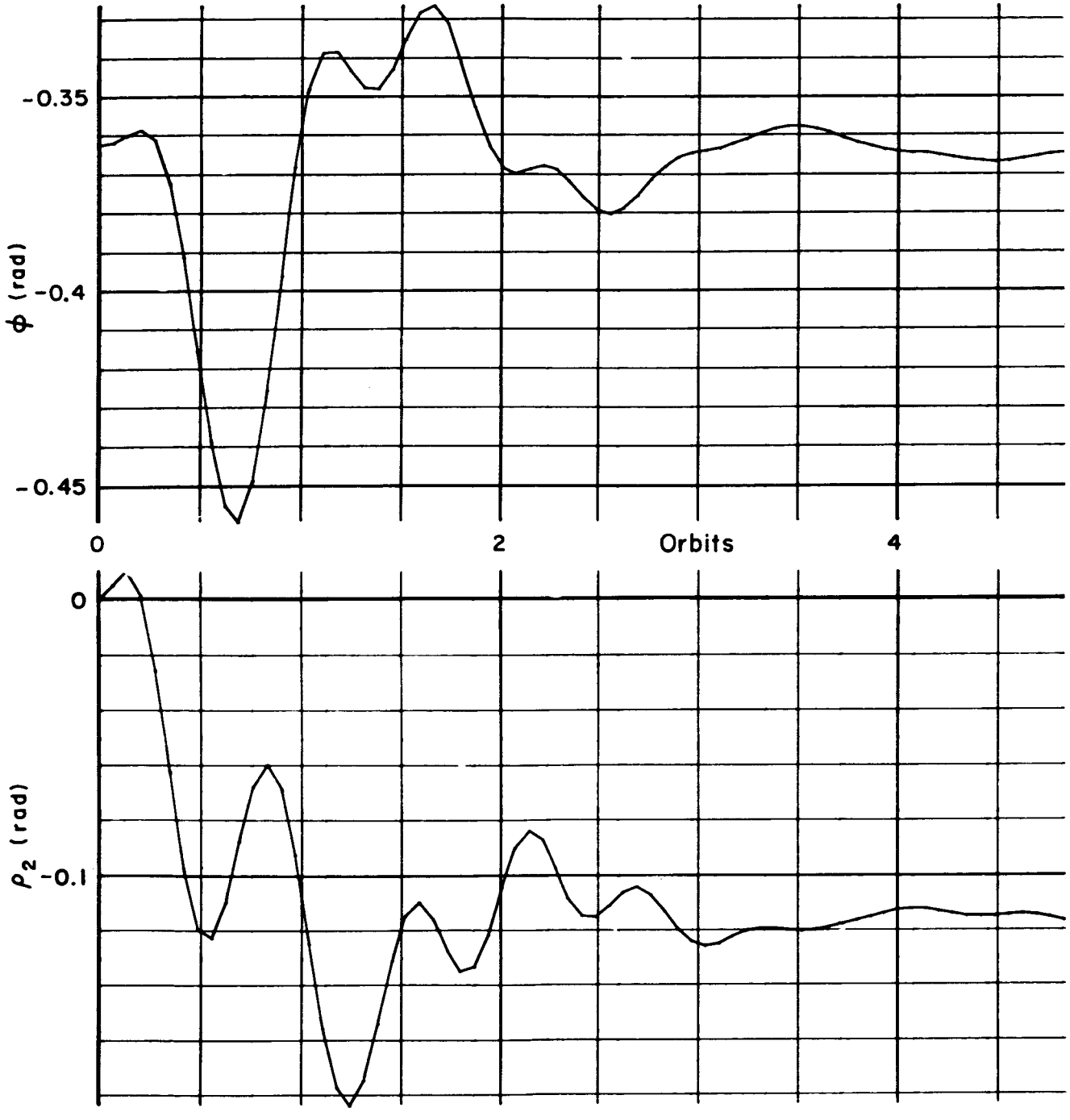

Fig. 24 (cont.)

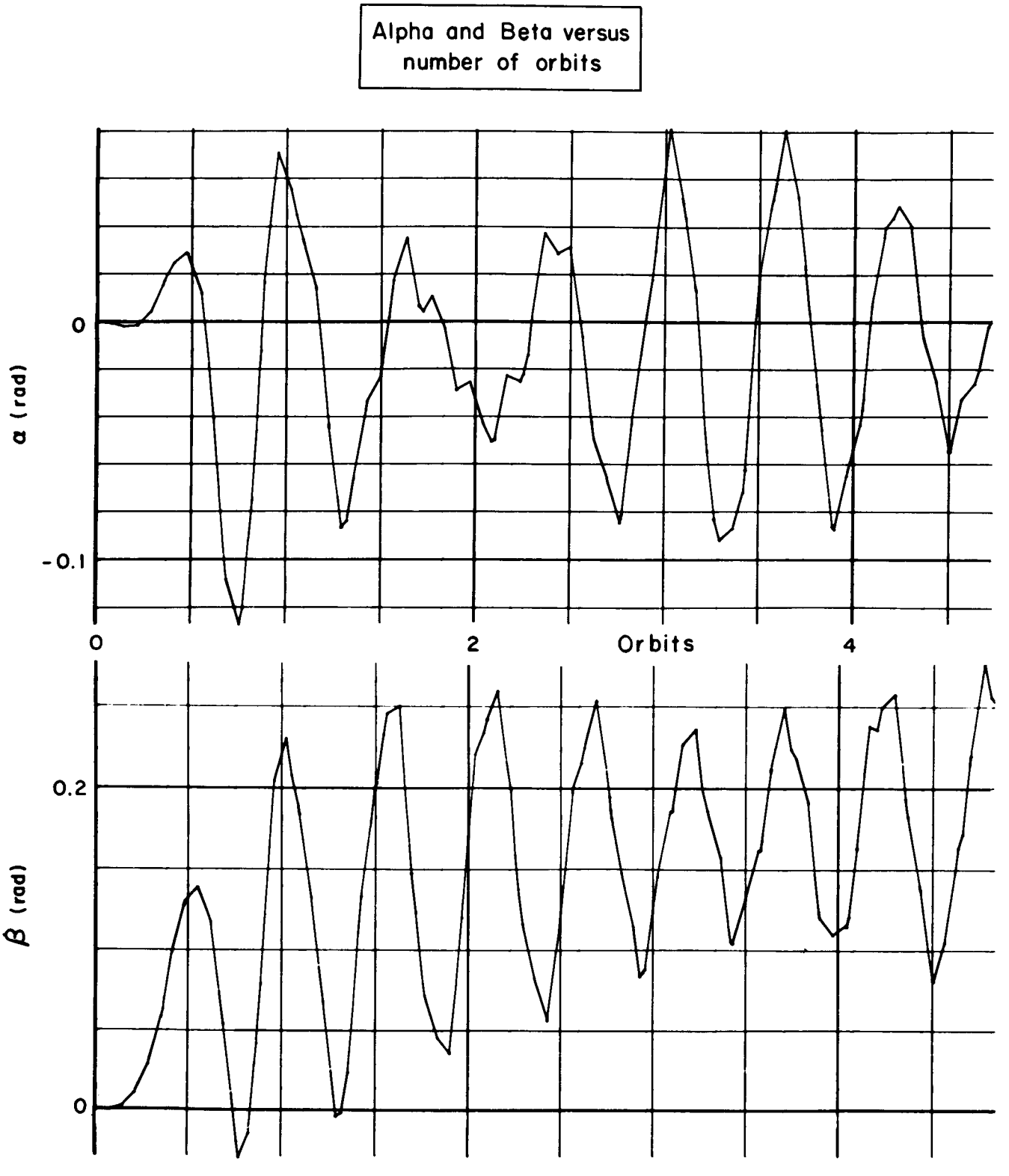

Fig. 25 — Forced response due to constant disturbing torques

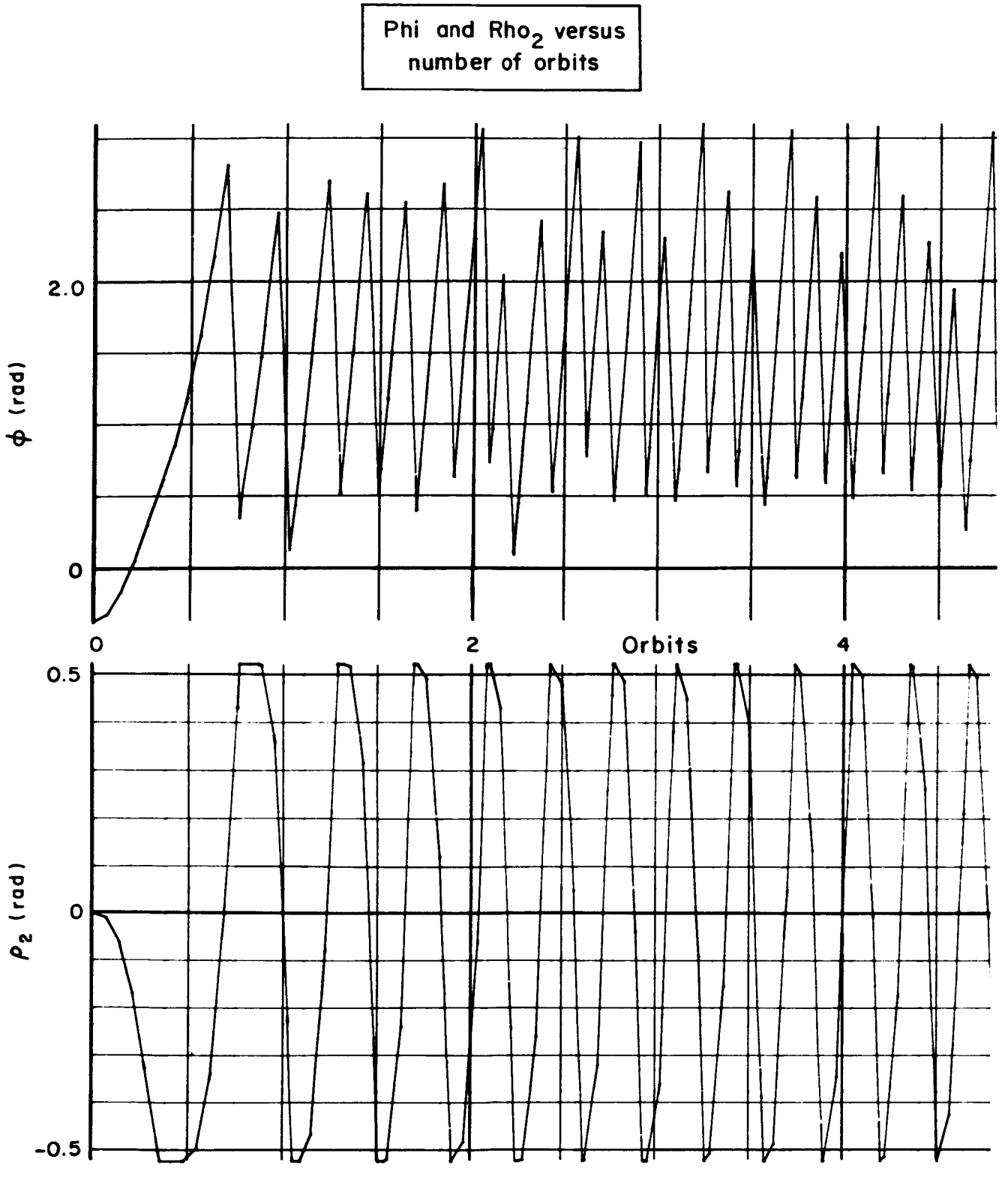
Phi and Rho2 versus number of orbits
2.0
0
ϕ (rad)
0
2
Orbits
4
0.5
0
-0.5
ρ2 (rad)

Fig. 25 (cont.)

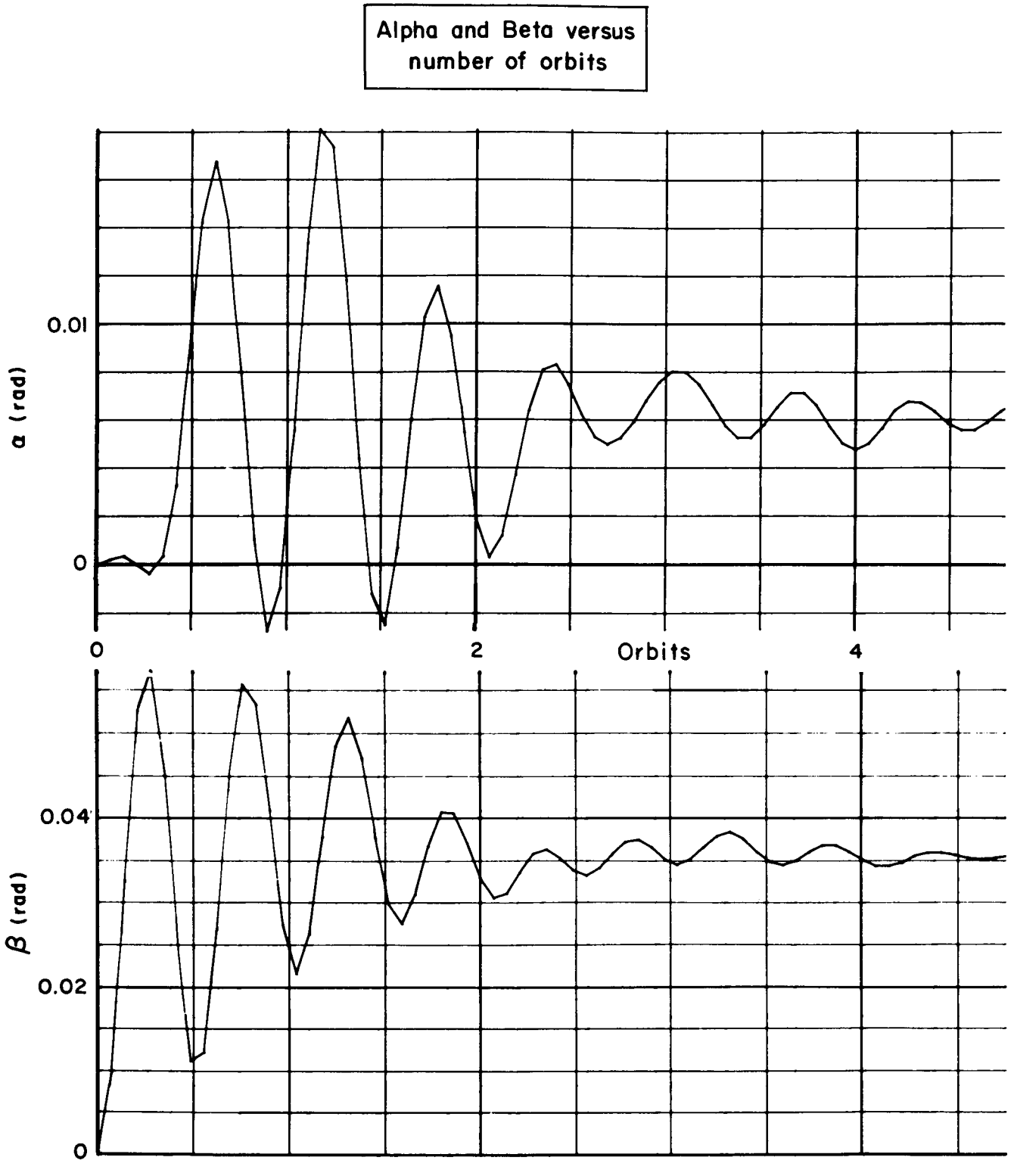

Fig. 26 — Forced response due to constant disturbing torques

Phi and Rho_2 versus number of orbits

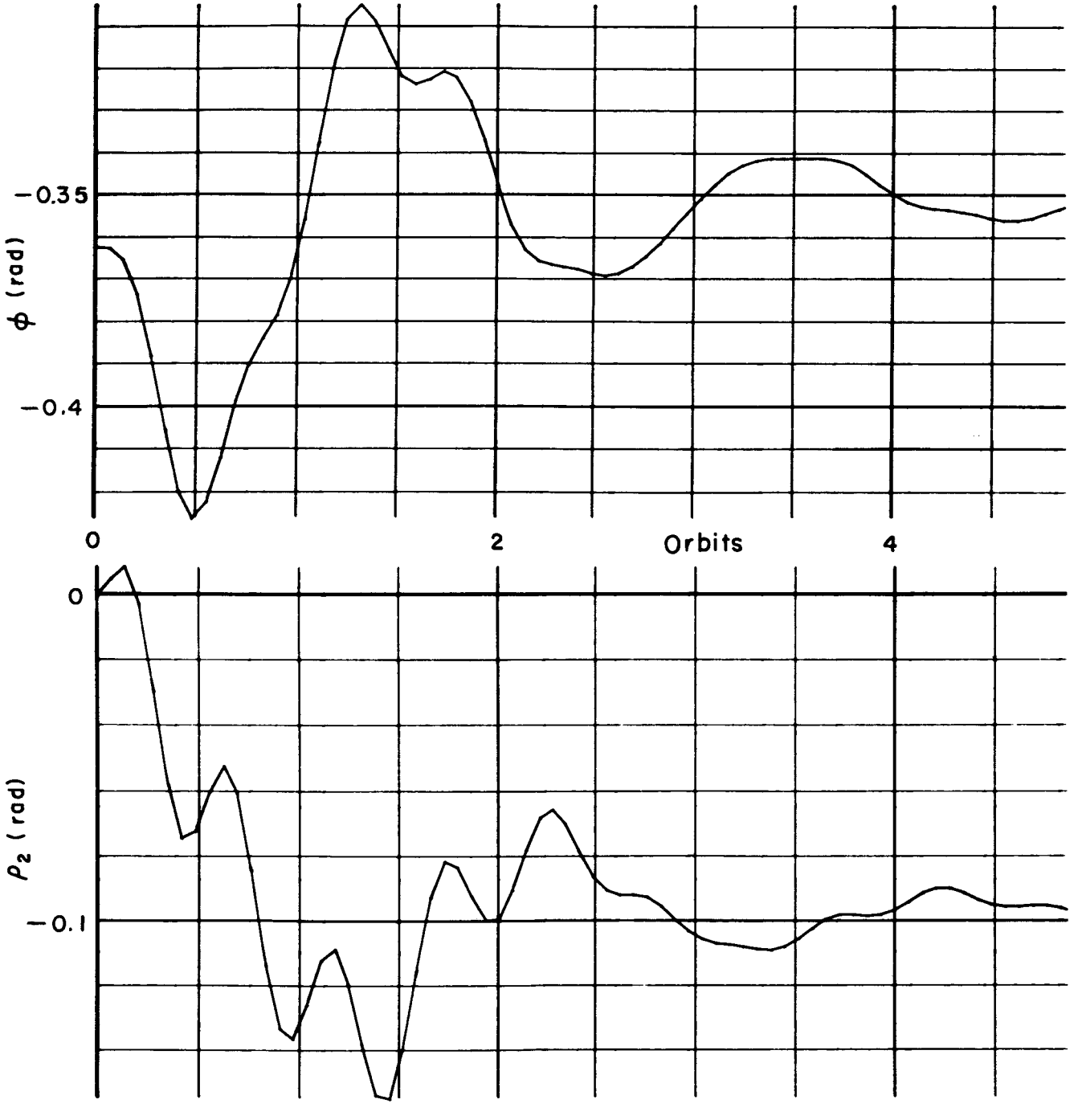

Fig. 26 (cont.)

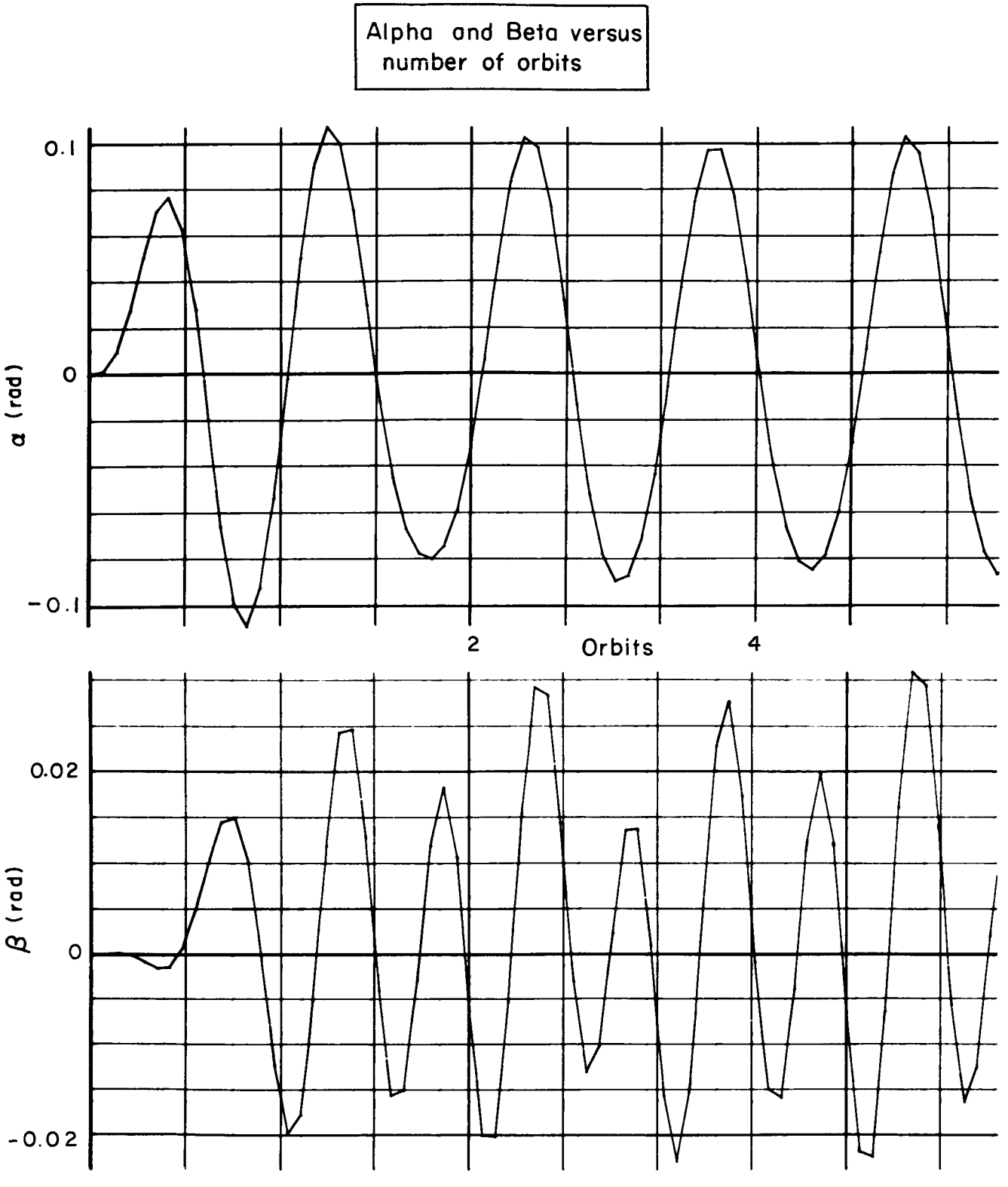

Fig. 27 — Forced response due to sinusoidal disturbing torques

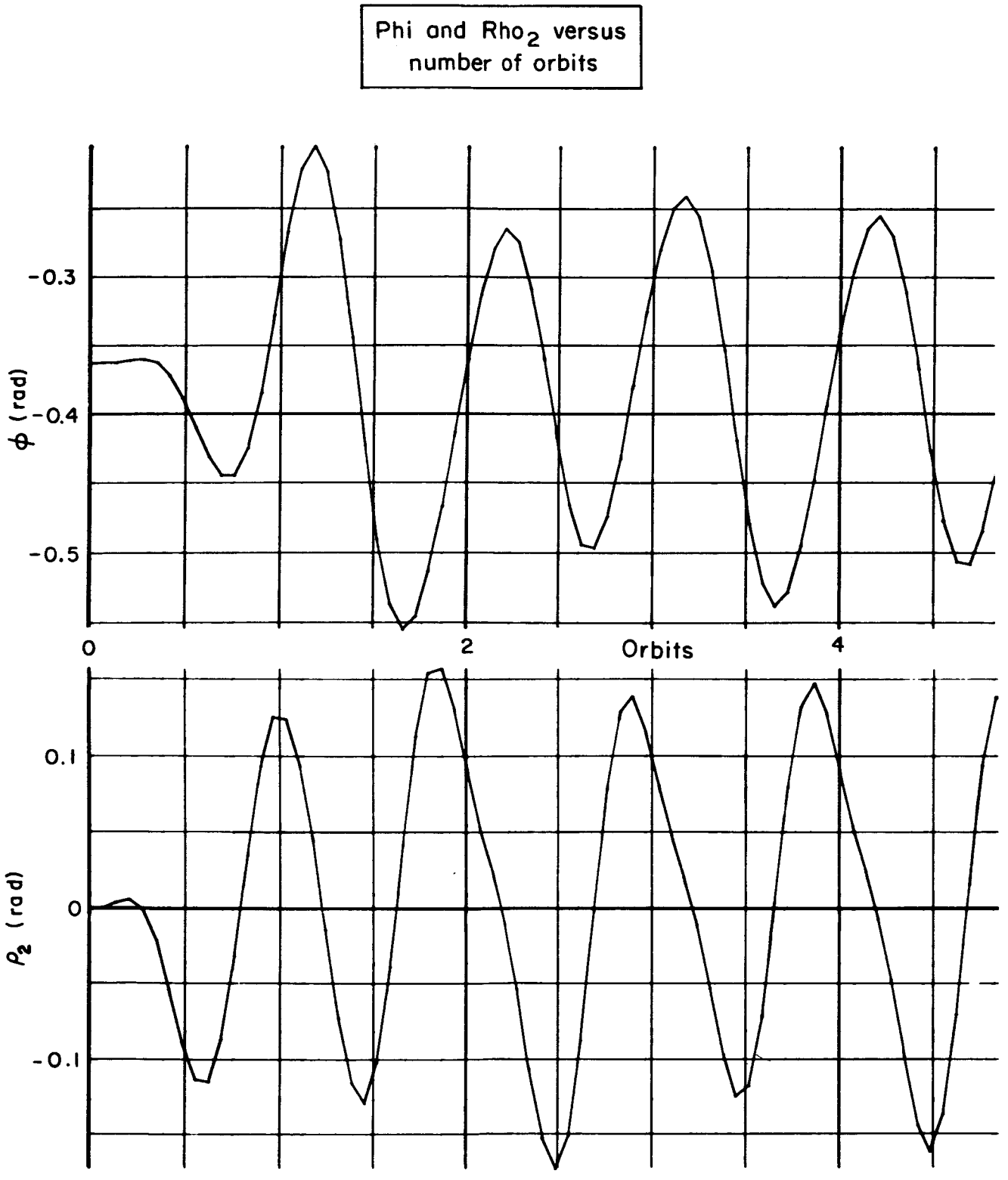
Phi and Rho2 versus number of orbits
-0.3
-0.4
-0.5
φ (rad)
0
2
4
Orbits
0.1
0
-0.1
ρ2 (rad)

Fig. 27 (cont.)

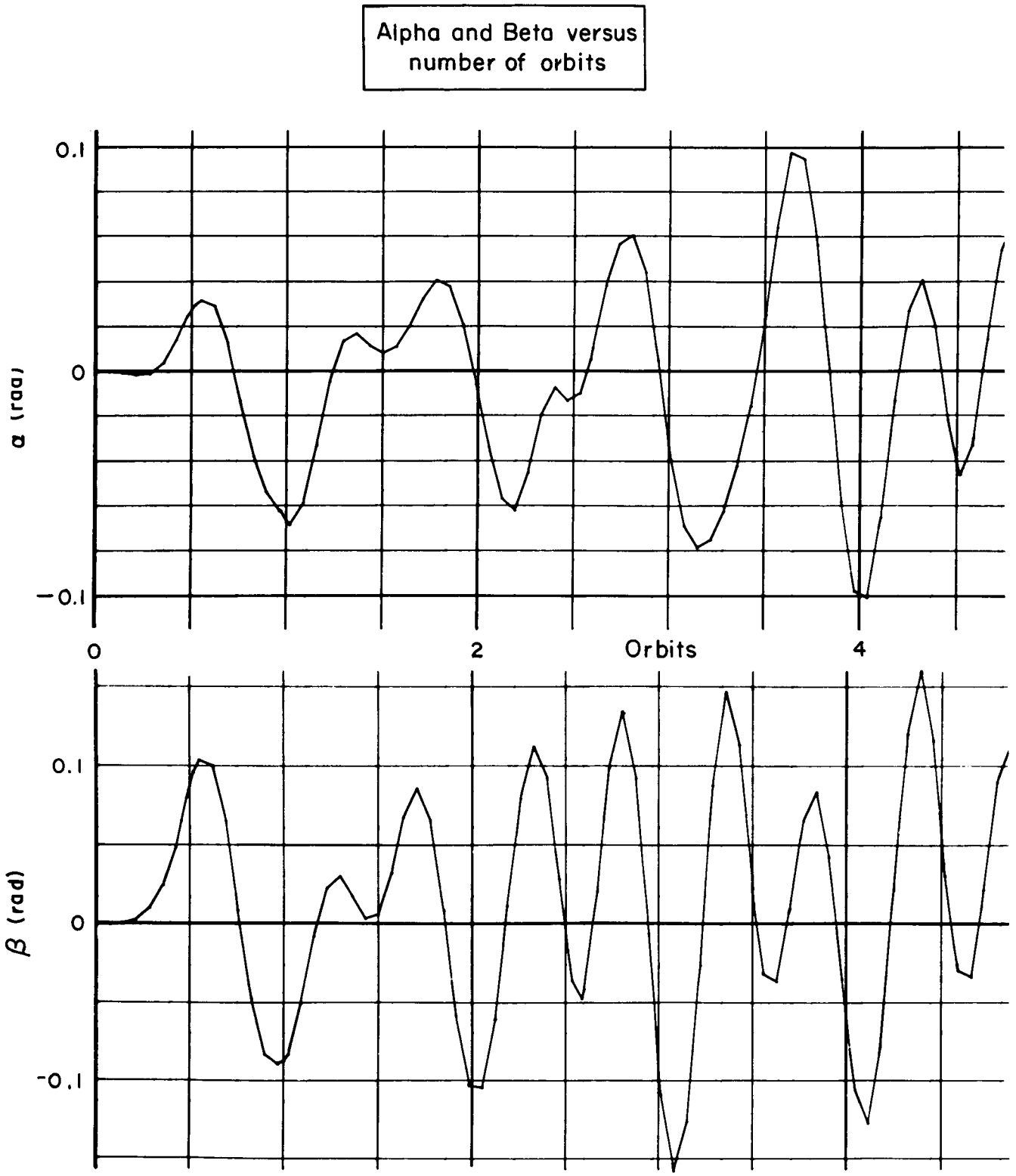

Fig. 28 — Forced response due to sinusoidal disturbing torques

Phi and Rho_2 versus number of orbits

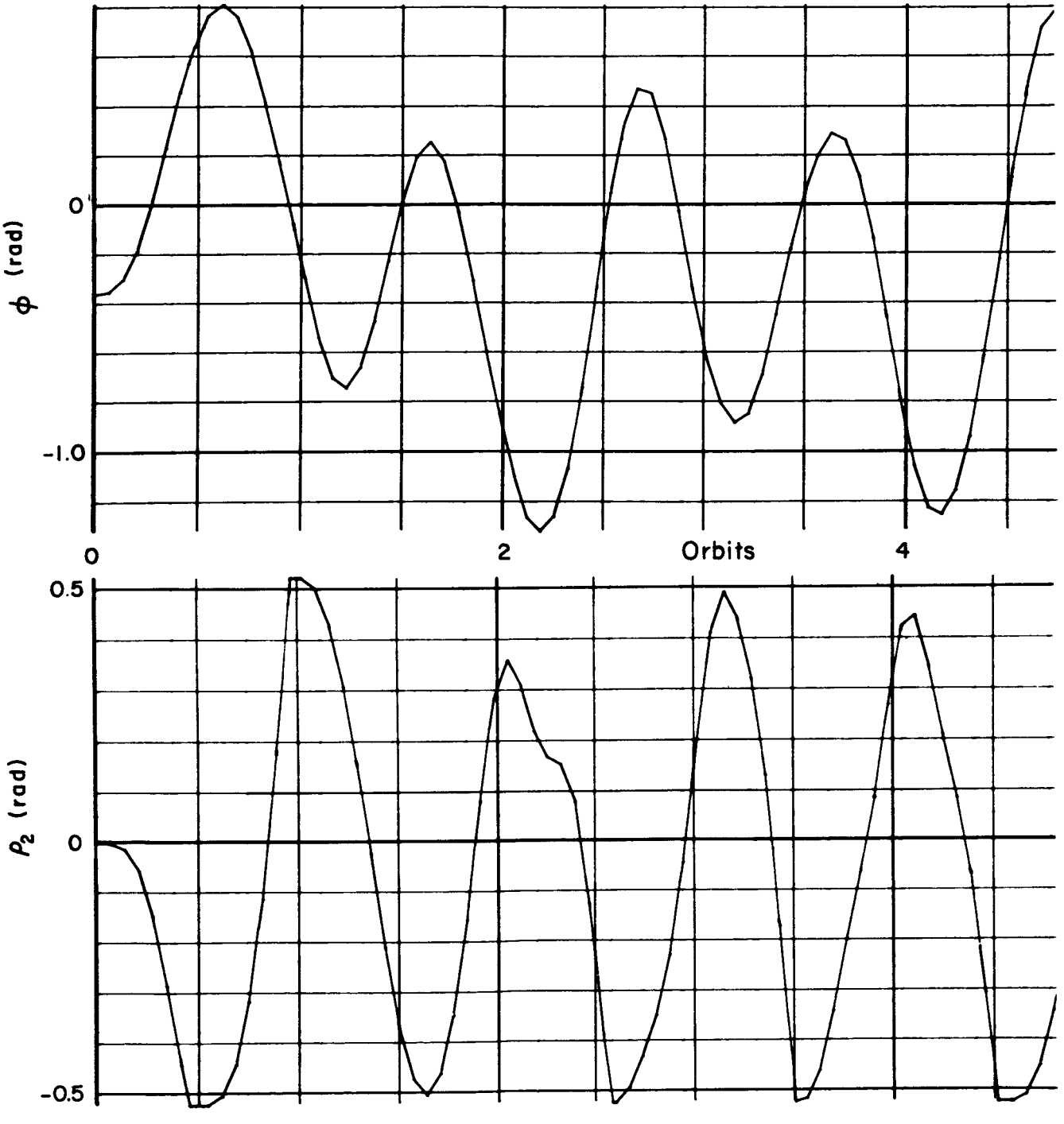

Fig. 28 (cont.)

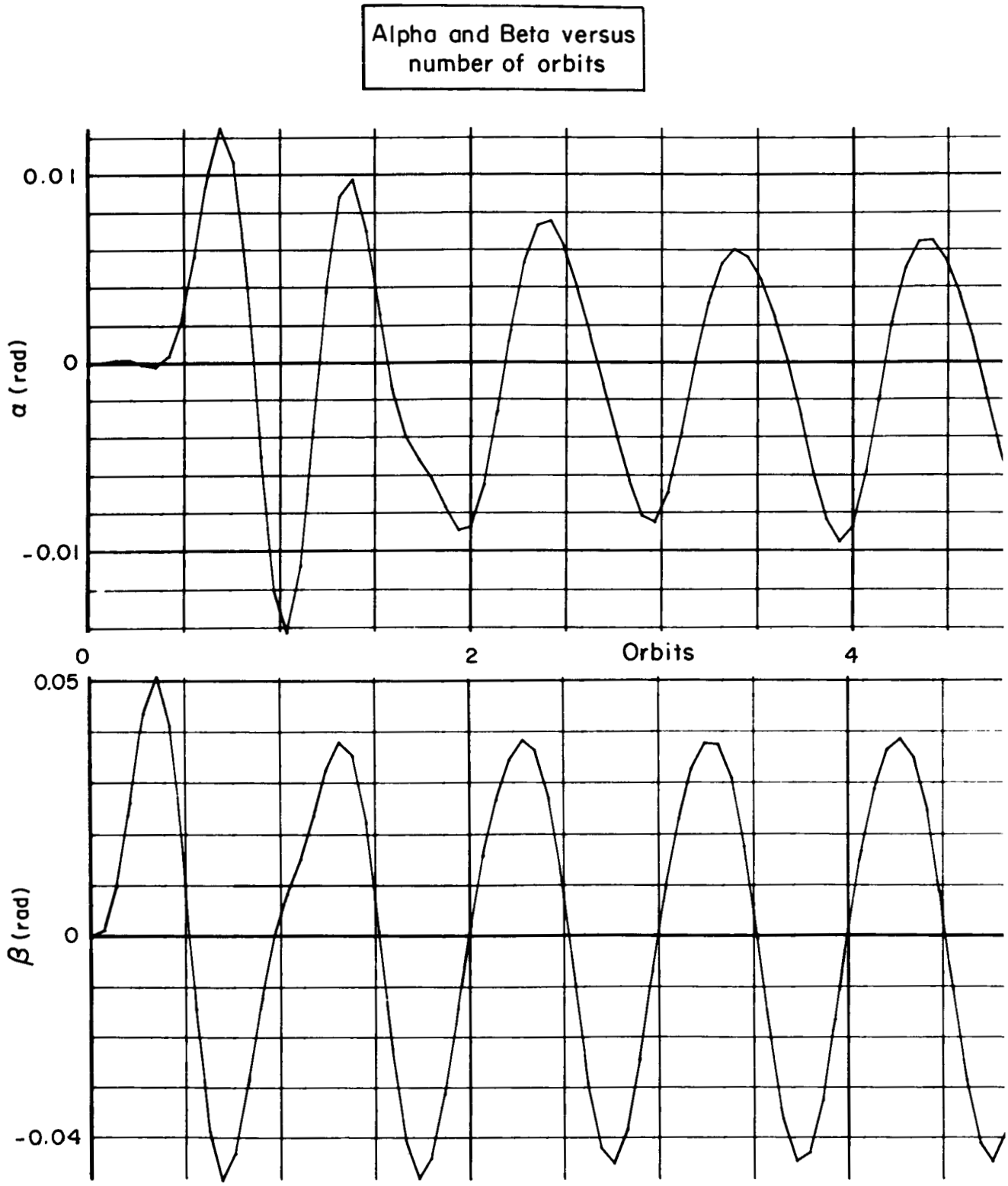

Fig. 29 — Forced response due to sinusoidal disturbing torques

Phi and Rho_2 versus number of orbits

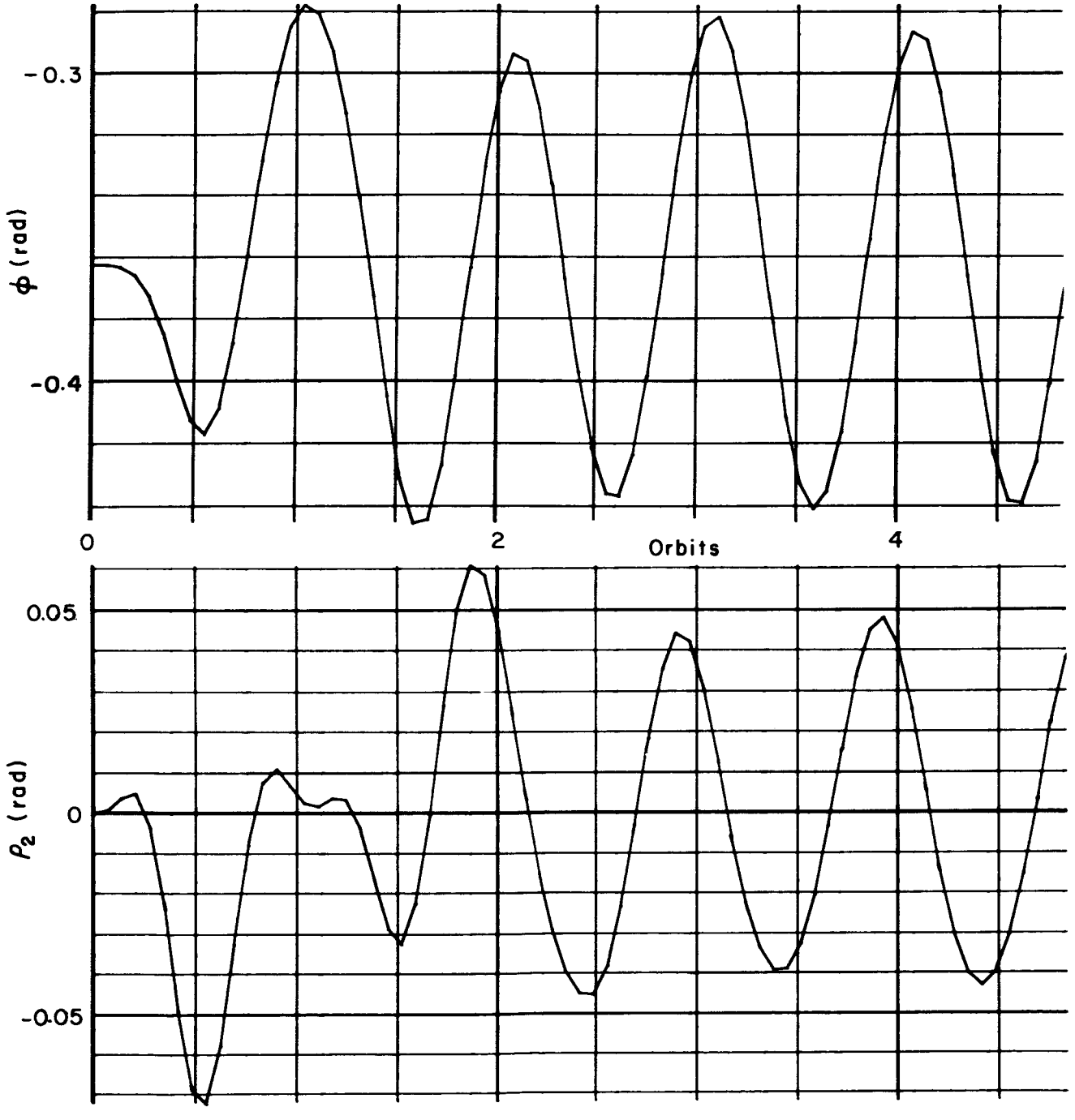

Fig. 29 (cont.)

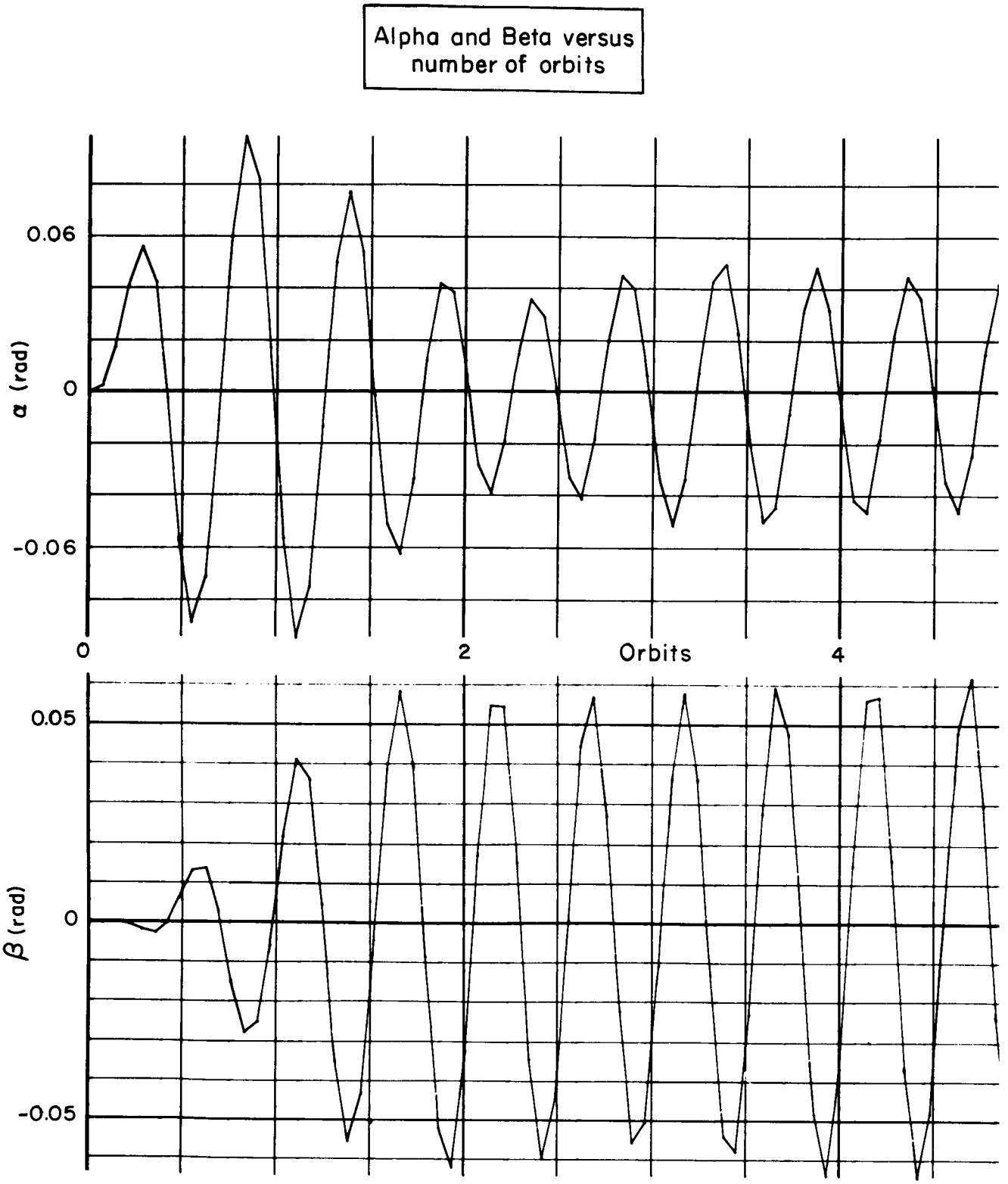

Fig. 30 — Forced response due to sinusoidal disturbing torques

Phi and Rho_2 versus number of orbits

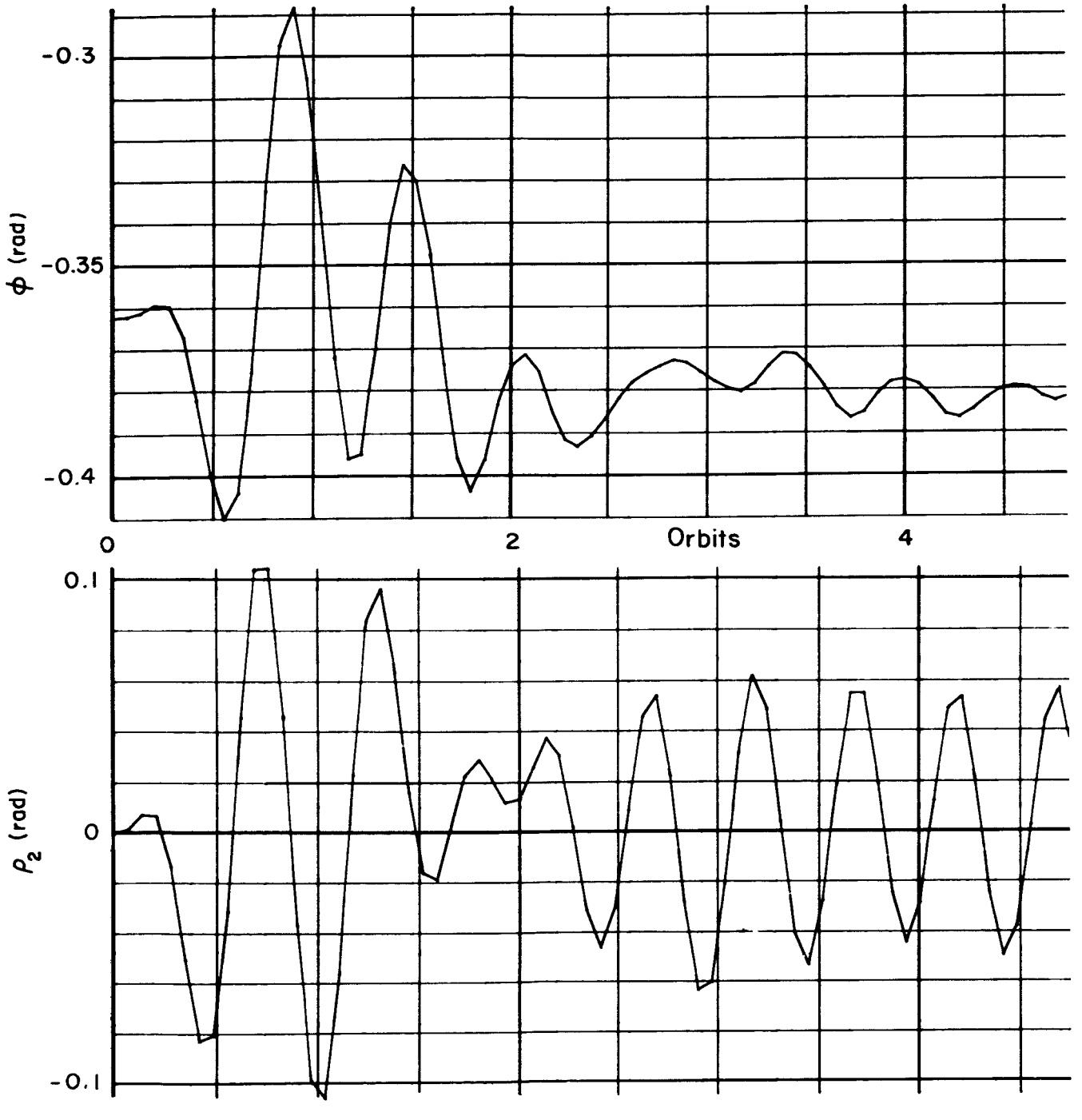

Fig. 30 (cont.)

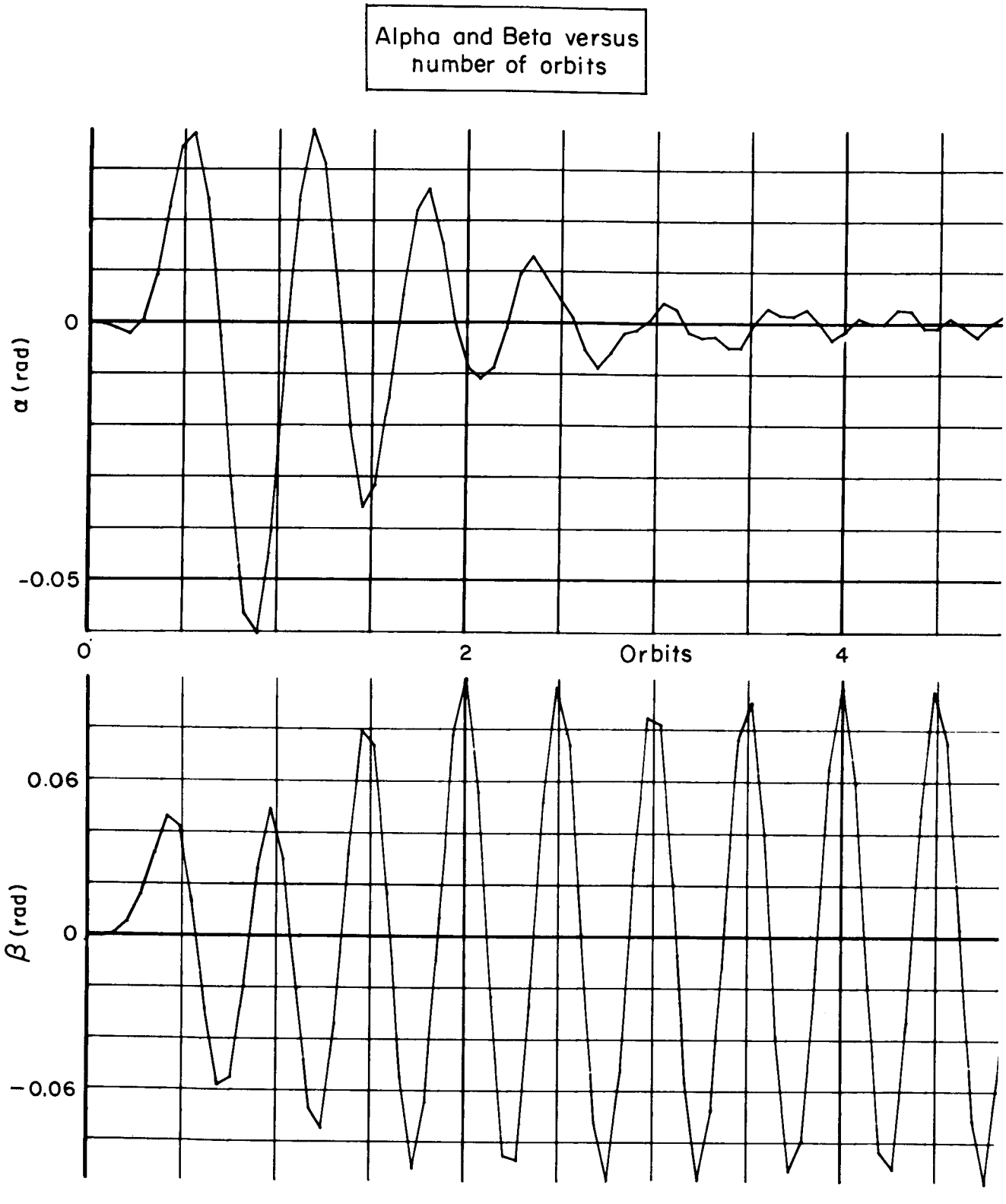

Fig. 31 — Forced response due to sinusoidal disturbing torques

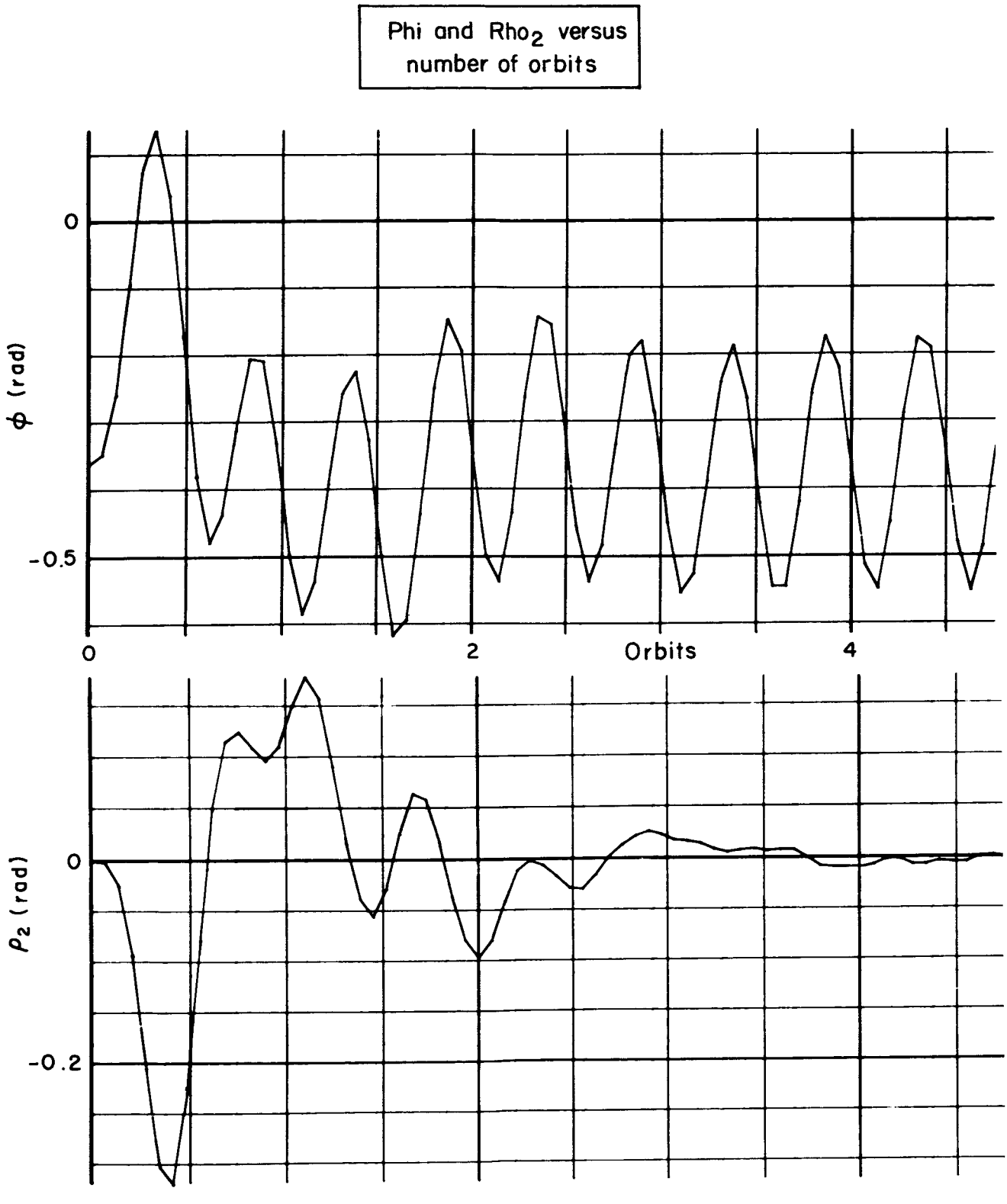
Phi and Rho2 versus number of orbits
0
-0.5
φ (rad)
0
2
Orbits
4
0
-0.2
ρ2 (rad)

Fig. 31 (cont.)

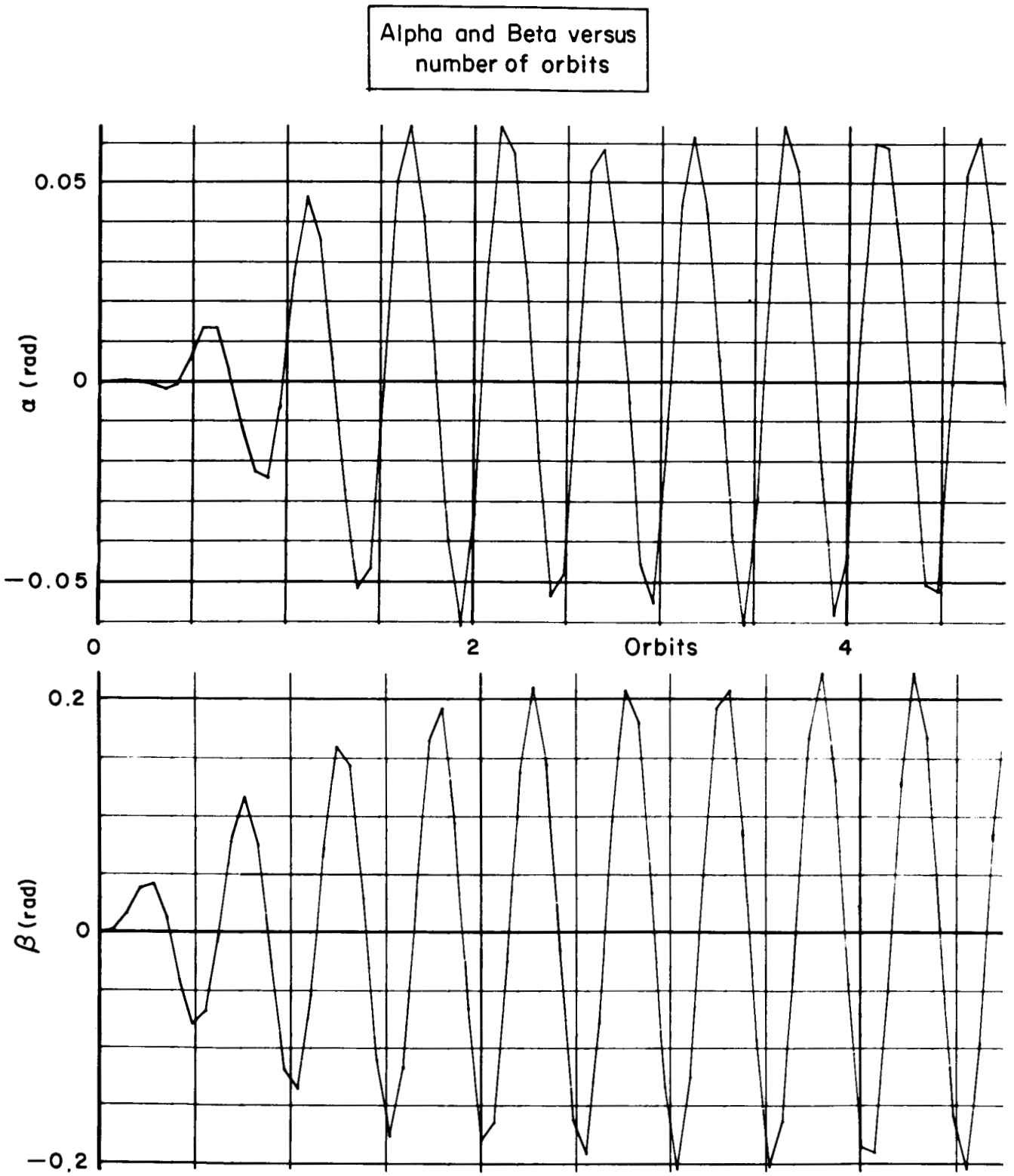

Fig. 32 — Forced response due to sinusoidal disturbing torques

Phi and Rho_2 versus number of orbits

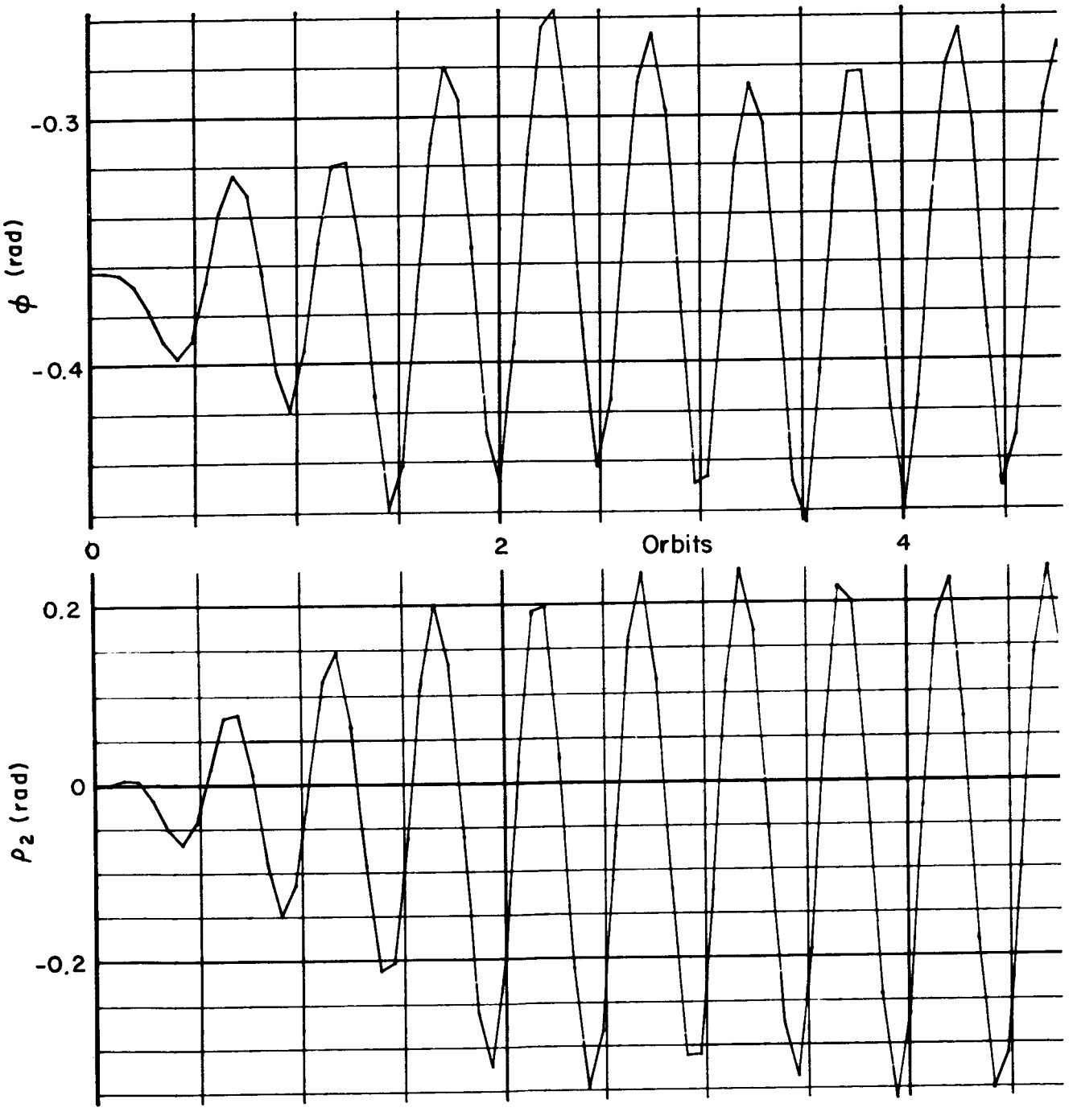

Fig. 32 (cont.)

REFERENCES

1. Roberson, R. E., (North American Aviation, Inc.), Attitude Sensing and Control for a Satellite Vehicle, The RAND Corporation, RM-1050, January 1953.

2. Newton, R. R., Damping of a Gravitational Stabilized Satellite, Johns Hopkins University Applied Physics Laboratory, TG487, April 1963.

3. Burt, E. G. C., On the Attitude Control of Earth Satellites, Space Department, Royal Aircraft Establishment, Farnborough, England, 1961.

4. Roberson, R. E., Methods For the Control of Satellites and Space Vehicles, Vol. 1, Systems Corporation of America, Sensing and Actuating Methods WADD Technical Report 60-643, July 1960.

5. Rowell, L. N. and M. C. Smith, "Effect of Geometrical Libration on the Damped Motion of an Earth Satellite," ARS Journal, March 1961.

6. Kamm, L. J., "An Improved Satellite Orientation Device," ARS Journal, Vol. 32, June 1962.

7. Wrench, E. H., Implementation of Vertistat, A Gravity Gradient Attitude Control System for Satellites, General Dynamics/Astronautics, San Diego, California, 1963.

8. Tinling, Bruce E. and Vernon K. Merrick, The Exploitation of Inertial Coupling in Passive Gravity-Gradient Stabilized Satellites, AMES Research Center, Moffett Field, California, Paper presented at the AIAA Guidance and Control Conference, MIT, August 1963.

9. Paul, B., J. W. West, and E. Y. Yu, "A Passive Gravitational Attitude Control System for Satellites," Bell Technical Journal, Vol. XLII, No. 5, September 1963.

10. Etkin, B., Attitude Stability of Articulated Gravity-Oriented Satellites, Part I, "General Theory and Motion in Orbital Plane," University of Toronto, Institute of Aerophysics Report No. 89, November 1962.

11. Roberson, R. E., "Attitude Control of Satellite Vehicles - An Outline of the Problem," Proceedings of the VIIIth International Astronautical Federation Congress, Barcelona, 1957.

12. Warren, H. R., The Use of Extensible Booms for Space Antennas and for Satellite Attitude Control, Hawker Siddeley Dynamics Ltd., London, England, September 1963.

13. Frick, R. H. and T. B. Garber, General Equations of Motion of a Satellite in a Gravitational Gradient Field, The RAND Corporation, RM-2527, December 1959.

14. Moran, John P., "Effects of Plane Librations on the Orbital Motion of a Dumbbell Satellite," ARS Journal, Vol. 31, No. 8, August 1961.

15. Frick, R. H. and T. B. Garber, Perturbations of a Synchronous Satellite, The RAND Corporation, R-399-NASA, May 1962.

16. Sterne, Theodore E., An Introduction to Celestial Mechanics, Interscience Publishers, Inc., New York, 1960.